UNIVERSITY OF ALBERTA
LIBRARY

Regulations Regarding Theses and Dissertations

Typescript copies of theses and dissertations for Master's and Doctor's degrees deposited in the University of Alberta Library, as the official Copy of the Faculty of Graduate Studies, may be consulted in the Reference Reading Room only.

A second copy is on deposit in the Department under whose supervision the work was done. Some Departments are willing to loan their copy to libraries, through the inter-library loan service of the University of Alberta Library.

These theses and dissertations are to be used only with due regard to the rights of the author. Written permission of the author and of the Department must be obtained through the University of Alberta Library when extended passages are copied. When permission has been granted, acknowledgement must appear in the published work.

This thesis or dissertation has been used in accordance with the above regulations by the persons listed below. The borrowing library is obligated to secure the signature of each user.

Please sign below:

Date	Signature	Institution

THE UNIVERSITY OF ALBERTA

AN ANALYTICAL STUDY OF INCLINED CRACKING IN REINFORCED CONCRETE BEAMS

by

JAMES RICHARD VINCENT WALTERS, B.Sc.(Alberta)

A THESIS

SUBMITTED TO THE FACULTY OF GRADUATE STUDIES

IN PARTIAL FULFILMENT OF THE REQUIREMENTS FOR THE DEGREE OF

MASTER OF SCIENCE

DEPARTMENT OF CIVIL ENGINEERING

EDMONTON, ALBERTA

JULY, 1966

ABSTRACT

The objective of this investigation was to derive, with the use of a digital computer, a rational solution to the shear strength of reinforced concrete beams. The theory assumed a shear compression type of behavior and attempts to predict the ultimate load by analyzing the complete cracked structure in the shear span. The effects of the shear carried by the longitudinal reinforcement, the shear transmitted across the crack through aggregate interlock and the effect of sections warping after cracking have been considered.

The results of the analysis were compared to the observed that values for 10 beams with reasonable success. To aid future investigators, a discussion of the various factors and recommendations are included in this report.

ACKNOWLEDGEMENTS

The author would like to express his grateful appreciation to the following for their contributions to this thesis:

Associate Professor J.G. MacGregor for his constructive criticism and assistance throughout the course of this investigation.

The National Research Council of Canada for the financial assistance provided to carry out the research.

The staff of the computing center at the University of Alberta for their assistance in writing the computer programs.

Mr. J.A. McLean for assistance in preparing the figures in this thesis.

Miss H. Wozniuk for the typing of the manuscript.

TABLE OF CONTENTS

TABLE OF CONTENTS (continued)

LIST OF FIGURES

LIST OF FIGURES (continued)

LIST OF TABLES

CHAPTER I

INTRODUCTION

1.1 GENERAL

This thesis is the result of an attempt to obtain a rational solution to the problem of the shear strength of reinforced concrete beams. Presently the methods of analysis and design found in building codes are empirical or semi-empirical and are not based on the observed behavior of the member as it fails in shear. Because of the many variables involved, the rational solution to this type of behavior will be extremely complex. However, when the behavior and the mechanism of failure are fully defined, the more important parameters may be incorporated into simplified design relationships.

1.2 OBJECT AND SCOPE

This thesis represents the second in a series of studies being carried out at the University of Alberta. The object of this investigation is to attempt to predict the inclined cracking and ultimate loads of reinforced concrete beams failing due to combined bending and shear by examining the mechanism of the crack structure in the shear span.

In order to accomplish this end many assumptions were made regarding material properties, beam behavior and stress distributions. These assumptions are elaborated upon in CHAPTERS 3 and 4.

The analysis presented in this thesis is an attempt to base the

shear strength of beams on a shear compression type of failure. In such a failure the behavior in flexure is extremely important while the shear stresses are important because they modify the stresses at the head of a flexural crack and the direction of such a crack.

This analysis is an attempt to go one step beyond the tooth theories of Moe (1962) and Kani (1964) by considering the cracked structure in its entirety rather than considering only one tooth in the structure. In order to accomplish this, extensive use was made of the University of Alberta's digital computing facilities. The effects of sections not remaining plane after cracking, shear force carried by the longitudinal reinforcement and shear forces transmitted by aggregate interlock and friction have been included in the analysis. The analysis was compared to the test results from 10 beams, which failed in diagonal tension, with reasonable success.

A brief literature survey is presented in CHAPTER 2. The assumptions necessary to define the material properties are presented and discussed in CHAPTER 3. The major step in the analysis of inclined cracking are presented in CHAPTER 4 along with the assumptions implicit in their derivation. The analysis is compared to test results in CHAPTER 5 and the variables affecting inclined cracking are briefly discussed in CHAPTER 6. Conclusions are drawn and recommendations made for future investigations in CHAPTER 7.

1.3 SYMBOLS

Most of the symbols are defined where they are first introduced.

They are collected here for ready reference.

A - an empirical constant in EQUATION 2.2.

- in the remainder of the thesis, the depth of the compression zone in the beam.

a - the length of the shear span

α - a crack spacing factor in EQUATION 2.2

B - an empirical constant in EQUATION 2.2

b - the width of the concrete beams

C - the distance from the tension face of the beam to the centroid of the reinforcement

C_1, C_2 - empirical constants in EQUATION 2.1

C_k - the total compressive force at section k

d - the distance from the compression face of the beam to the centroid of the reinforcement

ΔH - the total horizontal deflection of a tooth at the level of the reinforcement

ΔH_s - the horizontal deflection due to the shear transfer forces, at the level of the reinforcement

ΔT - the horizontal force on a tooth due to a difference in tension in the longitudinal reinforcement

ΔV - the total vertical deflection of a tooth at the level of the reinforcement

Δx - the crack spacing

E_{ci} - the initial tangent modulus of elasticity of concrete

E_s - the modulus of elasticity of the reinforcement

ϵ - the strain at any point on the beam cross-section

ϵ_y - the yield strain of the reinforcement

ϵ_s - the steel strain at a given load

ϵ_{cs} - the strain in the concrete, adjacent to the reinforcing

ϵ_u, ϵ_o - as shown in FIGURE 3.1

$\epsilon_{t1}, \epsilon_{to}, \epsilon_{tu}$ - as shown in FIGURE 3.2

ϵ_{s1} - the strain in the reinforcing assuming F equals unity

ϵ_{s2} - the additional strain in the steel due to bending of the teeth

f_c - the compressive stress in the concrete at some point of the cross-section

f'_c - the compressive strength of a 6" x 12" concrete cylinder at 28 days

f_s - the stress in the reinforcement

f_y - the yield stress of the reinforcement

f'_t - the ultimate tensile strength of the concrete as obtained from the split cylinder test

- in EQUATION 2.4, the modulus of rupture

f_r - the reduced stress at which cracking occurs, calculated as described in SECTION 4.10

f_{t1} - as shown in FIGURE 3.3

F - a steel strain compatibility factor calculated as described in SECTION 4.8.

γ - a cover coefficient in EQUATION 2.2

h - the total depth of the concrete beam

I - the moment of inertia of the concrete beam considering an uncracked section

I_{bar} - the moment of inertia of a reinforcing bar

j - ratio of distance between centroid of compression and centroid of tension to depth, d

K - a factor relating the tensile strength of concrete to $\sqrt{f'_c}$, see EQUATION 2.2

k_3 - 0.85 in this thesis

K_f - see EQUATION 4.3

k - a subscript referring to a given section

K_T - the stiffness of a tooth

λ - see EQUATION 4.3

L_{eff} - the effective length of reinforcing joining two adjacent teeth

M - the bending moment on a given section

m - a subscript referring to a given section

M_{VD} - the bending moment in the longitudinal reinforcing

P - the concentrated load on the beam

P_{cr} - the observed inclined cracking load

P_{code} - the inclined cracking load predicted using the A.C.I. Committee 326 Equation

P_u - the observed ultimate load of the beam

P_w - the ultimate load of the beam as predicted in this analysis

p - the percentage of longitudinal reinforcement in a given beam

$\emptyset$ - the angle at which a crack propagates, measured from a vertical axis

Q - the first moment of area about the neutral axis

Q_f - a foundation modulus, see EQUATION 4.3

R - the end reaction on a given beam

s - the height of a crack in the shear span in EQUATION 2.4

S - the predicted crack height in the region of shear and flexure or pure flexure

T - the tension in the reinforcing at a given section

T_t - the tooth stress on the critical element as shown in FIGURES 4.1 and 4.9

V - the total shear on a given section

V_{conc} - the shear force carried by the concrete

V_D - the shear force carried by the longitudinal reinforcing

v_c - the maximum allowable shear stress in the concrete before inclined cracking

v_{max} - the maximum calculated shear stress on a cracked section

v_s - the calculated shear stress at the head of the crack

X - a crack spacing factor, see TABLE 6.1

Y - the depth of the beam in which the concrete resists load in tension

CHAPTER II

REVIEW OF PREVIOUS WORK

2.1 INTRODUCTION

This chapter will be a brief review of previous inclined cracking theories for reinforced concrete beams. For a more complete review the reader is referred to a previous investigation done at the University of Alberta by Morrison (1965).

2.2 PREVIOUS THEORIES AND INVESTIGATIONS

In the past the problem of shear in reinforced concrete beams has been dealt with using three main approaches. The first and earliest approach was to consider the failure as being due to the horizontal shear force as expressed by the formula $v_c = VQ/Ib$. This approach was abandoned about 1910 and was replaced by considering failure to result from maximum principal tensile stresses computed in the cracked or uncracked beam. The majority of later theories and design formulae are based on this type of reasoning. In recent years the tooth failure theories of Kani (1964) and Moe (1962) have been presented. These theories idealize cracking as the breaking off of a "tooth" between two flexural cracks in the shear span.

The classical shear equation as found in the 1956 A.C.I. Building Code used the nominal shear stress $v_c = V/bjd$ as a measure of the diagonal tension. This equation, however, does not take into account the effect of moment on the shearing resistance of beams. Work by Clark (1951) and Moody (1954) showed that the shear strength of concrete beams was

equal to some function of the shear span or the ratio of moment to shear. This work led to the A.C.I. - A.S.C.E. Committee 326 Equation for the nominal concrete stress:

$$v_c = C_1 + C_2 \, Vpd/M \sqrt{f'_c} \qquad (2.1)$$

where C_1 and C_2 were constants which were evaluated empirically as 1.9 and 2500 respectively.

Van den Berg (1962) derived a test procedure whereby he could vary the moment and the shear independently of one another. Using his results he was able to derive an expression for the diagonal cracking load that was a function of the shear force and bending moment on a given section. Van den Berg also suggested that there was a shear force transferred across the crack and concluded that the parabolic shear distribution was undisturbed by the formation of flexural cracks.

Krahl (1963) developed an analytical procedure for predicting the failure load for a concrete beam failing by inclined cracking. The procedure developed by Krahl defined an inclined crack for a given set of beam properties, load patterns and an assumed shear stress distribution. In his calculations a crack height was assumed and the load required to cause that crack height was calculated. The procedure was then repeated for slightly larger crack heights until at some crack height the load required to cause the crack was less than the previous load. Failure was assumed to occur when this condition occurred. This method of analysis is limited, however, since the cracked structure is not analyzed in its

entirety.

Moe (1962), by considering the concrete elements or teeth between cracks to be cantilevers anchored in the compression zone of the beam, loaded with forces in the tensile reinforcement as well as shear stresses transferred across the inclined cracks, was able to derive equations for the shear stress in the concrete at failure. The transfer shear stresses were made up of two parts, those due to dowel action of the longitudinal reinforcement and those due to aggregate interlock. The transfer stresses were assumed to be a function of the crack width and as such were a function of the stress in the longitudinal steel and the bond properties of the longitudinal steel. Moe's final equation was given as:

$$v_c = \left(\frac{f_s}{f_s - B}\right)\left(\frac{\alpha j}{6\gamma(1 - A)}\right) K\sqrt{f'_c} \qquad (2.2)$$

where $K\sqrt{f'_c}$ = the tensile strength of the concrete

αd = the spacing of the cracks

γd = the distance from the centroid of the longitudinal reinforcing to the neutral axis.

A and B are constants and v, j and f_s have their normal meanings.

If the following values are assumed K = 5.0, α = 0.3, γ = 0.6, j = 7/8, A = 0.808 and B = 2850 then EQUATION 2.2 becomes

$$v_c = 1.9\sqrt{f'_c}\ \frac{f_s}{f_s - 2850} \qquad (2.3)$$

which is identical to an equation derived by the A.C.I. - A.S.C.E. Committee 326 and can be rearranged to give EQUATION 2.1.

Kani (1964) proposed a tooth theory to predict the shear strength of reinforced concrete beams. Kani, like Moe, only considered one tooth in his mechanism. Kani further simplified his expressions by neglecting any doweling shears or concrete shears which might be transferred across the crack. By considering a crack height and only a horizontal force due to the longitudinal steel stress he was able to derive EQUATION 2.4 for the critical moment.

$$M_{cr} = \frac{7}{8} \frac{f'_t}{6} \frac{\triangle x}{s} \text{ bad} \qquad (2.4)$$

where f'_t is the modulus of rupture of the concrete; $\triangle x$ is the crack spacing; s is the crack height; a is the shear span; and b and d are the dimensions of the cross-section. The term $\triangle x/s$ was to be determined from tests but as yet this has not been published.

The tooth analysis of Kani and Moe are only applicable in the range of shear span to depth ratios, a/d, greater than about 2.5.

2.3 CONCLUSIONS

Past work has suggested some of the factors that are involved in the development of inclined cracks in reinforced concrete beams. The more significant factors seem to be: the concrete strength, the percentage of longitudinal reinforcement, the bond characteristics of the reinforcing, the shear span to depth ratio, the crack spacing, the shear force and

bending moment acting on a given section, the shear transferred across a crack by particle interlock or by dowel action and the flexural capacity of the member.

From the number of variables involved it can be seen that the problem is extremely complex and there will probably not be any simple solution to it. So far, all solutions have been of an empirical or semi-empirical nature.

CHAPTER III

MATERIAL PROPERTIES

3.1 INTRODUCTION

The properties of steel and concrete presented in this chapter have been derived empirically from a survey of tests reported in the engineering literature.

The properties themselves, while they directly influence the results of the analysis, can be changed for future applications of the analysis.

3.2 CONCRETE

Concrete was assumed to be an elasto-plastic material. For this thesis the specific effects of creep, shrinkage and composition were ignored. The following sections in this chapter will deal with mathematical expressions for the stress-strain curves in compression and tension.

3.2.1 CONCRETE STRESS-STRAIN PROPERTIES IN COMPRESSION

The strength which concrete exhibits in compression is usually taken as a fraction of the 28 day compressive strength of a 6 inch by 12 inch cylinder, because the conditions of stress, restraint, casting and curing are different for concrete in a beam and that in a control cylinder. In this thesis the strength of the concrete in the structure

is expressed as $k_3 f'_c$ where k_3 is taken as 0.85. This value is well documented in tests by Hognestad (1951) and Hognestad, Hanson, McHenry (1955). In these same tests the value of ultimate strain in compression was found to range from about 0.0030 to 0.0045 depending on a number of variables. The ultimate compressive strain of 0.0038 used by Hognestad (1951) has been adopted in this thesis.

The general shape of the stress-strain curve in compression is shown in FIGURE 3.1. It can be described as a second-degree parabolic curve to a maximum stress and a horizontal line at the maximum stress until a maximum strain is reached. The parabolic portion is mathematically expressed as:

$$f_c = k_3 f'_c \left(2 \frac{\epsilon}{\epsilon_o} - \left(\frac{\epsilon}{\epsilon_o}\right)^2\right) \qquad (3.1)$$

where $$\epsilon_o = \frac{2k_3 f'_c}{E_{ci}}$$

The initial tangent modulus is based on work by Pauw (1960) and is given by EQUATION 3.2. It corresponds closely to the expression in the 1963 A.C.I. Building Code.

$$E_{ci} = 60{,}000 \sqrt{f'_c} \qquad (3.2)$$

The portion of the curve between ϵ_o and ϵ_u was considered horizontal for ease in programming the computer. This stress-strain curve

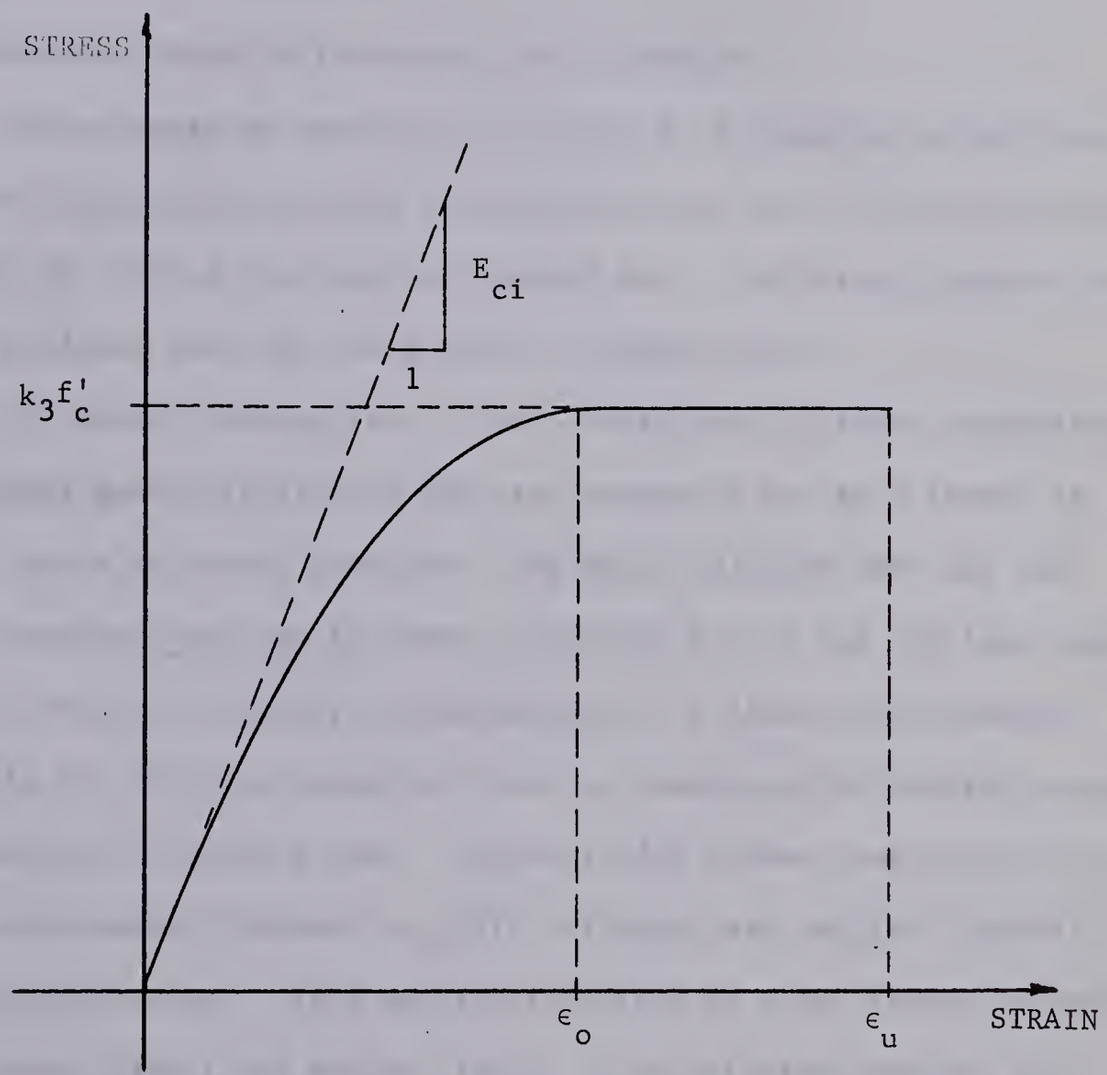

FIGURE 3.1 STRESS - STRAIN CURVE

FOR CONCRETE IN COMPRESSION

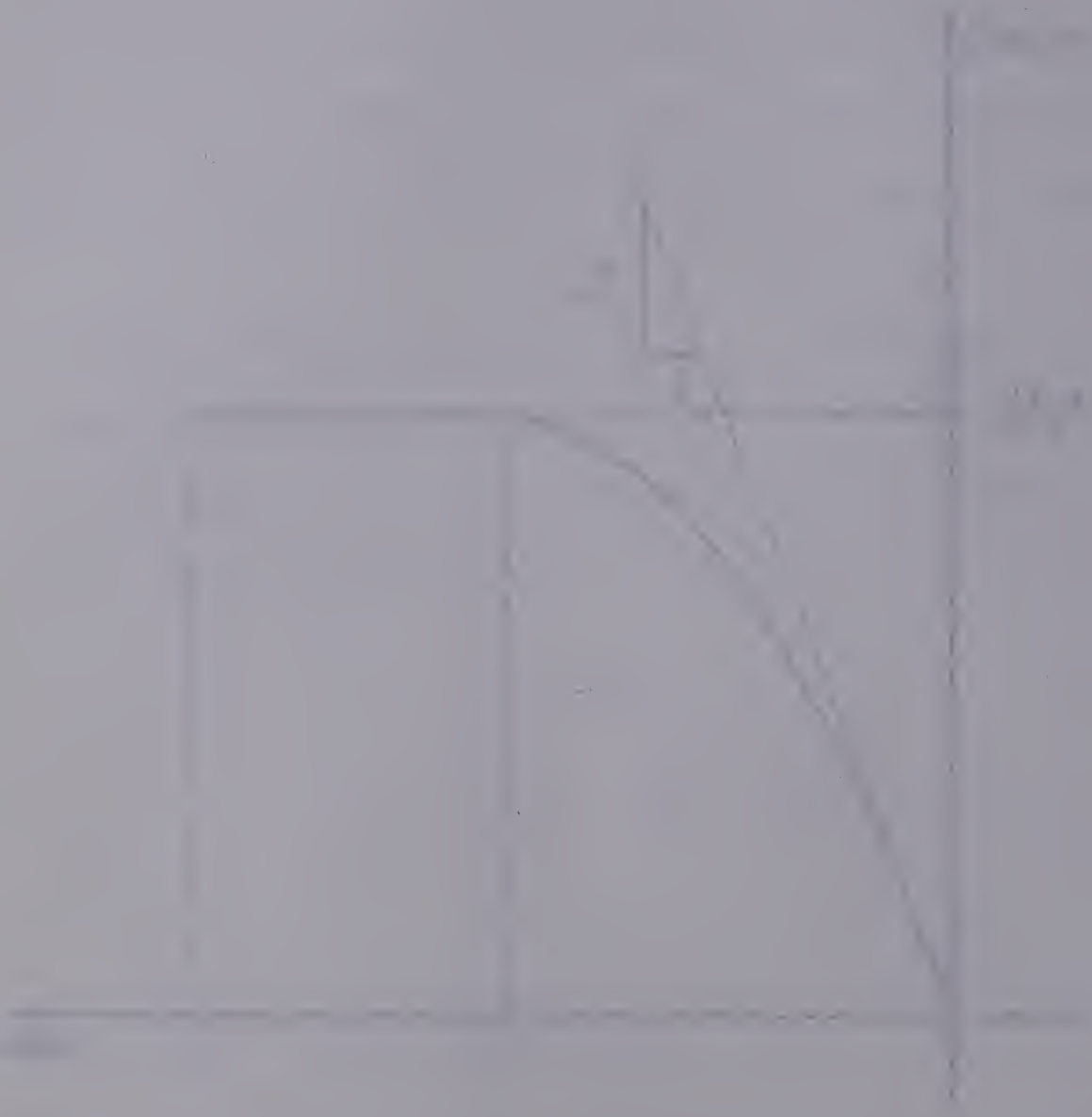

was first used by Manuel (1966).

3.2.2 CONCRETE STRESS-STRAIN PROPERTIES IN TENSION

The strength of concrete in tension is a function of the type of test and the assumptions made in analyzing that test. The three most common ways of testing the tensile strength are: the direct tension test, the split cylinder test and the modulus of rupture test.

The direct tension test is very sensitive to stress concentrations and accidental eccentricities in the test apparatus and as a result is used very little in actual practice. The split cylinder test and the modulus of rupture test are the most convenient to run and are less susceptible to errors. However, the assumption of a linear stress-strain relationship for concrete leads to errors in computing the tensile strength from the modulus of rupture test. Narrow (1963) showed that there is a definite relationship between the split cylinder test and the flexural or modulus of rupture test. This was substantiated by other investigators including Oladapo (1964) and Wright (1955). A relationship between the direct tensile strength and the modulus of rupture was also shown as early as 1928 by Gonnermann and Shuman and later by Price (1951).

For this thesis, the tensile strength is based on the split cylinder test for a number of reasons. The split cylinder test seems to give results between those from the direct tension test and the flexural test, thus it could be regarded as an average value. More important, the stress conditions in the split cylinder test with compression and tension on perpendicular planes more closely approximate the actual stress con-

ditions in a beam at inclined cracking.

Neville (1963) reports the value of the modulus of rupture as $9.5\sqrt{f'_c}$ a value which is credited to the European Concrete Committee. This expression is in good agreement with the expression $f'_t = 3000/(4 + \frac{12,000}{f'_c})$ derived by Sozen, Zwoyer and Siess (1959). Wright (1955) stated that the split cylinder strength was two-thirds of the flexural strength and later work by Oladapo (1964) showed that the ratio varied from two-thirds to three quarters of the flexural strength. In this thesis the tensile strength has been taken as $7\sqrt{f'_c}$ which is approximately three-quarters of the value of $9.5\sqrt{f'_c}$ assumed for the modulus of rupture.

The ultimate tensile strains reported in the literature ranged from a low of 67 micro inches per inch (Oladapo, 1964) to a high 200 micro inches per inch (Neville, 1963). Linder and Sprague (1955) found that the limiting strain was a function of the beam size. Kaplan (1963) found that the volume of coarse aggregate also had an effect on the limiting strain of concrete in tension. The value of the limiting tensile strain was taken as 150 micro inches per inch for the purposes of this thesis. This value tended to be on the upper side of observed cracking strains from tests reviewed in the literature.

The shape of the stress-strain curve was chosen to be linear initially and parabolic for the later stages of loading. This type of curve is shown in FIGURE 3.2 and is similar to a stress-strain curve proposed by Linder and Spraque (1955). Mathematically the curve may be expressed as follows:

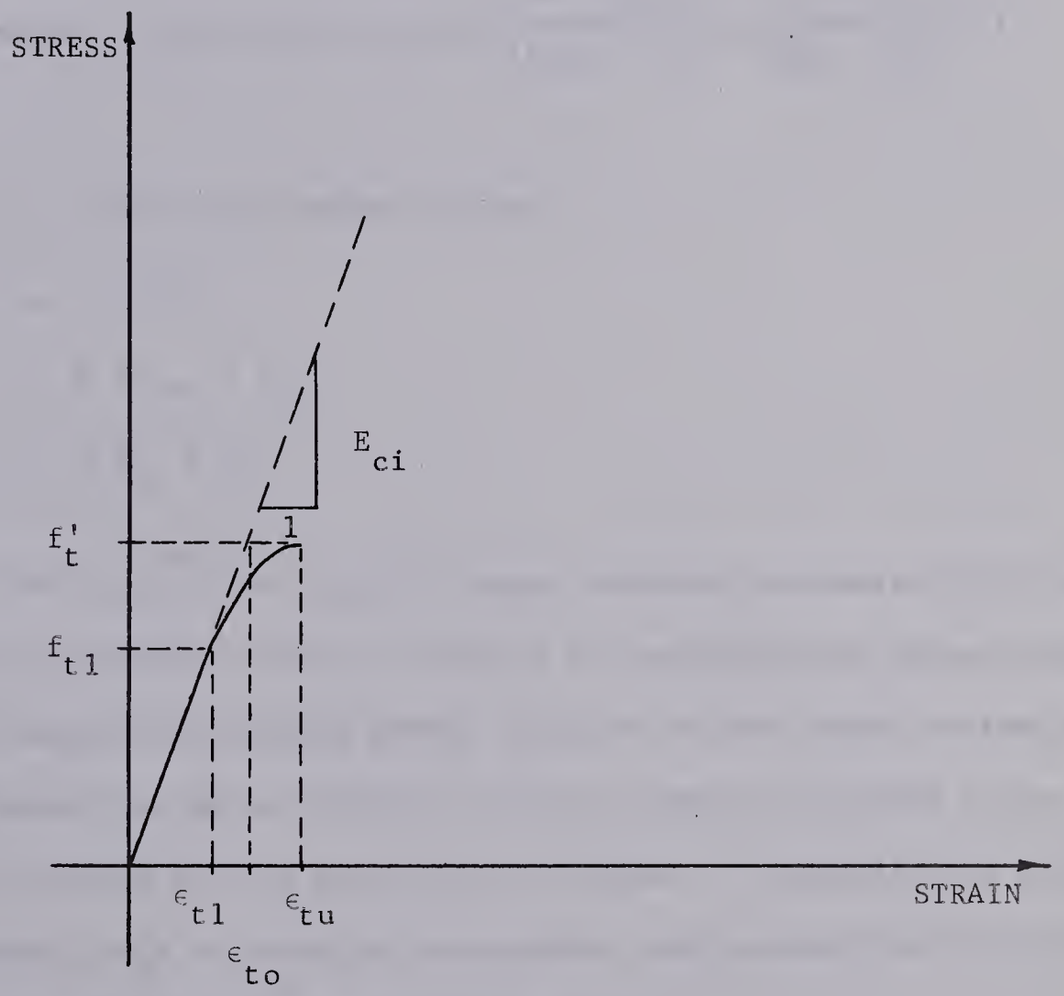

FIGURE 3.2 STRESS - STRAIN CURVE

FOR CONCRETE IN TENSION

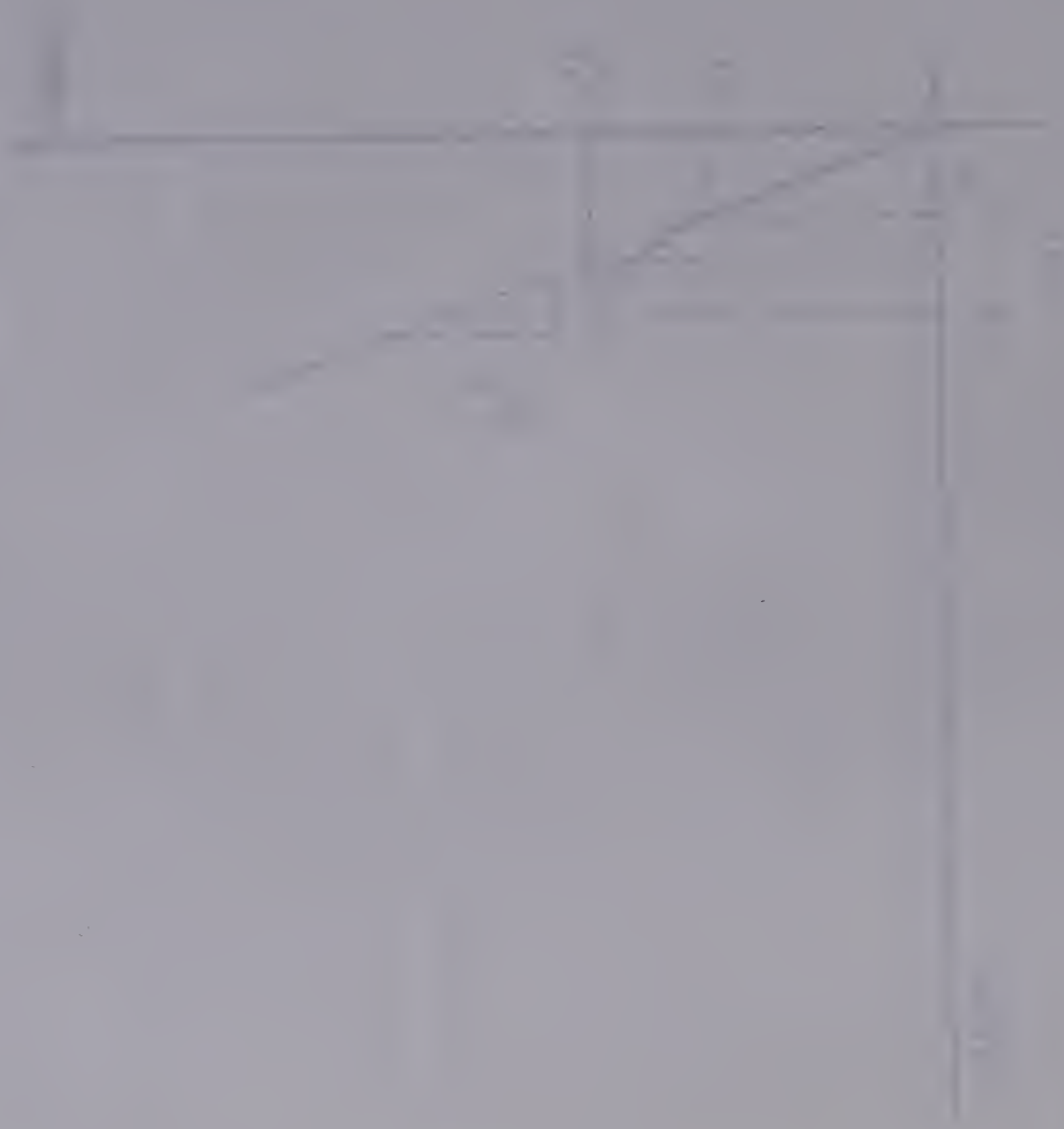

$$\epsilon \leq \epsilon_{t1} \quad f_t = E_{ci} \times \epsilon_t \tag{3.3}$$

$$\epsilon_{t1} \leq \epsilon \leq \epsilon_{to} \quad f_t = (f'_t - f_{t1}) \left(2 \frac{(\epsilon - \epsilon_{t1})}{(\epsilon_{tu} - \epsilon_{t1})} - \left(\frac{(\epsilon - \epsilon_{t1})}{(\epsilon_{tu} - \epsilon_{t1})}\right)^2\right)$$

where ϵ_{tu} = 150 micro inches per inch

$\epsilon_{to} = f'_t / E_{ci}$

$\epsilon_{t1} = 2\,\epsilon_{to} - \epsilon_{tu}$

$f_{t1} = E_{ci} \times \epsilon_{t1}$

The value of the initial tangent modulus of elasticity of concrete in tension was assumed to be the same as in compression as given by EQUATION 3.2. This particular tensile stress strain curve was chosen so that the cracking moment for an unreinforced concrete beam corresponded to the modulus of rupture for the concrete in the beam. In addition the shift in the neutral axis at cracking corresponded approximately with the shift measured in tests by Linder and Spraque (1955).

3.3 FAILURE THEORY FOR CONCRETE

Concrete is assumed to fail in tension when the principal tensile stress exceeds the tensile strength assumed for concrete. A limiting compression strain was used to define a compression failure. The principal stresses were calculated using a Mohr's circle. No attempt has been made to base the theory on a maximum shear stress critieria, a maximum strain criteria or a Mohr Rupture Line criteria.

3.4 REINFORCING STEEL

The stress-strain curve for the reinforcing steel has been assumed to represent an elasto-plastic material as shown in FIGURE 3.3.

The values of E_s and f_y have been taken from the results of tests of actual bars reported with the beam data in the literature. Where such information was not available E_s was assumed to be 30×10^6 psi and f_y = 40,000 psi.

3.5 CONCLUSIONS

The material properties in this section are based on mathematical approximations of actual results reported in the literature.

The assumptions regarding the tensile properties of the concrete probably have the most effect on the development of flexure and shear cracks. The assumptions made regarding concrete in compression and the reinforcing steel are very close to the usual assumptions.

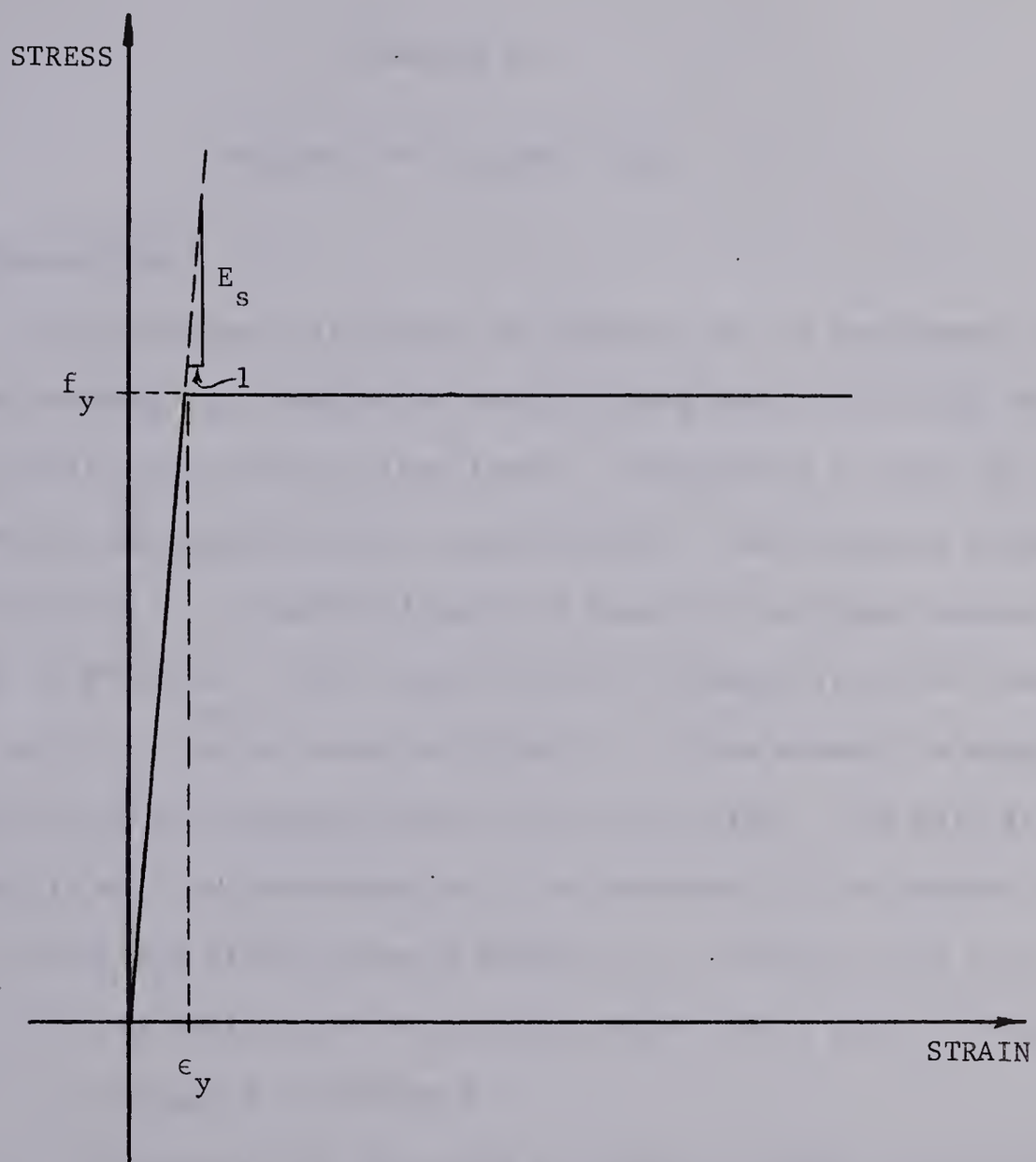

FIGURE 3.3 STRESS - STRAIN CURVE

FOR REINFORCING STEEL

CHAPTER IV

ANALYSIS FOR ULTIMATE LOAD

4.1 INTRODUCTION

This chapter will present an analysis of the development of inclined cracking in a reinforced concrete beam subjected to one or two symmetrically placed concentrated loads. The analysis is based on strength of materials and ignores stress concentrations. The structure assumed in the analysis is a reinforced concrete beam with uniformly spaced cracks as shown in FIGURE 4.7. The assumed critical element is on the load side at the top of a crack as shown in FIGURE 4.1. This element is acted on by shearing stress and flexural stress in two directions. The main steps in the analysis will be elaborated on in the remainder of the chapter and are shown in the block flow diagram of FIGURE 4.2. The main steps are:

(a) The calculation of the cracking moment for a given section as discussed in SECTION 4.3.

(b) The definition of the tooth structure in terms of calculated crack heights and an assumed crack spacing as discussed in SECTIONS 4.3 and 4.4.

(c) The calculation of a shear stress distribution as discussed in SECTION 4.5.

(d) The analysis of the indeterminate tooth structure for final steel strains and total deflections discussed in SECTIONS 4.6 and 4.8.

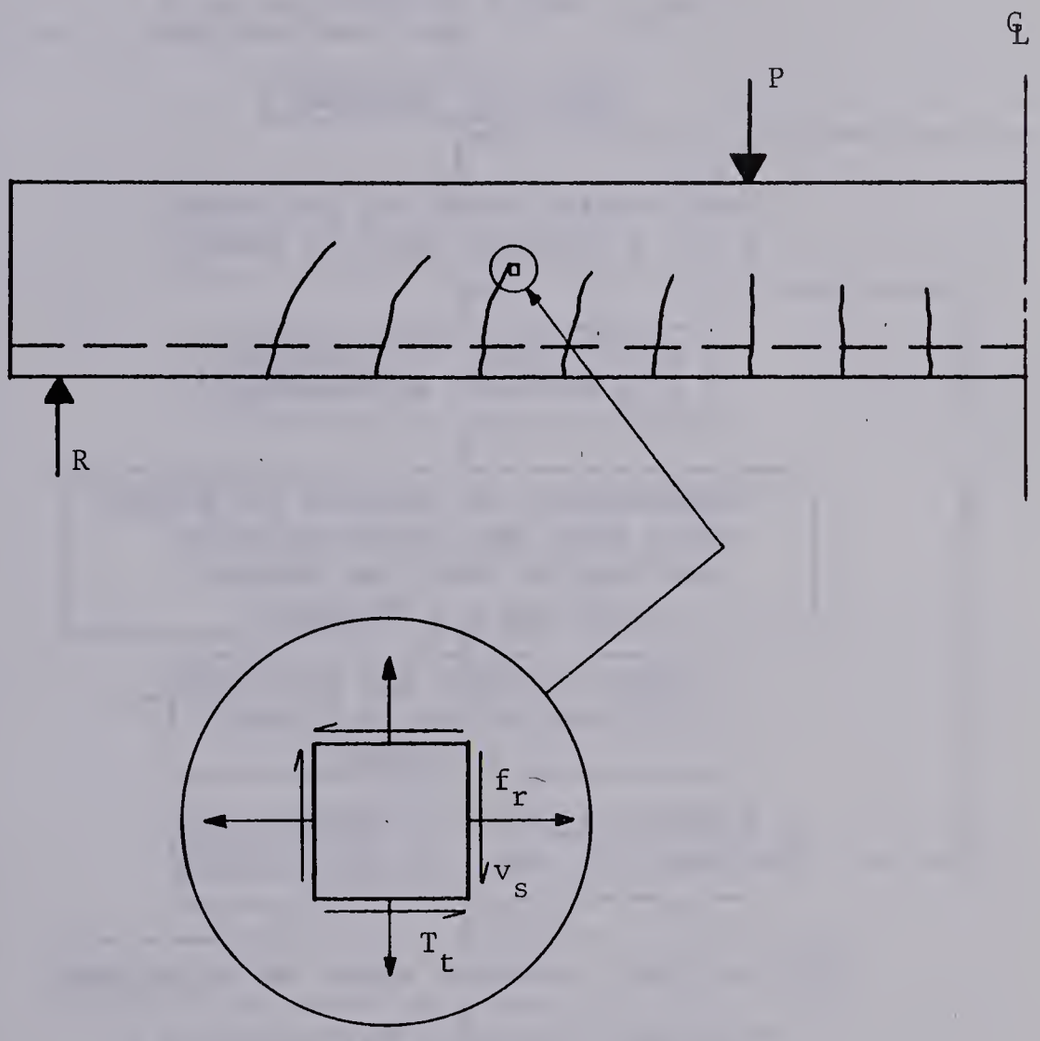

FIGURE 4.1 THE ASSUMED STRUCTURE AND CRITICAL ELEMENT

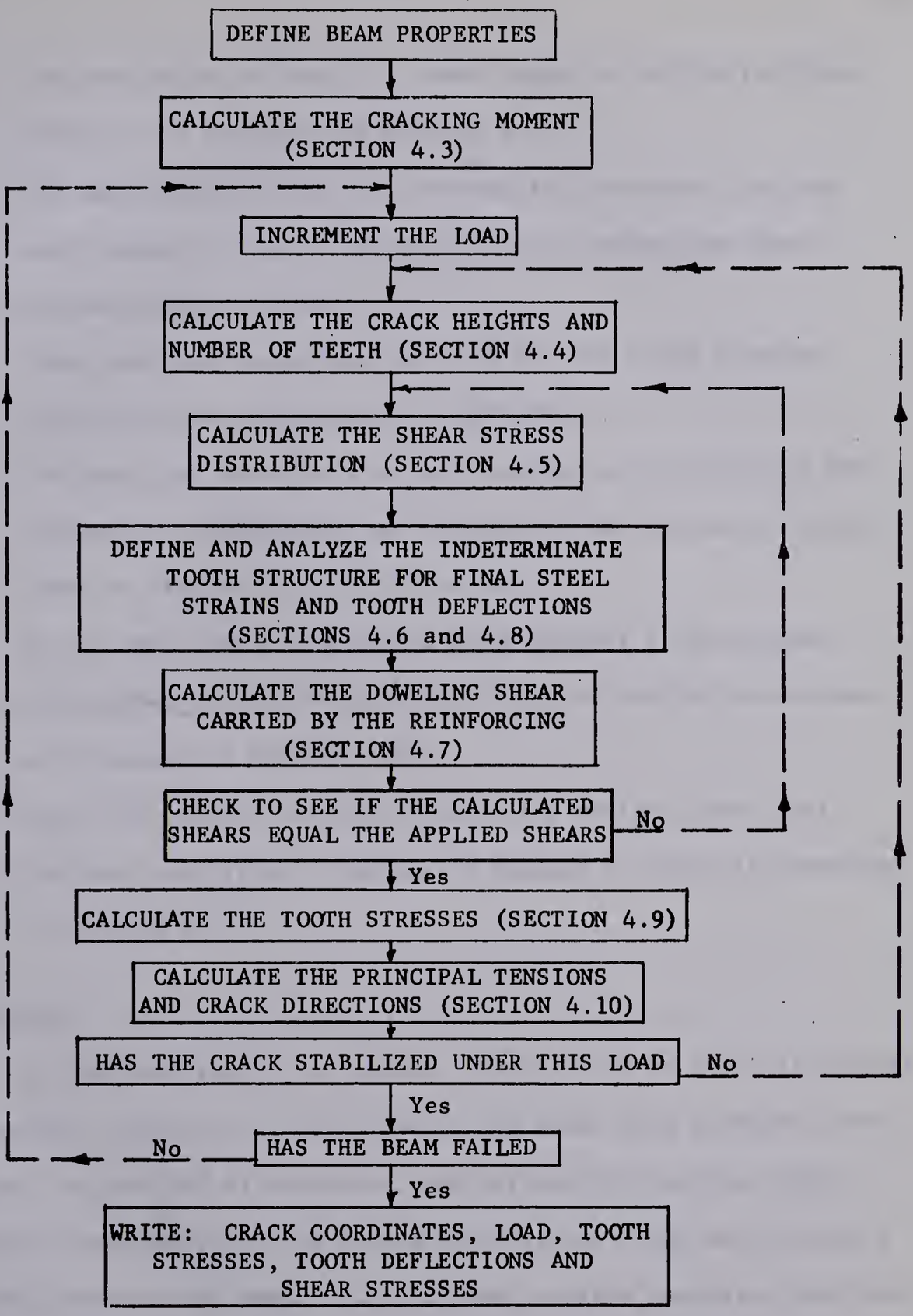

FIGURE 4.2 A BLOCK FLOW DIAGRAM OF THE ANALYSIS

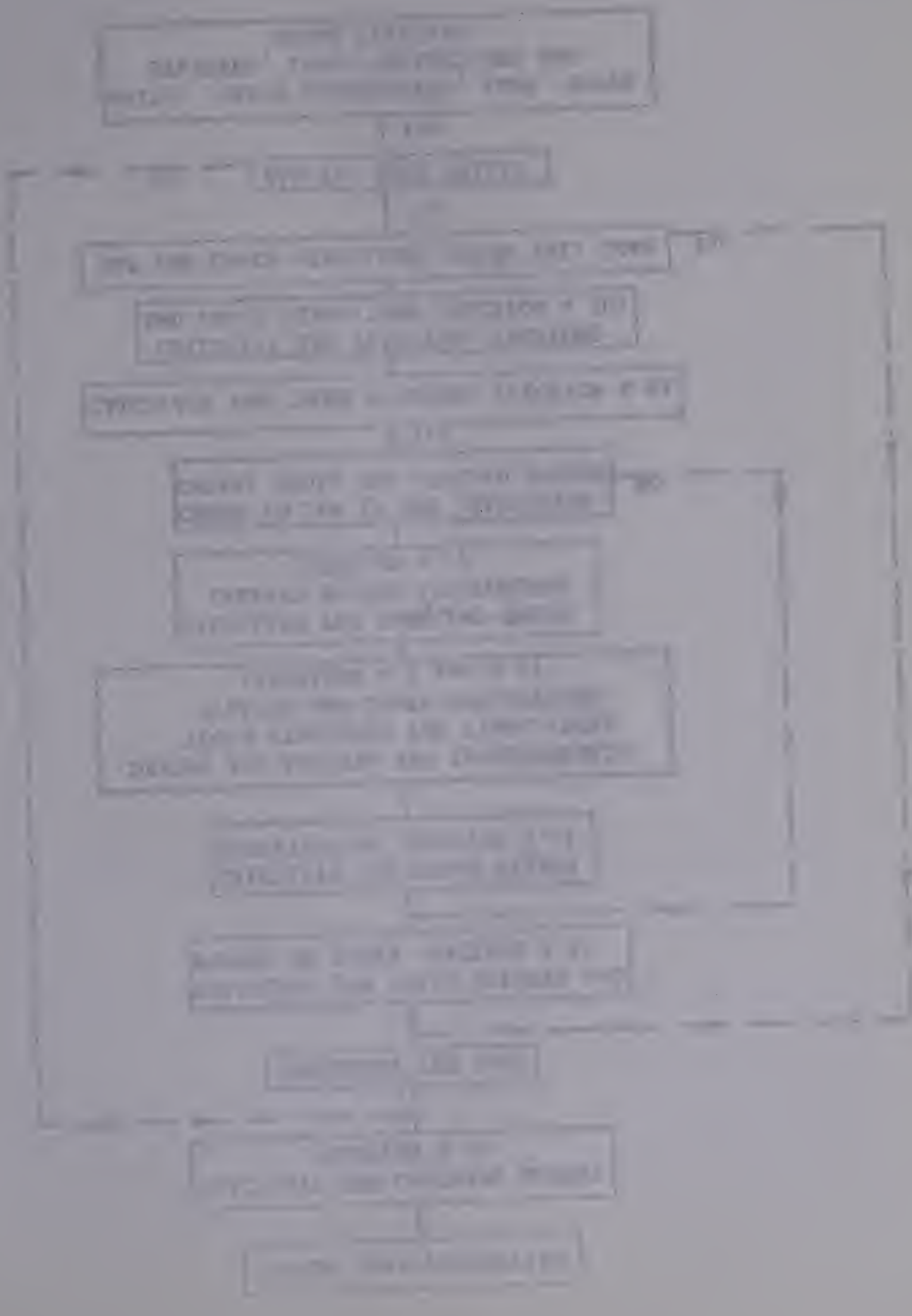

(e) The calculation of doweling shear using the deflection from step (d), as discussed in SECTION 4.7.

(f) The repetition of steps (c) through (e) to ensure that the total shear on a given section does not exceed the shear assumed in the section.

(g) Using the final stresses from step (f) the tooth stresses are calculated as discussed in SECTION 4.9.

(h) The magnitude and direction of the principal stresses on the assumed critical element at the head of the cracks are calculated as discussed in SECTION 4.10.

(i) At the same load a new set of crack heights is calculated using the principal stresses and their calculated directions as discussed in SECTION 4.10.

(j) Steps (b) through (i) are repeated for various loads until failure is achieved. Failure is assumed to occur as described in SECTION 4.11.

4.2 BEHAVIOR

In this analysis it is assumed that all cracks start as flexural tension cracks. Initially, the cracks in the shear span propagate vertically, but, as the load is increased, the effects of the shear force become more predominant and the cracks begin to lean over and propagate toward the center of the beam. It is assumed in this analysis that these cracks are caused by principal tension stresses and propagate in a direction normal to the principal tension stress. Under any given load the crack will propagate until a state of equilibrium is reached with a

stress equal to f_t' at the end of the crack. With increasing loads the cracks extend until a crushing failure occurs in the concrete in the compression zone or until the crack propagates through the beam. These two types of behavior result in what other investigators have called shear-compression failure or a diagonal tension failure.

It has been shown by Kani (1964) as well as other investigators that these types of failure can be expected to occur in beams with shear span to depth ratios (a/d) varying from about 2.5 to 5.0 with pure flexural failures occuring when the shear span exceeds about 5 times the depth of the beam.

In this analysis, the only failure modes that are considered are shear-compression, diagonal tension or pure flexural failures. Other modes of failure such as bond failure, shear tension failure, or a crushing of the end block have not been considered.

4.3 FLEXURAL CRACK HEIGHTS

At a cross-section where the cracking moment is exceeded, a flexural crack will develop and will extend into the beam until the internal stresses equilibrate the applied moment. The flexural crack height was calculated as follows:

(a) A crack height was assumed and the tensile strain at that height was taken as the ultimate strain in tension, ϵ_{tu}.

(b) The compressive strain was varied until the sum of the compression and tension forces on the cross-section was equal to zero.

(c) The resisting moment due to the internal forces was calculated and compared to the actual moment at the section under consideration.

(d) The crack height was then varied until the resisting moment was equal to the actual moment on the section.

The major assumptions involved in this computation were:

(a) The concrete strains were assumed to vary linearly across the depth of the beam. The reinforcement strains were related to the concrete strains by a strain compatibility factor, F.

(b) In the first cycle, the flexural crack was assumed to extend to a point where the strain is equal to ϵ_{tu}. In subsequent cycles the flexural stress at the head of the crack was reduced as described in SECTION 4.10 which discusses the computation of the principal tension stresses.

(c) The properties of the materials were taken as outlined in Chapter III.

A strain compatibility factor, F , was introduced in order to relate the tensile strain in the steel to the strain resulting from a linear strain distribution. The strain in the steel was expressed as $\epsilon_s = F \times \epsilon_{cs}$. The value of F was initially assumed to be 1.0 and later modified to a value obtained by solving for the steel strains in the cracked portion of the beam as an indeterminate structure.

The cracking moment of the cross-section was calculated using a procedure similar to that described above except that the crack height was known to be zero at the start of cracking. The value of cracking moment obtained was then assumed to apply to all sections in the beam. To facilitate the remainder of the calculations, cracks which did not reach the height of the reinforcing were neglected.

4.4 SPACING OF FLEXURAL CRACKS

For the purposes of this investigation the spacing of the cracks was assumed to be two times the distance from the tension face of the beam to the centroid of the tension reinforcing. The first crack was assumed to form directly under the load point. This spacing of cracks is based on work by Broms (1965). The theory presented by Broms predicted a crack spacing for one and one-half times the cover but when he checked this against tests he found that the measured distances were closer to two times the cover. The assumed relationship was checked against photographs of beams and was found to be sufficiently accurate for this investigation.

4.5 SHEAR STRESS DISTRIBUTION

The distribution of shearing stresses assumed in this thesis consisted of a second degree parabola in the uncracked portion of the cross-section and a fourth degree parabola in the cracked portion of the cross-section as shown in FIGURE 4.3.

This distribution shows two notable features. The first is that the maximum shearing stress was assumed to occur at the neutral axis computed from the flexural crack height procedure outlined in SECTION 4.3. The second feature is that there is some shear transferred across the crack and a considerable shear stress at the head of the crack. The latter assumption was justified by consideration of an element at the head of the crack, as shown in FIGURE 4.1. If no shearing stress acted on this element, a Mohr's circle would suggest that the crack would propagate at one of two angles, either horizontal or vertical. However, an inclined crack propagates at an angle that is neither horizontal or vertical and as a result it appears

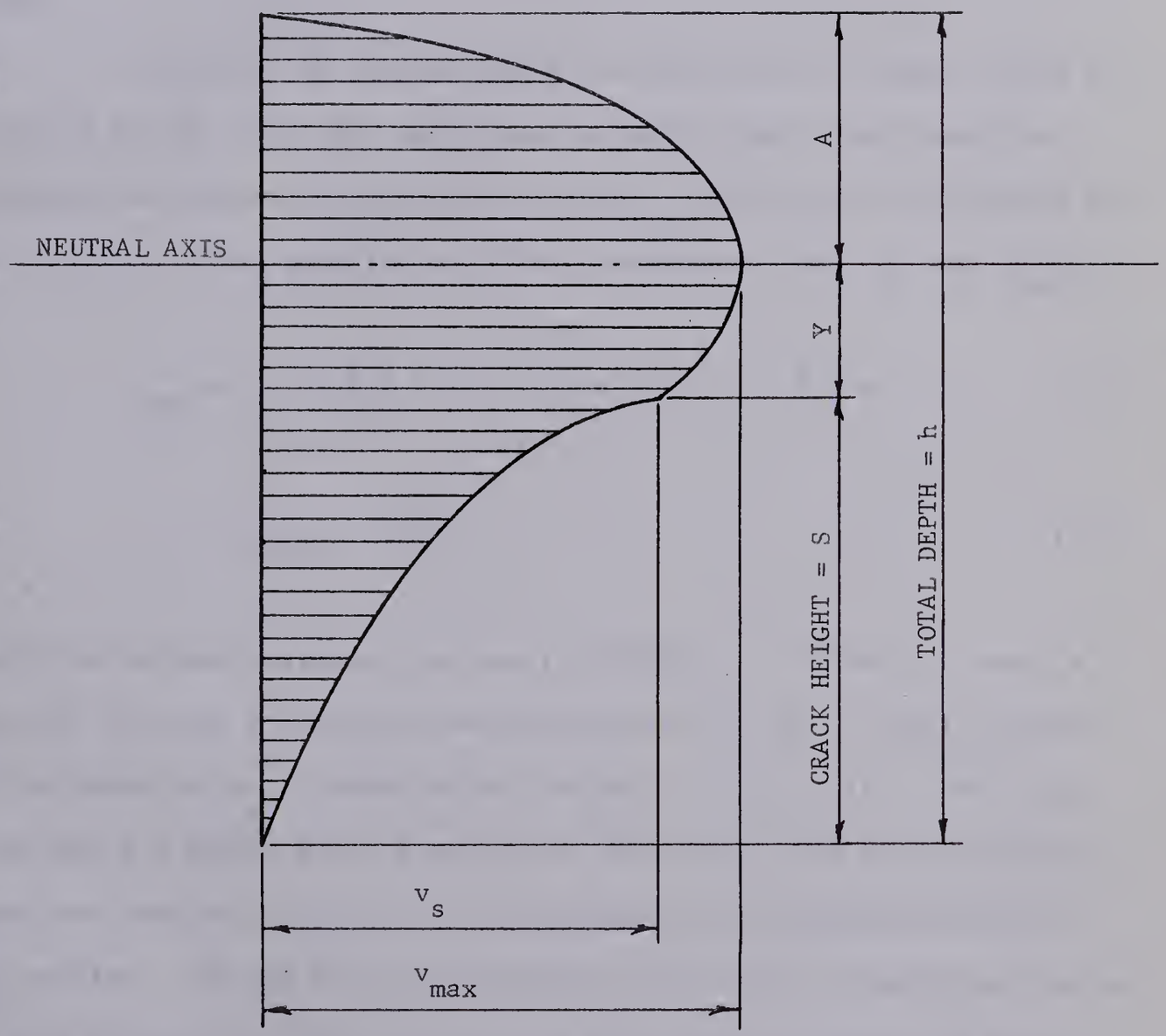

FIGURE 4.3 ASSUMED SHEAR STRESS DISTRIBUTION

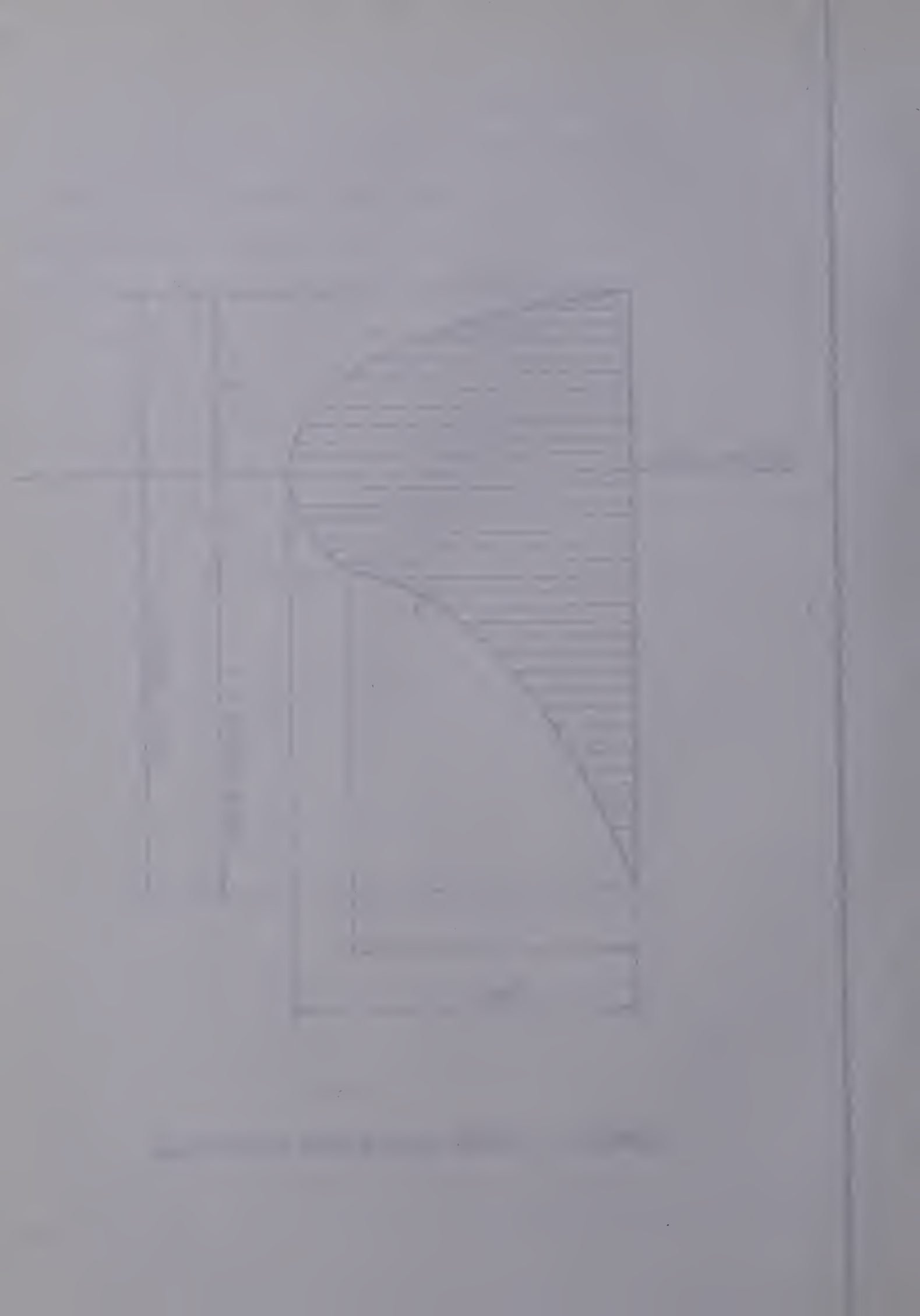

there must be a shear stress present. Such a stress would be transmitted by aggregate interlock or friction between two adjacent teeth as they deflect. The fourth degree parabola was chosen empirically on the assumption that the shear transmission across a crack decreases rapidly as the crack opens.

The values of the maximum shear stress and the shear stress at the head of the crack were determined by making the volume under the assumed distribution of shear stress equal to the total shear carried by the concrete. This gave the following expressions for v_s and v_{max}.

$$v_{max} = V_{conc} / \left[\left(\frac{2}{3} A + Y + \frac{S}{5}\right) + \left(\frac{Y}{A}\right)^2 \left(-\frac{Y}{3} - \frac{S}{5}\right) \right] b \qquad (4.1)$$

$$v_s = v_{max} \left(1 - \frac{Y}{A}\right)^2 \qquad (4.2)$$

where the various terms are defined in FIGURE 4.3. FIGURE 4.4 shows a plot of the shear distribution measured by Van den Berg (1962) compared to the distribution of shear stress assumed in this thesis. The volume under Van den Berg's shear distribution was 115 percent of the applied shear and thus would appear to over-estimate the shearing stresses in the section. Van den Berg extrapolated all his shear distribution curves to pass through zero shear stress at a point one inch above the base of the beam. This was done regardless of whether the beam was cracked or not and has not been explained at any time.

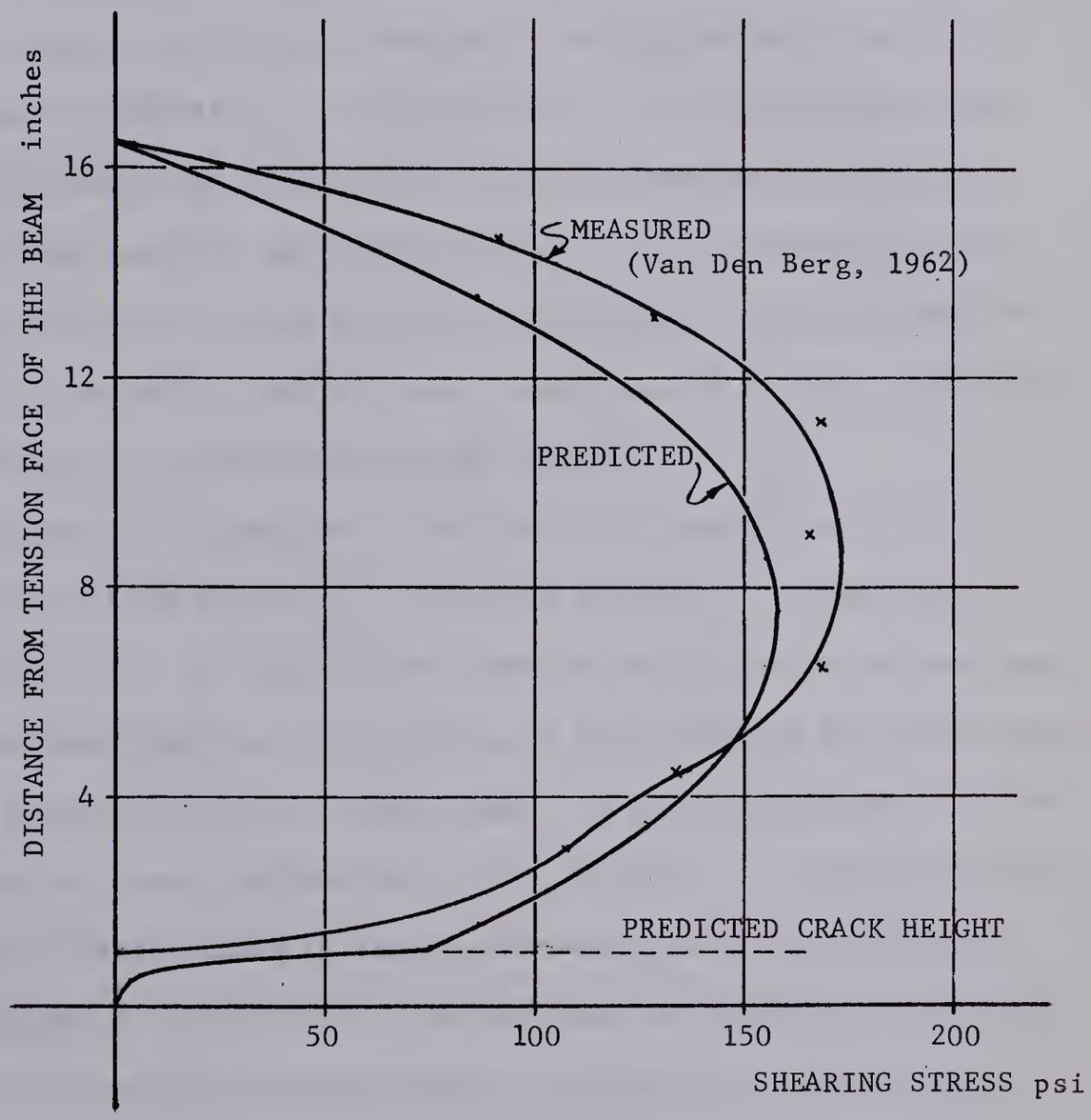

FIGURE 4.4 A COMPARISON OF MEASURED

TO PREDICTED SHEAR STRESS DISTRIBUTION

4.6 TOOTH STIFFNESSES AND DEFLECTIONS

The concrete between cracks in the shear span will be called a tooth because a slender beam will resemble a comb with a number of teeth as the beam reaches its ultimate strength. The forces acting on such a tooth are shown in FIGURE 4.5. The deflection of the tooth under these forces was calculated using an elastic analysis assuming the modulus of elasticity of the concrete was constant at E_{ci}. This assumption is not unreasonable when one realizes that the deflections of the teeth and the strains due to the deflections are small when compared to the strains that occur on vertical cross-sections through the beam.

The vertical dimension of the tooth, S , was chosen as the height of the crack on the side of the tooth farthest from the load, as shown in FIGURE 4.5. To simplify the computations the value of doweling shear and concrete shearing stress acting on both sides of the tooth were taken to be those values at the crack where the crack height was defined.

The horizontal deflections of the tooth due to the shear force and differing tensile forces in the reinforcement were then calculated using the method of virtual work. The stiffness of the tooth in the horizontal direction was also computed using the method of virtual work considering the effects of both flexural and shearing deflections. The vertical deflections of the sides of the tooth at the height of the steel (Points A & B) were evaluated in a similar manner.

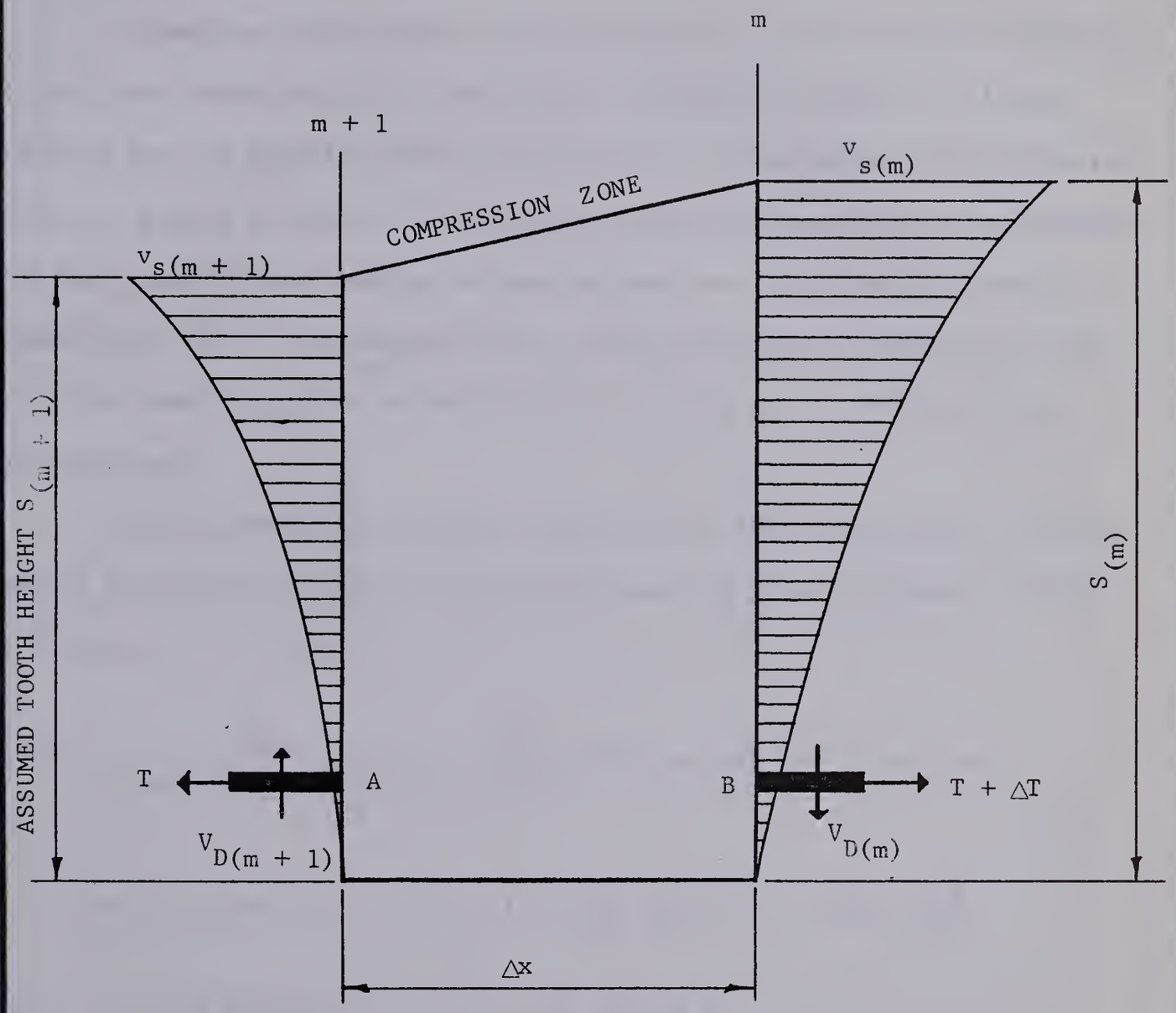

FIGURE 4.5 TOOTH FORCES

4.7 DOWEL SHEAR

Doweling shear forces are introduced as a result of the deflections of one tooth relative to the next tooth as shown in FIGURE 4.6. An expression for the doweling shear was obtained by considering the reinforcing to act as a beam on elastic foundation. Using this approach it was assumed that the concrete surrounding the bar between the cracks was the elastic foundation. The forces acting on the reinforcing bar are shown in FIGURE 4.6. For simplicity, the effect of axial tension on the dowling forces was neglected.

The relationship between deflection of the reinforcement and the moments and shears acting on the reinforcement is given by Hetenyi (1946) as follows:

$$\Delta V = \frac{\lambda}{K_f(\sinh^2\lambda\Delta x - \sin^2\lambda\Delta x)} \Big[2V_D(\sinh\lambda\Delta x(\cosh\lambda\Delta x + \cos\lambda\Delta x) - \sin\lambda\Delta x\,(\cos\lambda\Delta x + \cosh\lambda\Delta x) - 2M_{VD}\,(\sinh\lambda\Delta x + \sin\lambda\Delta x)^2 \Big] \tag{4.3}$$

where $\lambda = 4\,Q_f d/4\,E_s I_{bar}$ $\qquad K_f = \lambda 4\,E_s I_{bar}$

and Q_f = a foundation modulus.

In order to simplify the above expression it was assumed that the flexural cracks had a width of 0.01 inches or less and the moment in the dowel at the face of the concrete was set at the maximum expected value of:

$$M_{VD} = 0.005\ V_D \tag{4.4}$$

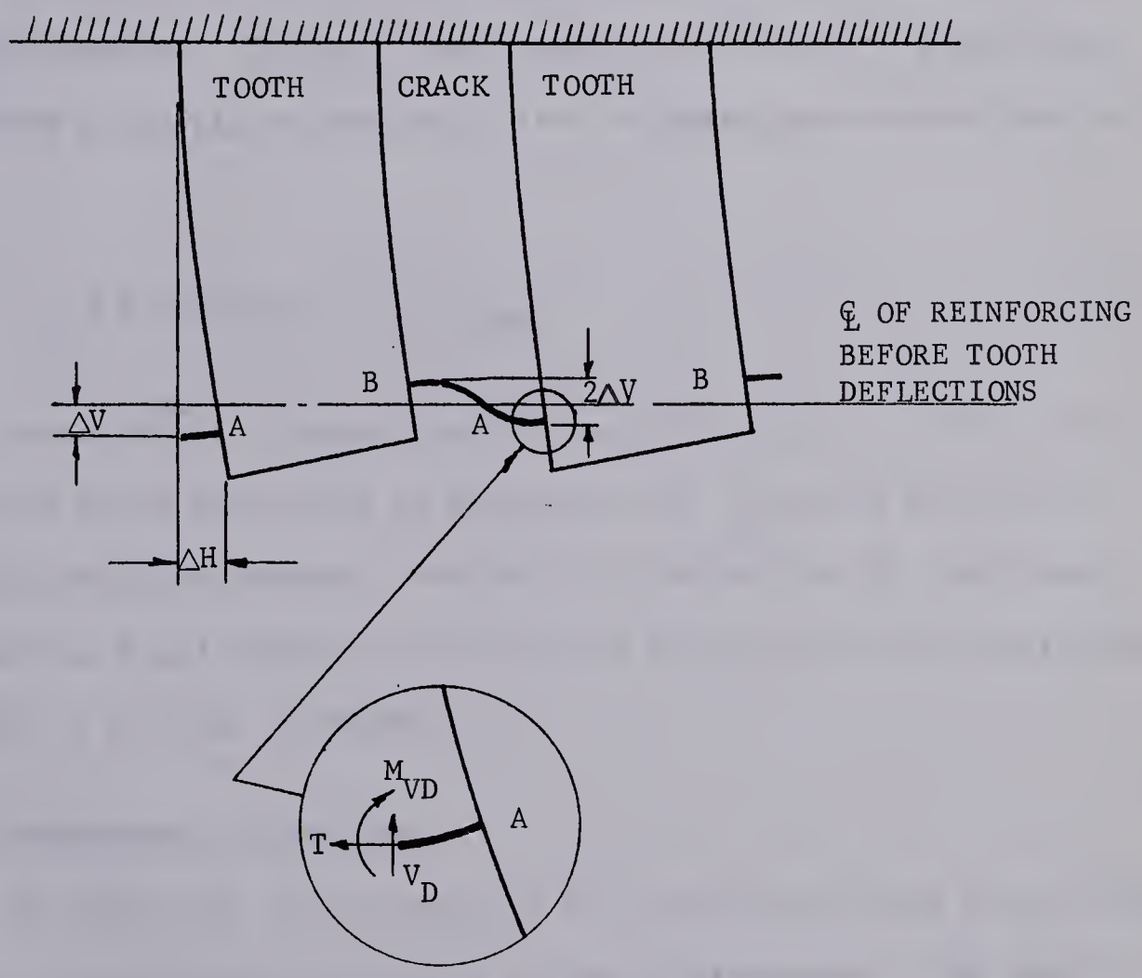

FIGURE 4.6 DOWELING SHEAR

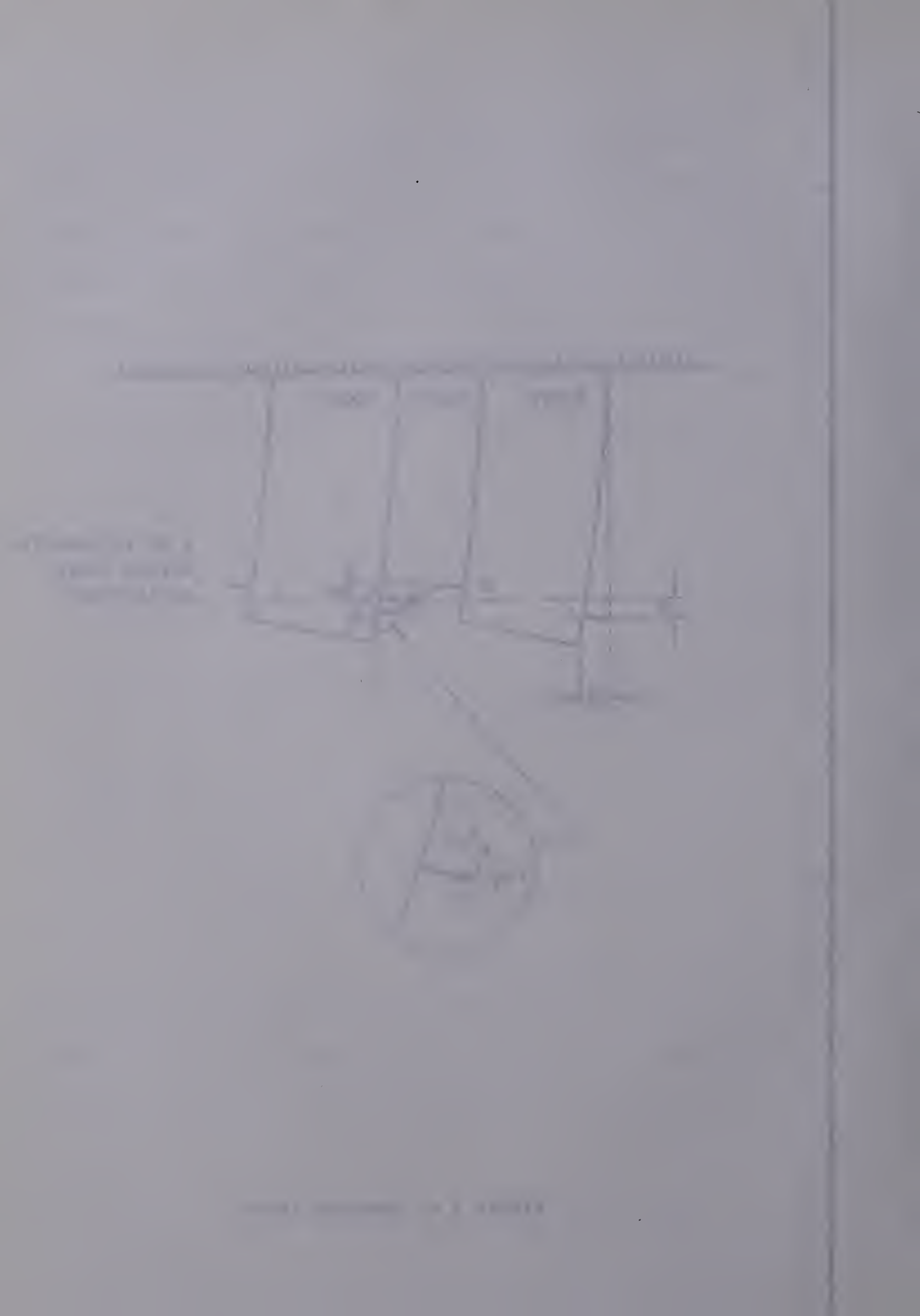

This assumption led to little error since the effect of moment was small compared to the shear.

A number of investigations have proposed values for the foundation modulus, Q, ranging from 0.92×10^6 psi to 2.56×10^6 psi depending on the type of test and analysis. The value used in this thesis was 1.5×10^6 psi selected by A.C.I. COMMITTEE 325 (1956) for steel bars embedded in concrete. For bar sizes ranging from #5 to #9 it was found that EQUATION 4.3 could be reduced to the following approximate relationship:

$$\Delta V = 1.90\ V_D / \lambda^3\ 4\ E_s I_{bar} \qquad (4.5)$$

The constant 1.90 was found to vary from 1.83 to 1.98. By rearranging the above expression an expression for V_D can be written in terms of the other parameters. The vertical deflection ΔV, was taken as one half the total relative deflection of two adjacent teeth calculated in SECTION 4.6 as shown in FIGURE 4.6.

4.8 THE INDETERMINATE STRUCTURE

At this point in the analysis all the forces acting on the tooth have been estimated except the force in the reinforcement. The steel strains, ϵ_{s1}, have been computed assuming that plane sections remain plane. However, it has also been assumed that the teeth will deflect under the various forces acting on them, resulting in an additional steel strain, ϵ_{s2}. The indeterminate structure shown in FIGURE 4.7 was solved to determine the additional steel strain due to the tooth deflections.

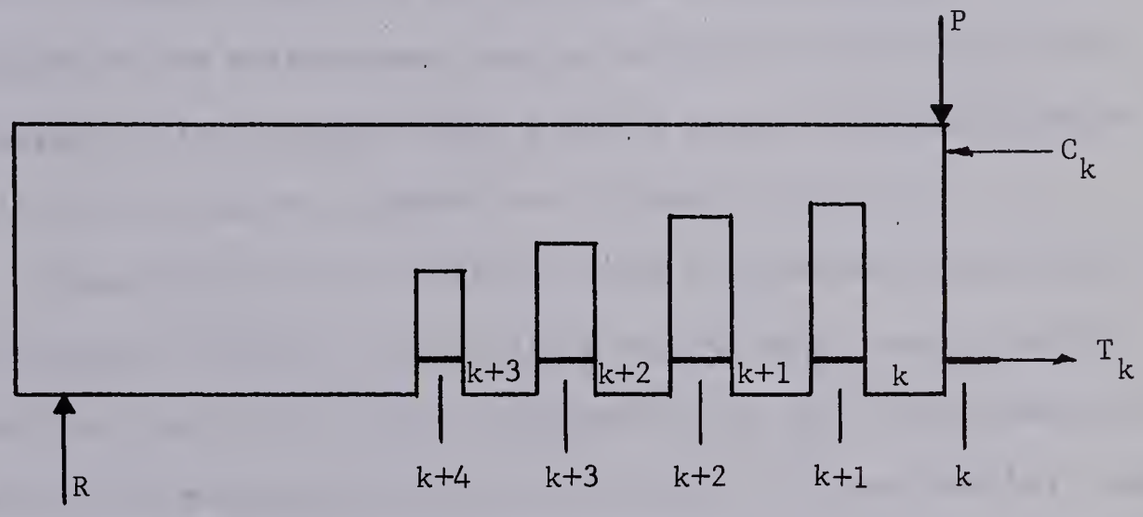

FIGURE 4.7 THE INDETERMINATE TOOTH STRUCTURE

The indeterminate structure consisted of a number of teeth joined by sections of reinforcement. The lateral stiffness of the teeth was defined in terms of the deflection equations described in SECTION 4.6. In order to define the stiffness of the reinforcement it was necessary to define the effective unbonded length of the bar connecting the teeth. The effective length of the reinforcement may be defined as that length which when multiplied by the average strain give the same elongation as would be found if the strains were summed over a length of bar Δx .

A knowledge of how the steel strains vary between two adjacent cracks is necessary before the effective unbonded length can be defined. It is known that there is a strain concentration in the reinforcing at a crack and that for deformed bars the steel strains are approximately equal to the strain in the surrounding concrete at some distance from a crack. University of Illinois Bulletin 479 (1965) presents several theoretical distributions of steel and concrete strains between two adjacent flexural cracks. The most common forms of distribution presented are linear, parabolic and sinusoidal. In this analysis the strain in the bar is assumed to vary parabolically from a maximum at the crack to a minimum at the center of the tooth and the strain in the concrete is assumed to vary parabolically from a minimum at the crack to a maximum at the center of the tooth as shown in FIGURE 4.8. If the parabolas are assumed to be of the second degree then the effective length of the bar can be calculated to be $\Delta x/3$. In future investigations, it may be desirable to make the effective length a function of the level of stress in the bar and to check the deformations in a region of pure flexure.

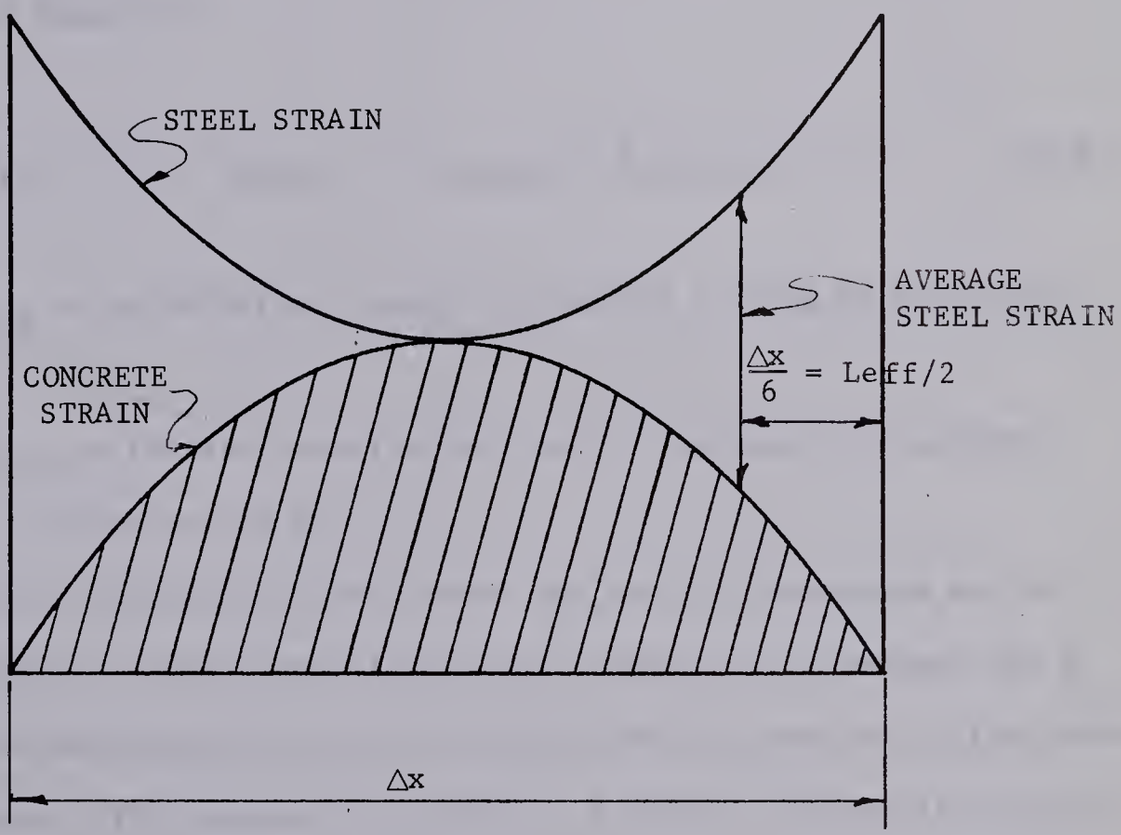

FIGURE 4.8 ASSUMED CONCRETE AND STEEL

STRAIN DISTRIBUTIONS ACROSS A TOOTH

In order to derive the simultaneous equations used to solve the indeterminate structure the following approach was used. The horizontal deflection of the k tooth was assumed to be the summation of the portion of the steel strains resulting from the tooth deflections multiplied by the effective length of the bars. This approach resulted in the following equation:

$$\Delta H_{(k)} = L_{eff} \left(\epsilon_{s2(k+1)} + \epsilon_{s2(k+2)} + \epsilon_{s2(k+3)} \text{-----}\right) \qquad (4.6)$$

where: L_{eff} = the effective length of the bars joining equally spaced teeth

$\epsilon_{s2(k)}$ = the additional strain due to the tooth deflections; to be solved for

The horizontal deflection of the k tooth can also be considered as the flexibility of tooth k times the difference in total strain between the k and the k+1 cross-section plus the horizontal deflections due to the shear transfer forces. This approach resulted in a second equation as follows:

$$\Delta H_{(k)} = K_{T(k)} \left[\left(\epsilon_{s1(k)} + \epsilon_{s2(k)}\right) - \left(\epsilon_{s1(k+1)} + \epsilon_{s2(k+1)}\right) \right] + \Delta Hs_k \qquad (4.7)$$

where: $\Delta Hs_{(k)}$ = the horizontal deflection of tooth k due to the shear transfer forces

$K_{T(k)}$ = the flexibility of tooth k

$\epsilon_{s1(k)}$ = the strain at section k assuming plane sections remain plane

By equating EQUATIONS 4.6 and 4.7 the following equation can be written:

$$- \epsilon_{s2(k)} K_{T(k)} + \epsilon_{s2(k+1)} (L_{eff} + K_{T(k)}) + \epsilon_{s2(k+2)} L_{eff} - - - -$$

$$= (\epsilon_{s1(k)} - \epsilon_{s1(k+1)}) K_{T(k)} - \Delta Hs_{(k)} \qquad (4.8)$$

EQUATION 4.8 can be written for each crack location in the structure. In order to solve the resulting set of equations it was assumed that there was no additional strain in the steel at the crack directly under the load, i.e. $\epsilon_{s2(1)} = 0$. These equations can then be solved for the strains, ϵ_{s2}, and by adding these to the corresponding strains ϵ_{s1} the total steel strain at each section can be found.

The strain compatibility factor, F, can now be defined as the total strain in the steel divided by the strain resulting from the flexural crack height computations assuming a linear strain distribution. The flexural crack height computations can then be repeated as can all the previous calculations with each cycle varying the F factor slightly until there is no significant change. A value of F larger than 1.0 will result if the teeth deflect toward the load point. As the value of F increases the crack height will decrease as discussed in CHAPTER 6.

4.9 TOOTH STRESSES

When the total steel strains computed in SECTION 4.8 and the shearing stresses computed in SECTIONS 4.5 and 4.7 are known it is possible

to compute the flexural stresses in the tooth shown in FIGURE 4.5. The only stress which has any significance in this analysis is the tensile stress at the base of the tooth. This stress was calculated using standard beam theory and assuming the modulus of elasticity of the concrete to be constant and equal to E_{ci}. The errors due to using this value of the modulus of elasticity are normally small since the deflections of the tooth are small. This computation ignores any "deep beam" action in the tooth. The errors due to this simplification are discussed by Lorentsen (1965).

4.10 COMPUTATION OF PRINCIPAL TENSIONS

To compute the magnitude and direction of the principal tensions the critical element shown in FIGURE 4.1 must be examined. Since this analysis assumes that a crack occurs if the tensile stress exceeds f'_t then the flexural stress in the longitudinal direction must be less than f'_t. The following stresses are assumed to act on this element: a tension stress in the vertical direction equal to the tooth stress as calculated in SECTION 4.9, a shearing stress equal to v_s, as calculated in SECTION 4.5 and a principal tension stress equal to f'_t at an angle to the horizontal. The reduced flexural tension in the horizontal direction and the direction at which the crack will propagate can then be calculated using a Mohr's circle as shown in FIGURE 4.9.

The flexural crack height computation can then be repeated for the reduced flexural tensile stress with the crack now propagating at an angle as calculated above. The remainder of the calculations are repeated

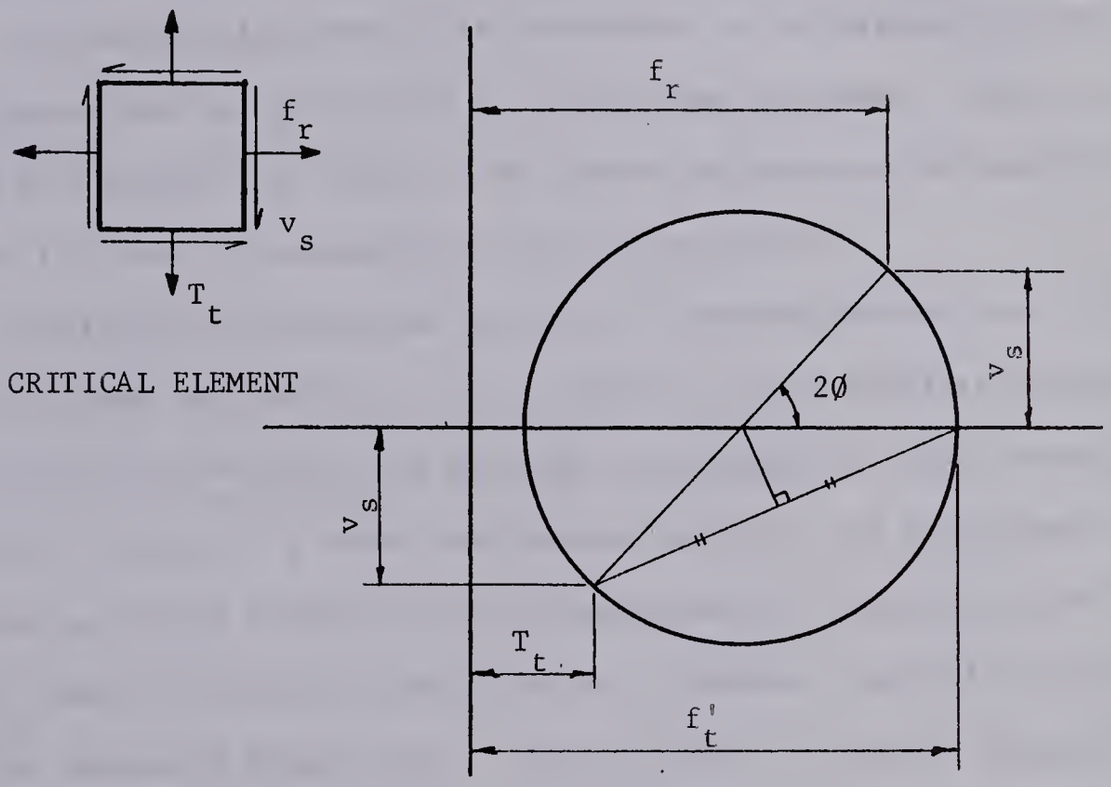

FIGURE 4.9 MOHR'S CIRCLE CALCULATION

FOR THE REDUCED FLEXURAL TENSION STRESS

until there is a negligible increase in the crack height at a given load. The coordinates of the end of the crack are assumed to represent those in the actual beam.

4.11 FAILURE MODES

The calculations and cycles described in the preceeding parts of this chapter are carried out at one given load increment. When, as described in SECTION 4.10, there is no longer any appreciable growth of the crack, the load is incremented until failure occurs.

Failure of the beam was detected in three different ways. If after an increase in load the concrete could no longer mobilize enough force to resist the tension, the concrete was assumed to crush, resulting in a failure similar to a shear compression failure. The second mode of failure was caused by yielding of the reinforcement. Yielding of the reinforcement results in infinite rotations at a constant load and thus the analysis as presented breaks down. The third mode of failure occurred as the result of the crack height being incremented up until the tension and compression forces could not be balanced on a given cross-section. This third type of failure is the result of too coarse an increment in crack height. If one examines moment versus crack height curves such as given by Morrison (1965) or in FIGURE 4.10 it can be seen that near the ultimate load a very small increase in crack height can result in a very large increase in the bending moment. If the crack height is incremented above the maximum possible crack height for the load under consideration an unstable condition will occur in that the forces on the cross-section can not be balanced. When this type of failure appeared to occur the crack height

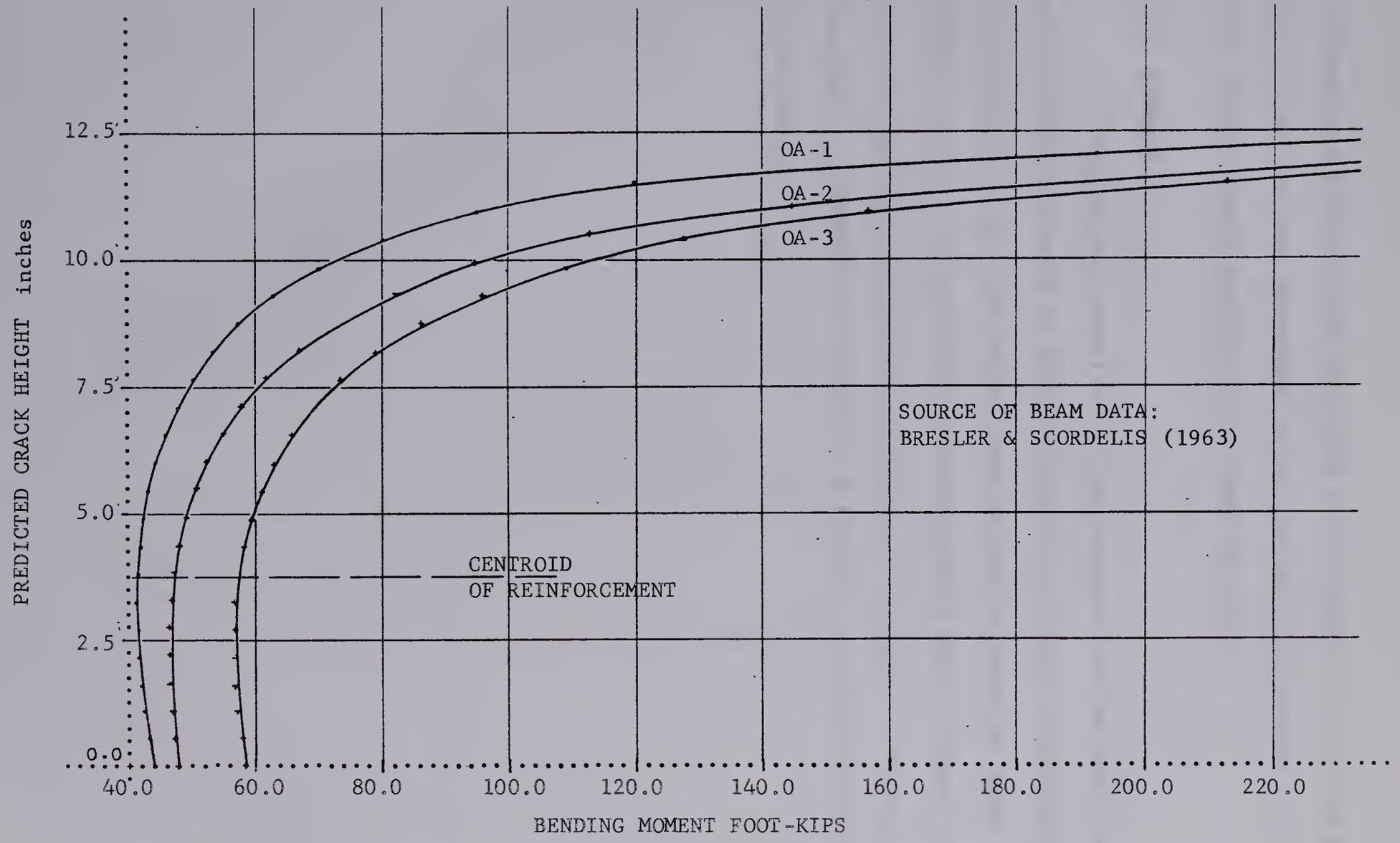

FIGURE 4.10 TYPICAL BENDING MOMENT VERSUS PREDICTED CRACK HEIGHT RELATIONSHIPS

increment was progressively decreased in an attempt to bring the beam to equilibrium. If this procedure failed, the beam was assumed to be close to an unstable state and was said to have failed.

4.12 SUMMARY

The analysis described in this chapter involves many iterations at one load to converge on final values of the strain compatibility factor, F, the crack height, the crack direction and the doweling shear values. FIGURE 4.2 will help the reader understand where most of these cycles occur and the order in which the calculations are made. The more complete flow chart in APPENDIX A shows some of the more intricate steps involved in the analysis.

CHAPTER V

COMPARISON OF ANALYSIS TO TEST RESULTS

5.1 INTRODUCTION

The analysis presented in CHAPTER IV was applied to 10 beams of varying shear span to depth ratios, concrete strengths and steel yield strengths. The crack patterns in the shear span obtained from the analysis are presented and where possible are compared to those patterns actually obtained from tests. The measured and computed shear failure loads are compared.

5.2 RESULTS OF THE ANALYSIS

The properties of the beams which were analyzed are presented in TABLE 5.1. The numbering of the beams is identical to that used in the references from which the data was taken. The concrete strengths in the beams considered varied from about 2500 psi to about 5500 psi and the steel yield strength varied from about 55,000 psi to about 105,000 psi. The reinforcement ratios ranged from a high of 0.0338 to a low of 0.0041.

The results of the analysis are presented in TABLE 5.2. The most important values are P_{cr} , the observed inclined cracking load; P_u , the observed ultimate load; P_{code} , the load value obtained by using the ACI Code expression $v_c = 1.9 \sqrt{f'_c} + 2500 \frac{pVd}{M}$; and P_w , the load predicted by the analysis in CHAPTER IV. The results of the analysis agree quite well with test results but in all cases the predicted ulti-

TABLE 5.1

PHYSICAL PROPERTIES OF THE BEAMS ANALYZED IN THIS THESIS

Beam	Source	d	b	p	h	f'_c	f_y	E_s	Reinf.	a	a/d
		in.	in.	%	in.	psi	psi	ksi		in.	
XOB-1	Bresler & Scordelis 1964	18.03	9.1	2.44	21.8	3660	96,500	27,900	4 - #9	72	3.99
OA-2	Bresler & Scordelis 1963	18.35	12.0	2.27	22.1	3440	80,500	31,600	5 - #9	90	4.90
OC-1	Bresler & Scordelis 1964	18.05	6.1	1.82	21.8	3920	96,500	27,900	2 - #9	72	3.98
11A-2	Krefeld & Thurston 1962	12.36	6.0	3.41	15.0	4380	57,000	29,200	2 - #10	36	2.91
12A-2	Krefeld & Thurston 1962	9.36	6.0	4.50	12.0	4360	57,000	29,200	2 - #10	36	3.84
4CC	Krefeld & Thurston 1962	10.00	6.0	2.63	12.0	2480	57,100	27,900	2 - #8	60	6.00
C	Krefeld & Thurston 1962	19.00	8.0	1.56	21.0	2430	57,100	27,900	3 - #8	60	3.16
OCa	Krefeld & Thurston 1962	17.94	10.0	2.22	20.0	5550	53,700	29,000	4 - #9	72	4.02
VIb 23	Mathey & Watstein 1963	15.86	8.0	0.84	18.0	4430	102,500	27,500	2 - #5 1 - #6	45	2.84
VIa 24	Mathey & Watstein 1963	15.86	8.0	0.47	18.0	3820	100,900	27,400	3 - #4	60	3.78

mate load is less than the observed ultimate load. In most cases the observed diagonal cracking load was very close to the ultimate load predicted in this thesis.

As shown in TABLE 5.2 the ratio of the observed diagonal cracking load to the inclined cracking load predicted by the A.C.I. 1963 Building Code ranged from 0.89 to 2.72 with a mean value of 1.53. The ratio of the observed ultimate load to the ultimate load obtained from the analysis presented in this thesis ranged from 1.09 to 1.58 with a mean value of 1.25.

FIGURES 5.1 to 5.3 compare the actual crack patterns reported by Bresler and Scordelis (1963, 1964) to the predicted crack pattern. While the crack heights toward the center of the span agree closely with the tests, the characteristic diagonal cracks which occurred in these beams during the tests were not predicted by the analysis. For purposes of comparison the loads at which the crack propagated to a given height are shown. All computed points on the theoretical crack paths are not shown as this would result in confusion. The crack spacing used in analyzing these beams was taken as the average spacing observed in the tests so that closer agrument between actual and theoretical crack patterns could be achieved.

FIGURES 5.4 to 5.6 show the predicted crack patterns for the remaining seven beams. The cracks at which failure was predicted are marked with arrows at the ends. It can be seen that while no one crack always caused failure, there were more failures at the first crack from the load point than the others. A reason for this may be that at an

TABLE 5.2

RESULTS OF THE ANALYSIS

Beam	p	d	f'_c	a/d	P_{cr}	P_u	P_{code}	P_w	$\frac{P_{cr}}{P_{code}}$	$\frac{P_u}{P_w}$	Observed Failure Mode[2]	Predicted Failure Mode[1]	Predicted Critical Crack
	%	in.	psi		kips	kips	kips	kips					
XOB-1	2.44	18.03	3660	3.99	45	57.5	42.6	45	1.06	1.28	DT	CR	2
OA-2	2.27	18.35	3440	4.90	65	80	55.2	60	1.18	1.33	DT	US	2
OC-1	1.82	18.05	3920	3.98	25	34.9	28.6	28	0.89	1.25	DT	CR	4
11A-2	3.41	12.36	4380	2.91	30	33	23.1	28	1.48	1.18	DT	CR	3
12A-2	4.50	9.36	4360	3.84	25	28.8	17.4	24	1.44	1.20	DT	CR	2
4CC	2.63	10.00	2480	6.00	15.8	15.8	5.8	10	2.72	1.58	DT	CR	2
C	1.56	19.00	2430	3.16	38	38.0	14.9	32	2.55	1.19	DT	CR	10
OCa	2.22	17.94	5550	4.02	62	66	55.7	55	1.11	1.20	DT	Y	4
VIb 23	0.84	15.86	4430	2.84	27	33.7	17.5	31	1.54	1.09	DT	Y	3
VIa 24	0.47	15.86	3820	3.78	21	24.5	15.4	30	1.36	1.22	DT	US	2
								Mean	1.53	1.25			

Note: 1. Predicted Modes of Failure (SECTION 4.11)
CR - Crushing of the concrete above the critical crack
Y - Yielding of the steel at the critical crack
US - Unstable condition occurs at an increase in load

2. Observed Mode of Failure
All beams failed following the formation of a large diagonal crack extending from the bottom of the beam to close to the top.

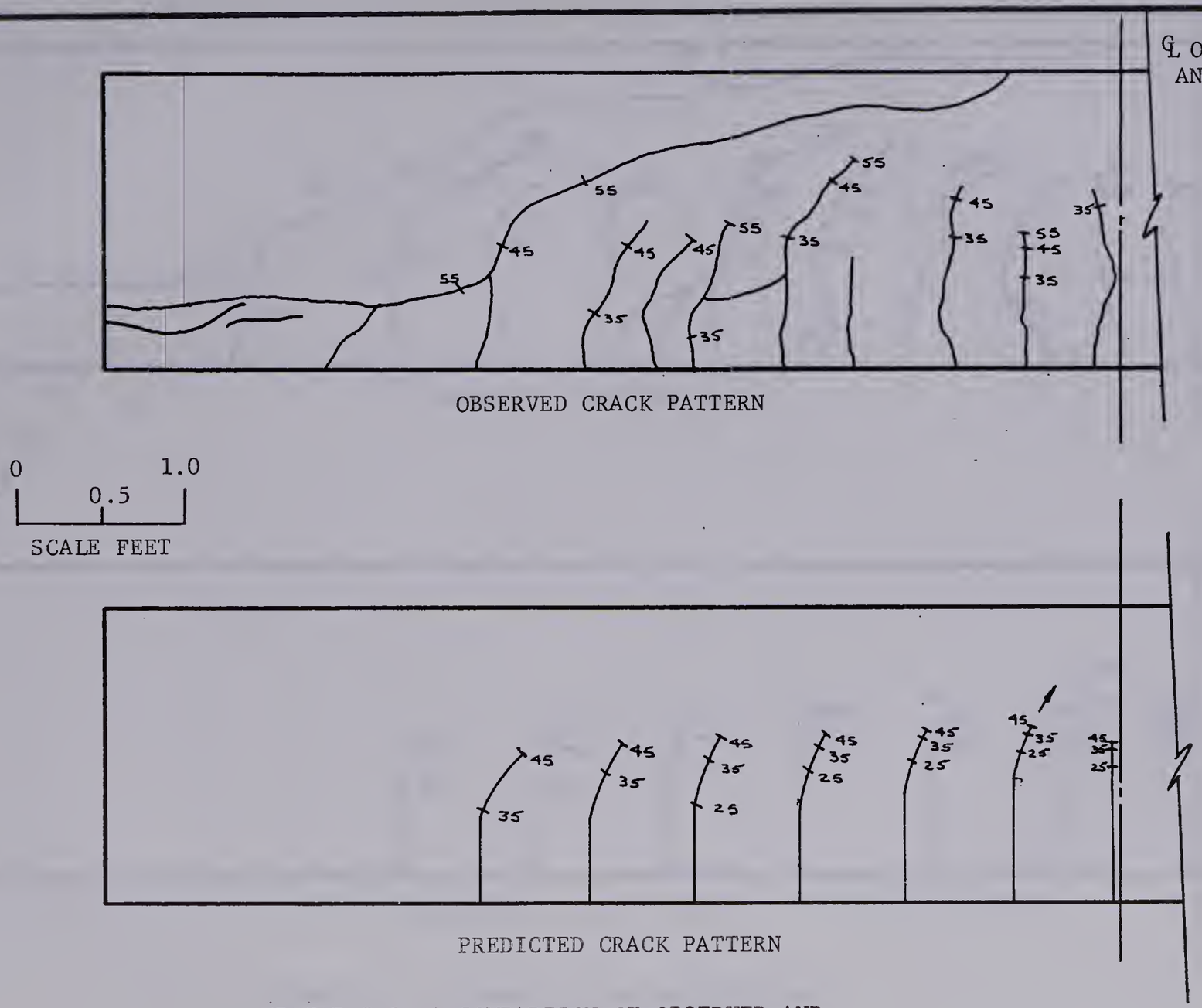

FIGURE 5.1 A COMPARISON OF OBSERVED AND PREDICTED CRACK PATTERNS FOR BEAM XOB-1

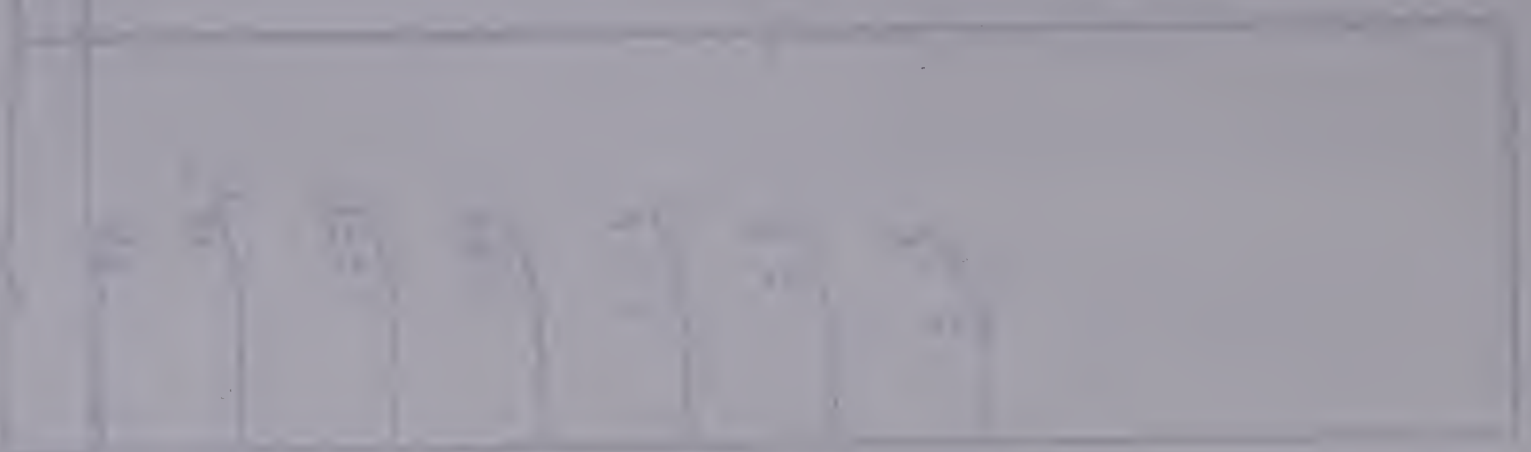

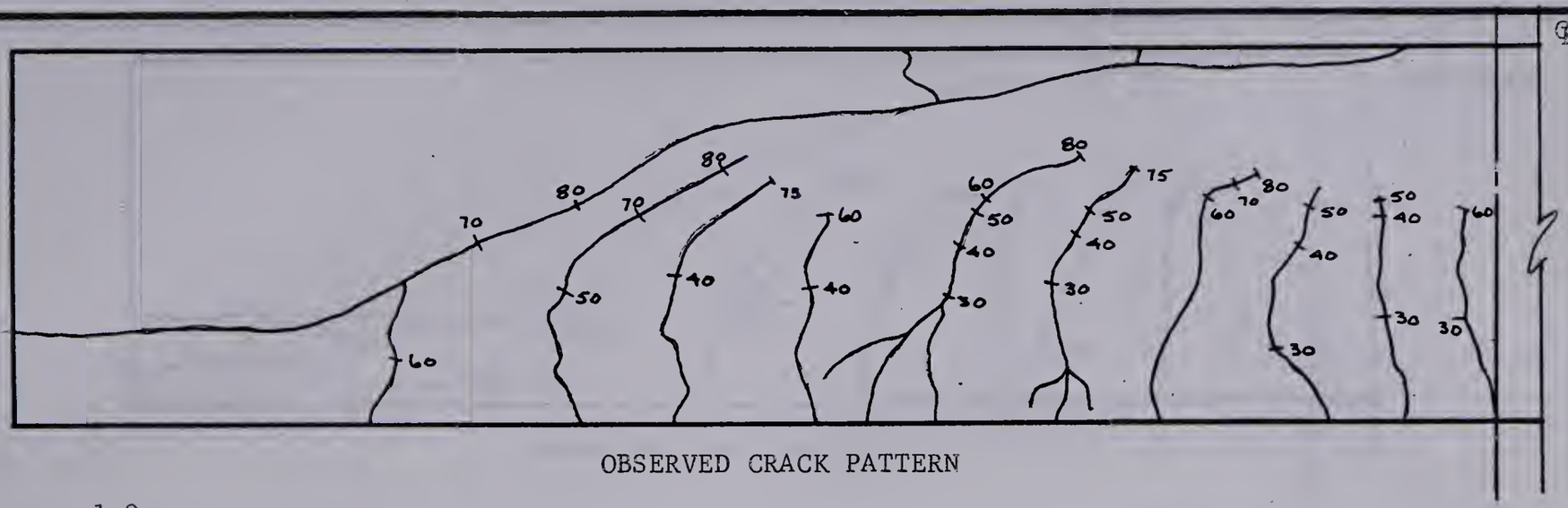

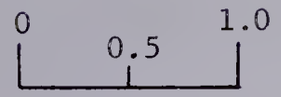

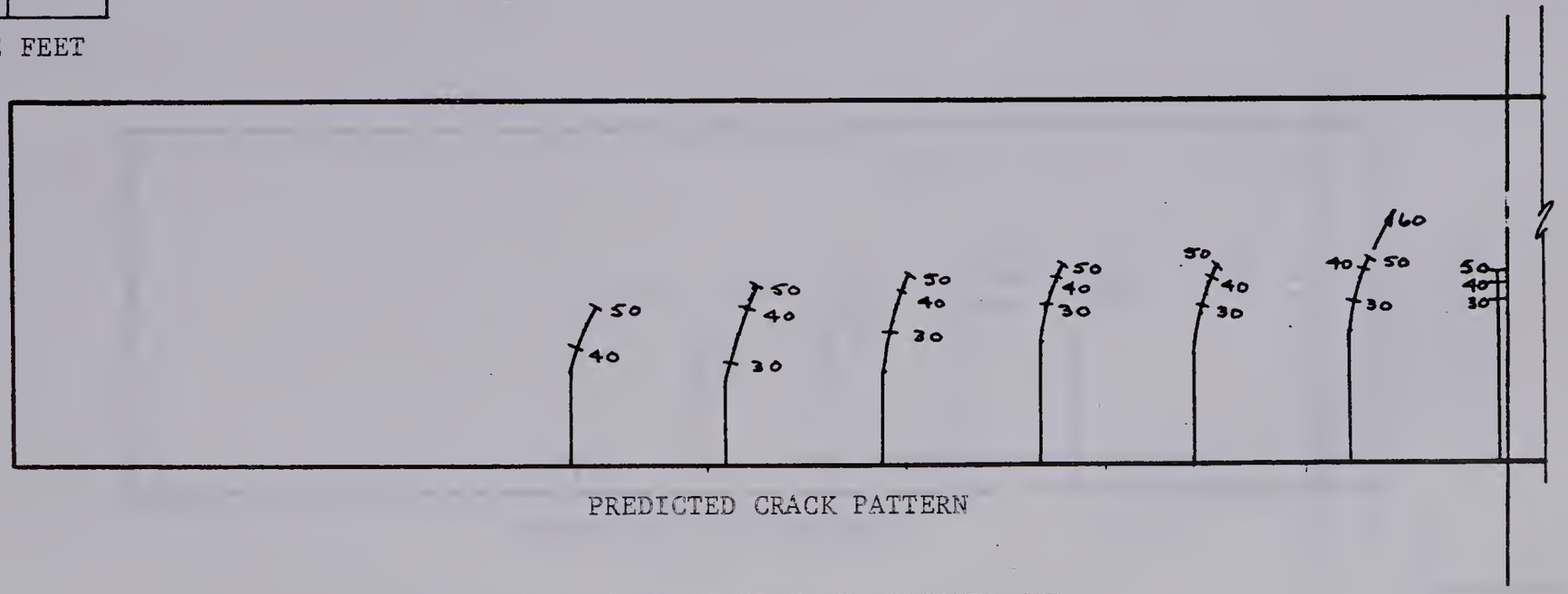

FIGURE 5.2 A COMPARISON OF OBSERVED AND PREDICTED CRACK PATTERNS FOR BEAM OA-2

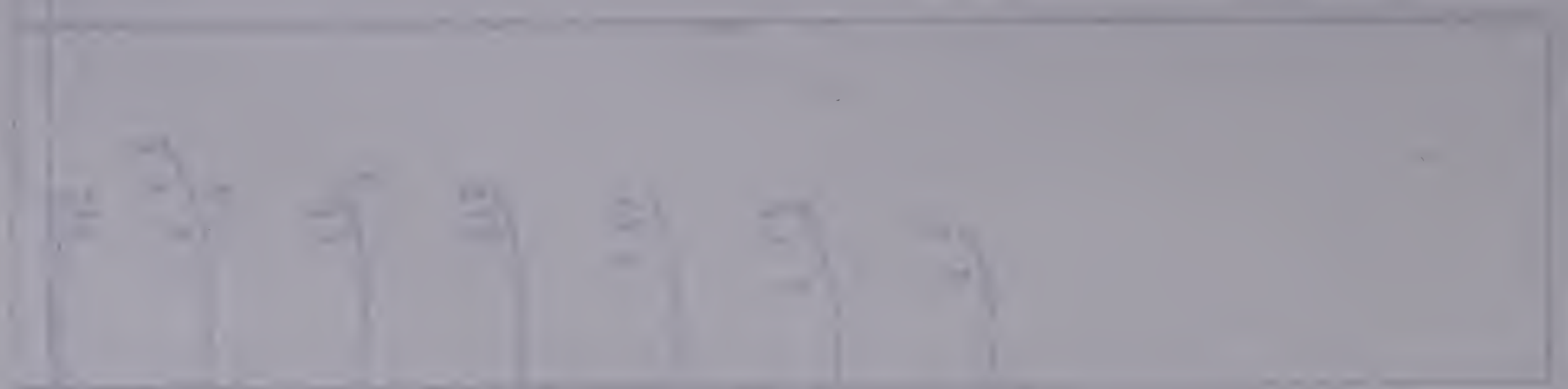

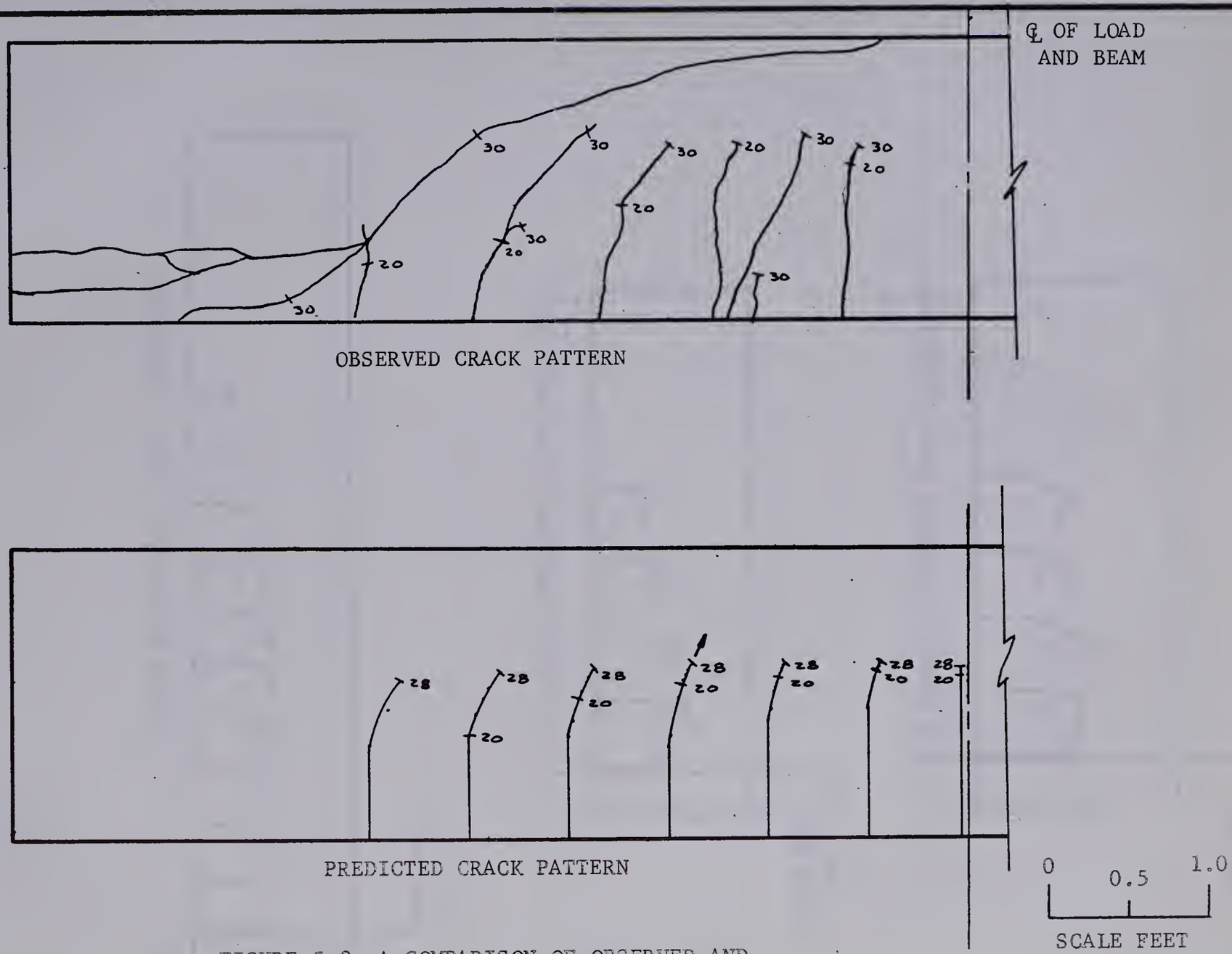

OBSERVED CRACK PATTERN

PREDICTED CRACK PATTERN

FIGURE 5.3 A COMPARISON OF OBSERVED AND PREDICTED CRACK PATTERNS FOR BEAM OC-1

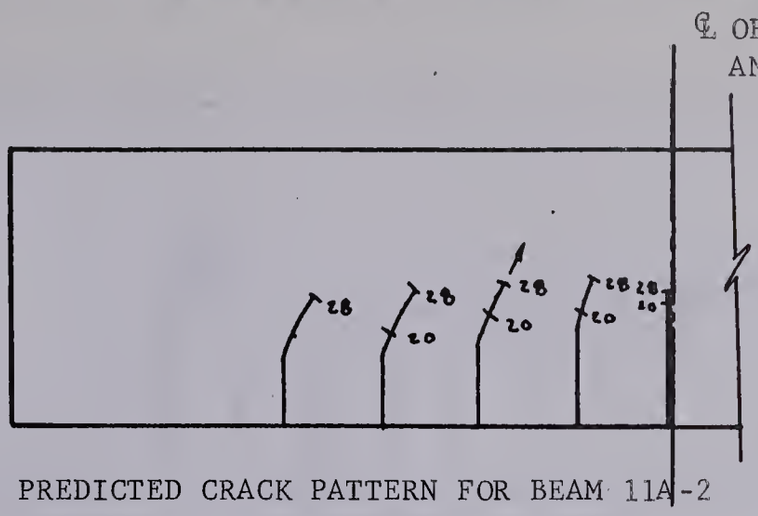

PREDICTED CRACK PATTERN FOR BEAM 11A-2

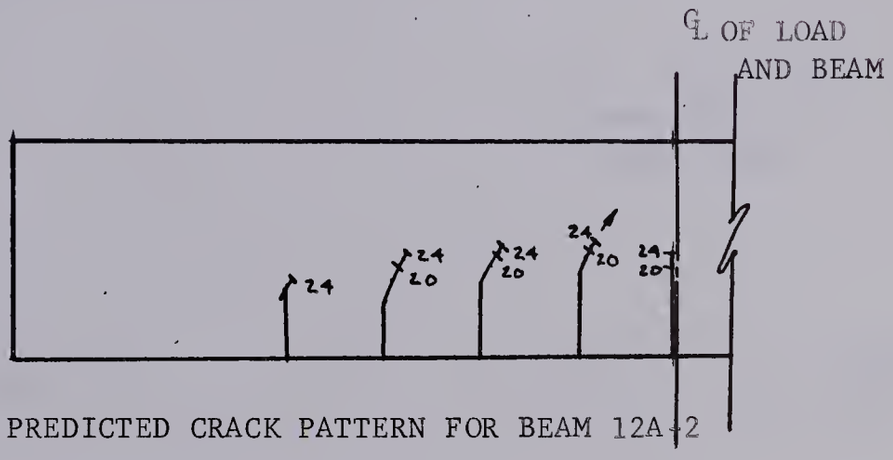

PREDICTED CRACK PATTERN FOR BEAM 12A-2

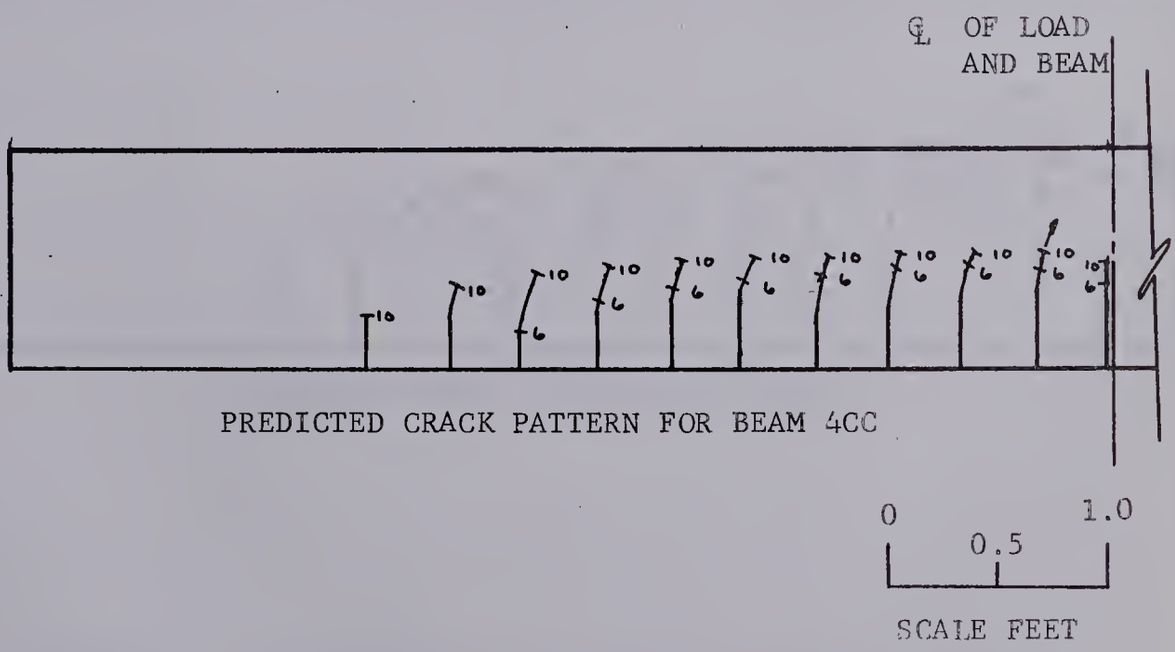

PREDICTED CRACK PATTERN FOR BEAM 4CC

FIGURE 5.4 PREDICTED CRACK PATTERNS FOR BEAMS 11A-2, 12A-2 AND 4CC

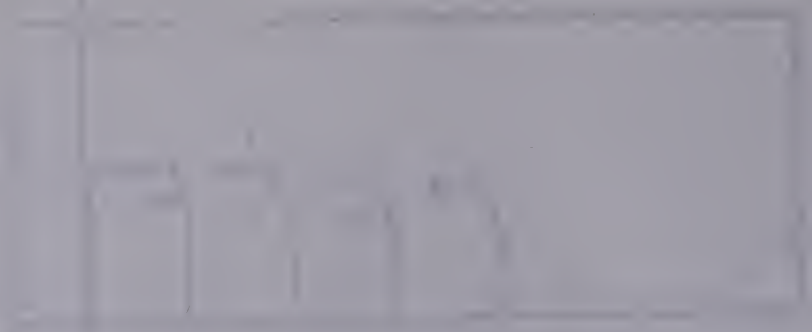

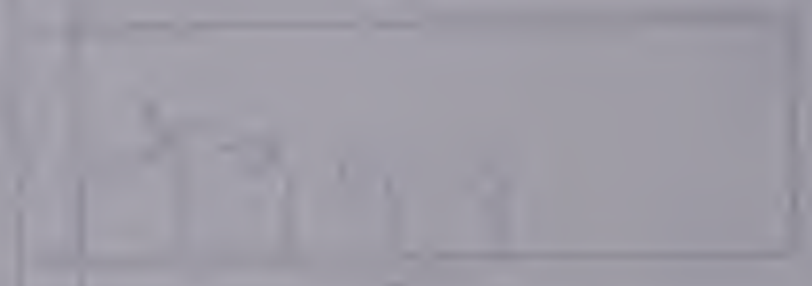

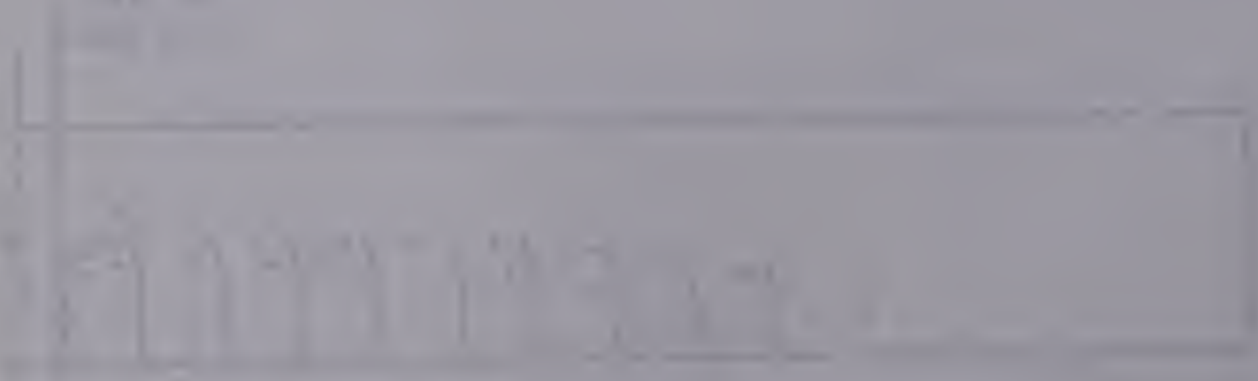

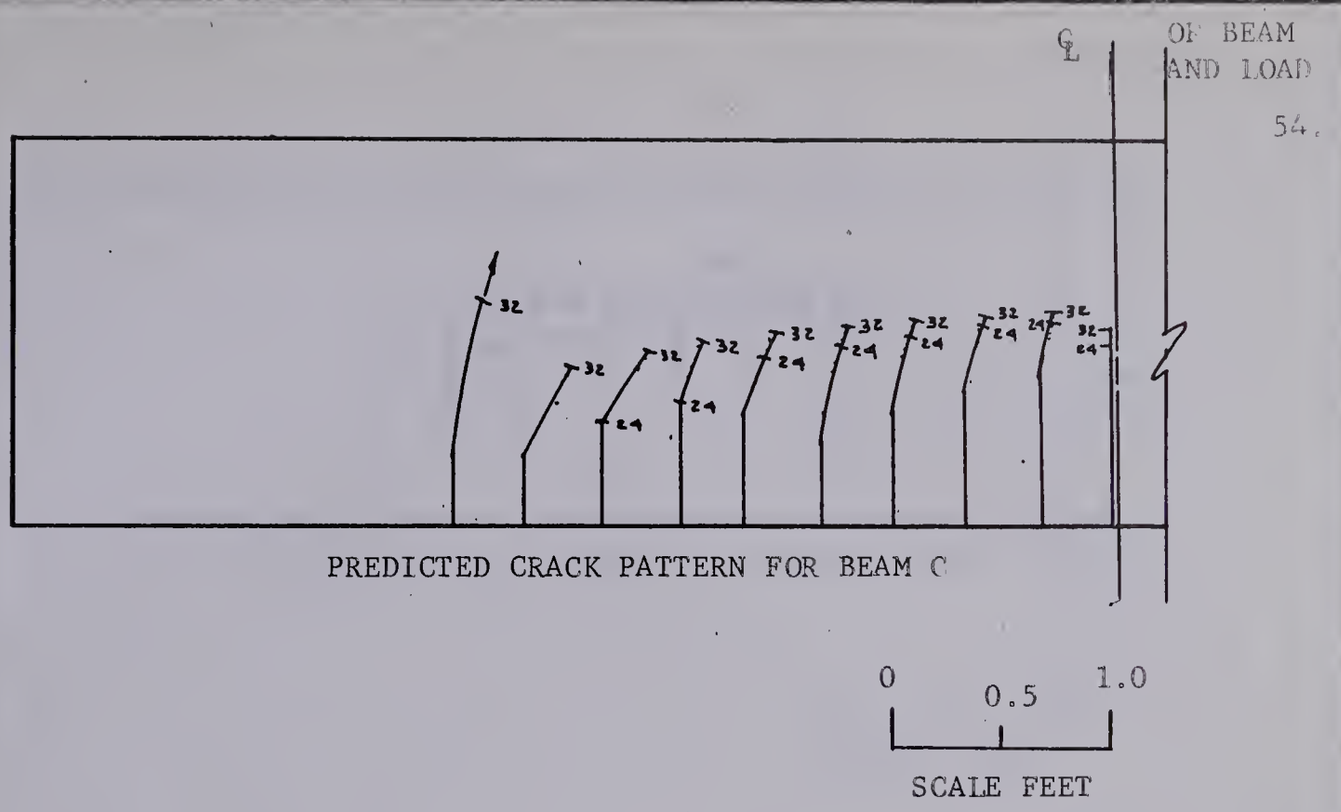

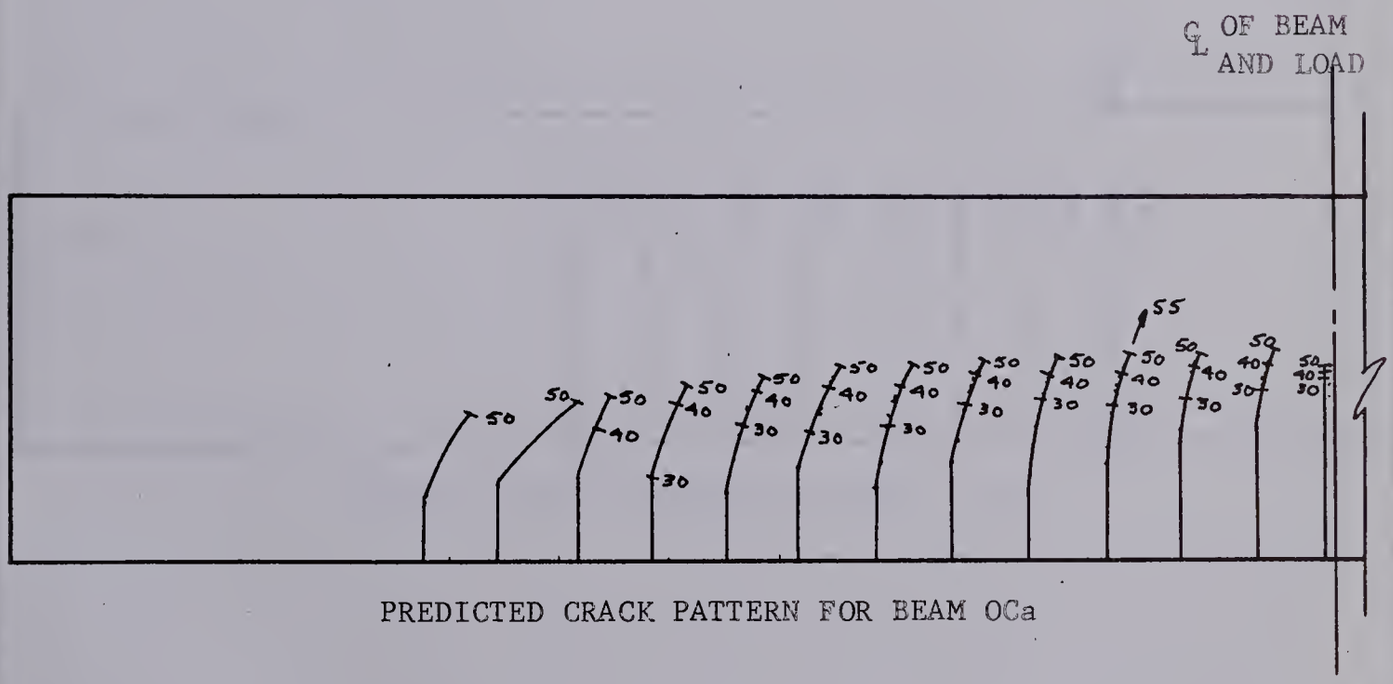

FIGURE 5.5 PREDICTED CRACK PATTERNS FOR BEAMS C AND OCa

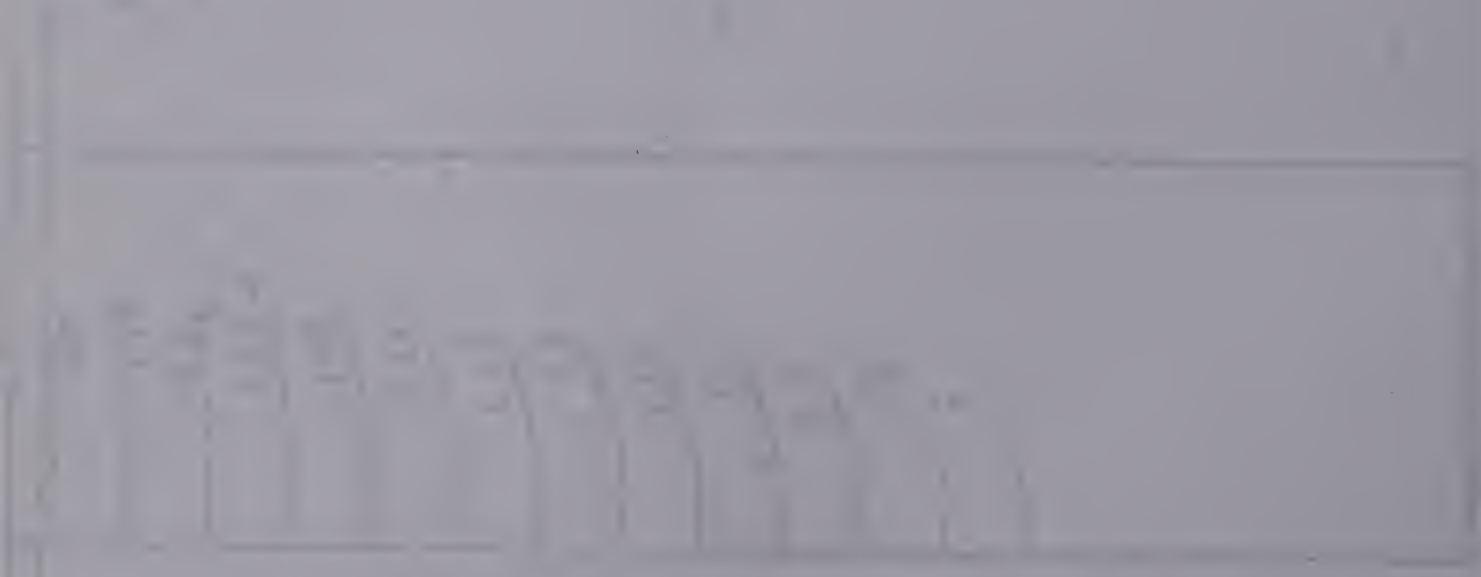

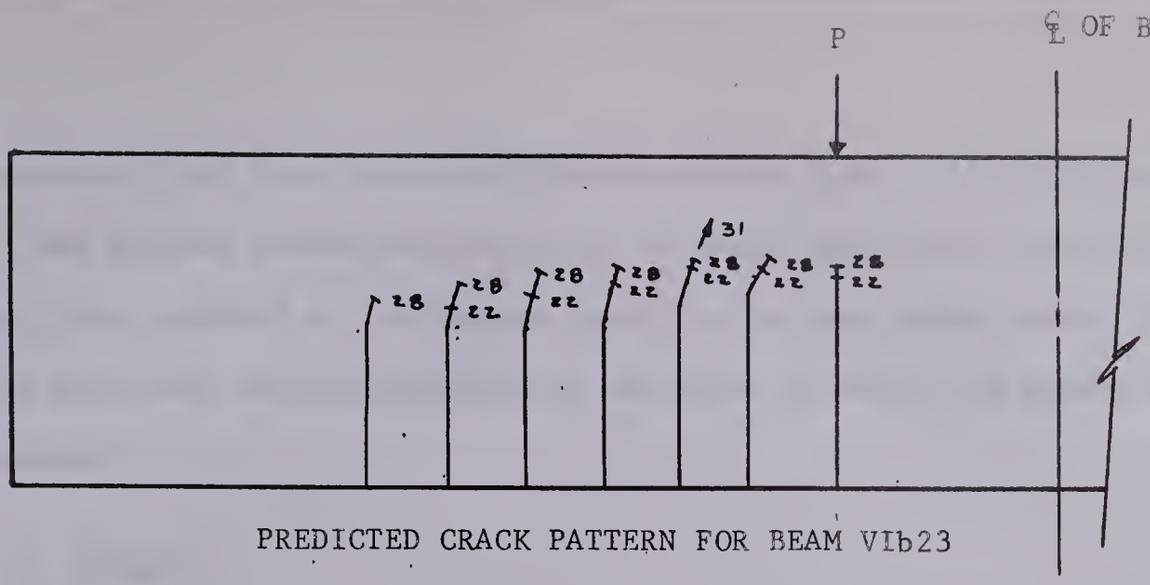

PREDICTED CRACK PATTERN FOR BEAM VIb23

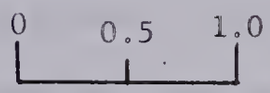

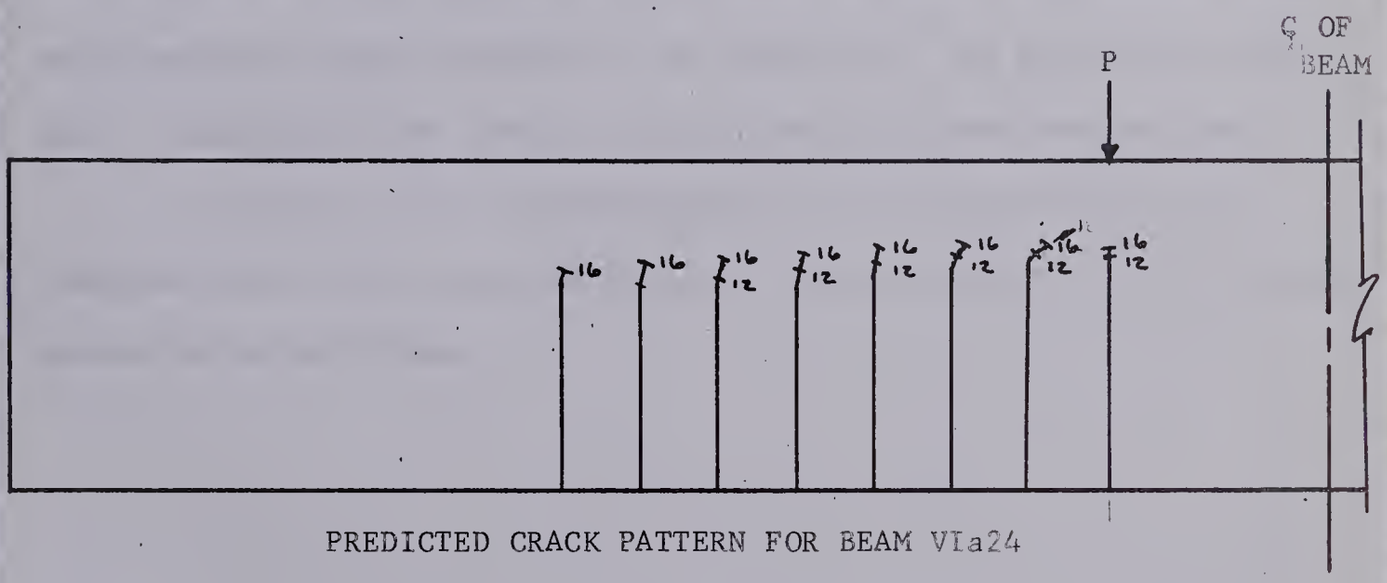

PREDICTED CRACK PATTERN FOR BEAM VIa24

FIGURE 5.6 PREDICTED CRACK PATTERNS FOR BEAMS VIb23 and VIa24

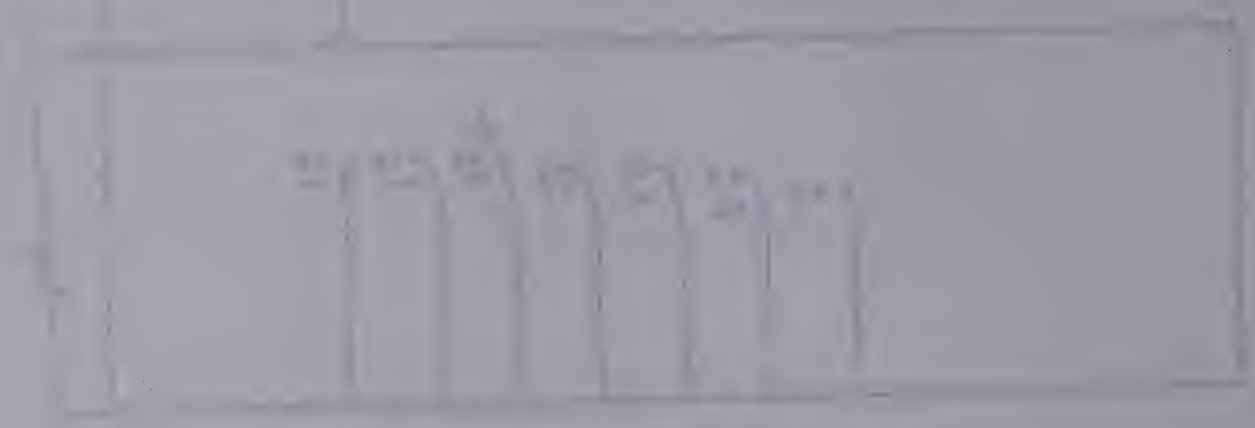

increased load this crack was always checked first. If some other crack in the pattern became unstable at a slightly lower load then failure may not have occurred at the second crack but at some other crack, but would not have been detected because of the order in which the cracks were checked.

5.3 SUMMARY

The analysis presented in this thesis predicts the ultimate load of reinforced concrete beams failing in diagonal tension or shear compression within about 25%. The crack patterns obtained from the analysis are similar to those observed during tests, although the diagonal crack which generally causes failure is not predicted. The predicted failure load is generally very close to the critical inclined cracking load.

In view of the accuracy with which the ACI Building Code equation predicts the inclined cracking load, the analysis in this thesis appears to be much better.

CHAPTER VI

DISCUSSION OF VARIABLES AND RESULTS OF THE ANALYSIS

6.1 INTRODUCTION

This chapter will present a discussion of the important variables which affect the shear failure load, the crack height and the relative magnitudes such secondary factors as tooth deflections and stresses, and the dowel and aggregate interlock shear forces. Factors which affect the ultimate crack height and failure load will also be discussed.

6.2 FACTORS AFFECTING THE CRACK HEIGHT

There are several factors which affect the crack height predicted by this analysis. These may be broken into two groups: those variables which have a direct effect on the flexural crack height, and those variables that influence the crack height under combined flexure and shear by their effect on the first group.

(a) Factors Affecting the Flexural Crack Height

The height of a flexural crack in a reinforced concrete beam is affected by such variables as the bending moment, the ultimate tensile stress and strain of the concrete, the ultimate compressive stress and strain of the concrete, the yield strength of the steel, the reinforcement percentage, p , the steel strain compatibility factor, F , and the cracking stress and strains of the concrete which may be altered as a

result of the computations of principal stress which are made in SECTION 4.10. The calculation of this reduced stress at which cracking occurs depends upon those variables which fall into the second group of variable affecting the crack height.

The effect of bending moment on the flexural crack height at any given section can be seen by examining FIGURE 4.10. This figure shows typical moment versus flexural crack height relationships for three beams. It can be seen that at the first stages of flexural cracking the moment resistance of a section increases very slowly or in some cases may decrease slightly as the crack propagates. In the later stages of loading the crack propagates very slowly as the moment resistance of the section increases rapidly. The reason for the initial decrease in moment resistance is that, just prior to cracking the concrete carries its maximum tensile force. This tensile force is reduced when the beam cracks and in many cases the increase in tensile steel force is not sufficient to maintain the previous value of moment resistance until the crack rises some distance into the beam. This decrease in moment capacity is particularly noticed in beams with low reinforcement ratios. As the crack height increases, however, the moment resistance begins to build at an ever increasing rate as the maximum concrete stress builds to a maximum, $k_3 f'_c$. Once the concrete stress has reached a maximum very little reduction of the compression zone can be tolerated and thus the moment resistance of a section increases rapidly for a small increase in crack height.

The effect on the crack height, of a change in the tensile

stress-strain curve assumed for the concrete can be seen by examining FIGURE 6.1. At the initial loading stages where the tensile strength of the concrete plays a major role in resisting the load, the effects of the tensile stress-strain curve on cracking are quite significant as would be expected. An increase in the ultimate tensile stress and strain of the concrete results in a higher cracking moment and consequently lower crack heights. In the final stages of loading there is little difference between the crack heights in the two beams although those corresponding to the concrete with the larger tensile values remain below those of the lower strength concrete. At this stage of loading the tensile strength of the concrete has little effect on the load carrying capacity of the member and the resulting lower crack heights are the result of the ultimate tensile strain being increased.

The effect of changing the ultimate compressive strength of the concrete in the beam on flexural cracking is shown in FIGURE 6.2. At the initial stages of loading the flexural crack heights are higher for lower strength concretes because the beam cracks earlier and the internal moment arm must be greater and the stress block must be more fully developed to resist the internal tension. Because the concrete in the low strength beams must be more highly stressed relative to its ultimate value, however, the moment-crack height curves for low strength concrete level off faster than those for high strength concrete. At the final loading stages, the cracks are shorter for the lower strength concretes. This is because a larger compression zone is required to resist the compression force developed when the beam approaches failure,

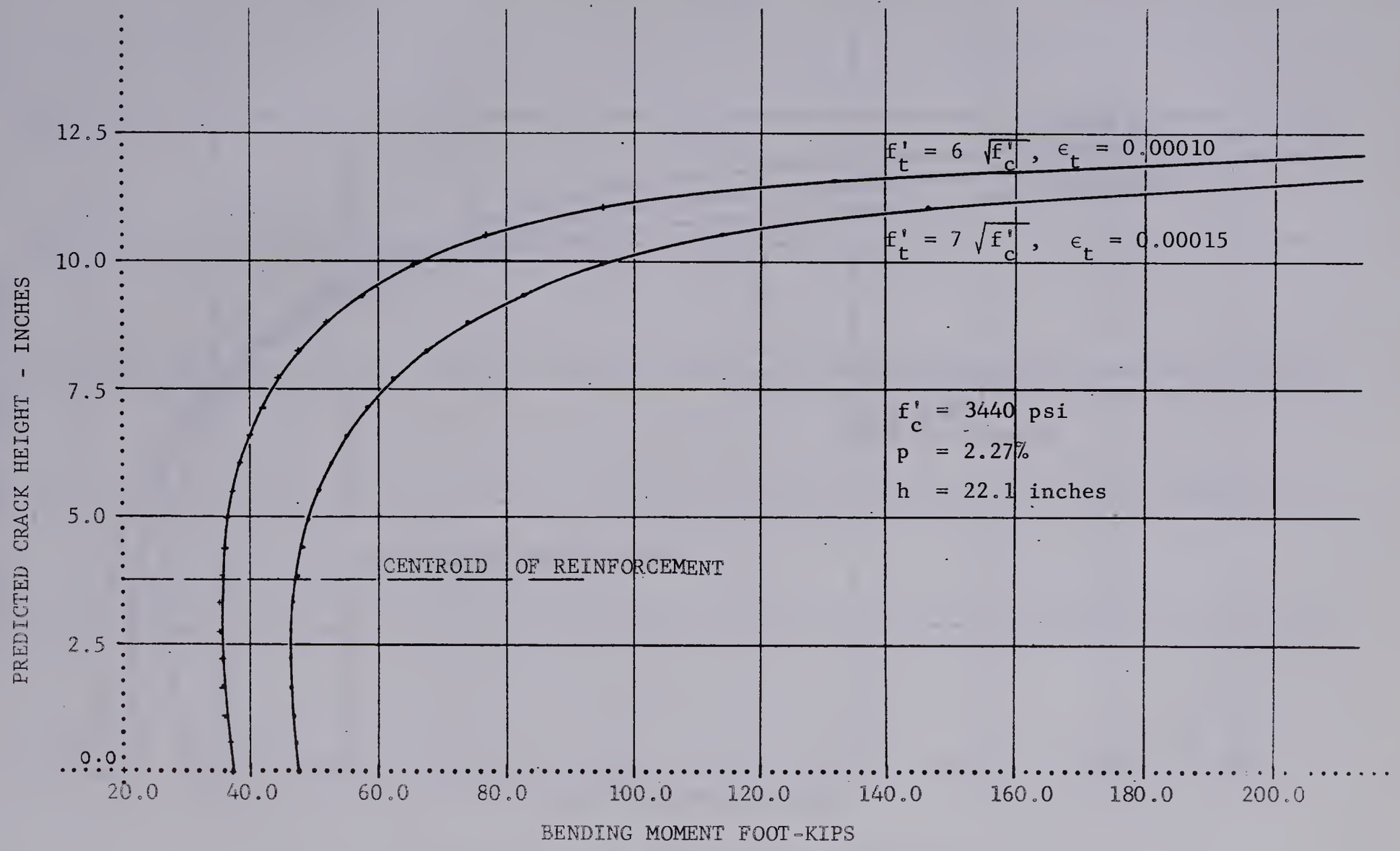

FIGURE 6.1 THE EFFECT OF THE TENSILE STRENGTH OF CONCRETE ON THE PREDICTED CRACK HEIGHT

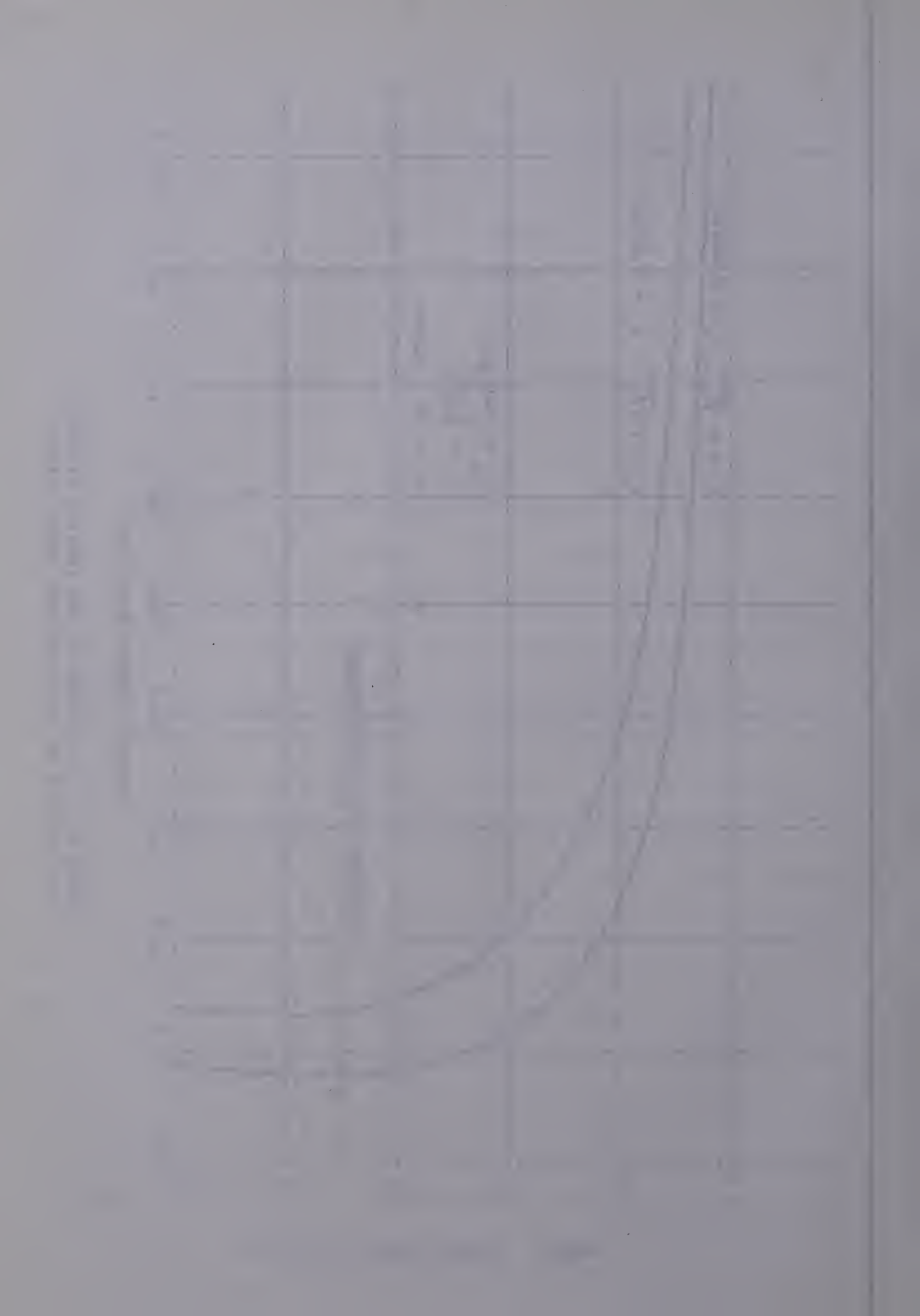

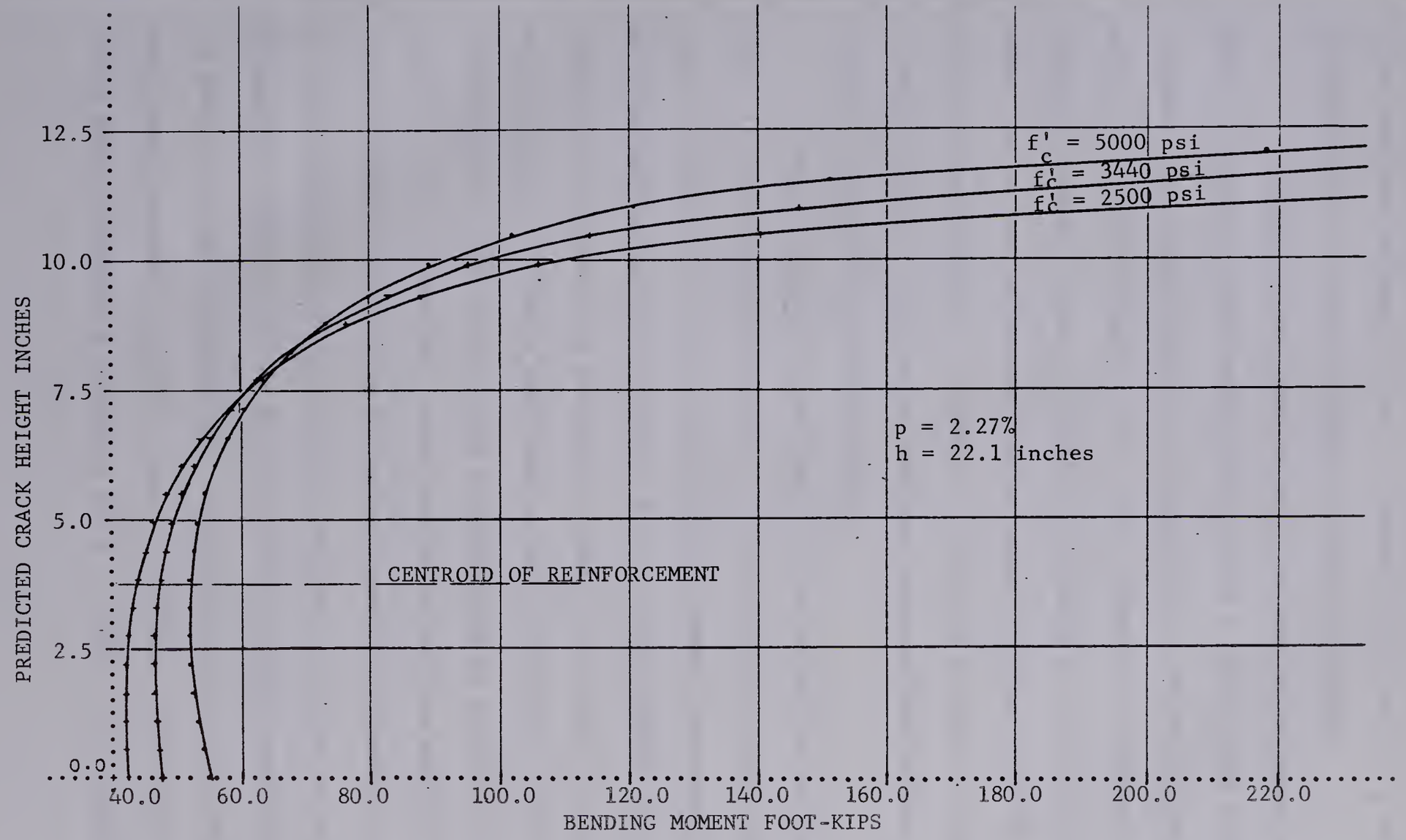

FIGURE 6.2 THE EFFECT OF A CHANGE IN f'_c ON THE PREDICTED CRACK HEIGHT

if the concrete strength is low. A change in the factor k_3 would have the same effect as a small change in concrete strengths.

A change in the yield strength of the reinforcement has no effect on flexural crack heights except that a lower yield stress reinforcement will cause failure of an under-reinforced section sooner than would a high yield strength steel. The ultimate crack height of the section, assuming failure is caused by yielding of the steel, would be lower. In an over-reinforced section where the steel does not yield until after the concrete fails, a change in the yield strength of the steel has no effect unless it results in that beam changing from an over-reinforced section to an under-reinforced section.

One of the most significant factors affecting the flexural crack height is the reinforcement ratio, p . The effects of this factor are shown in FIGURE 6.3. The flexural cracking moment increases slowly as the steel percentage is increased. For low reinforcement ratios initial cracking is followed by a decrease in moment resistance which eventually builds up again. Under a dead loading the initial crack would extend vertically until the crack height corresponding to the applied load was reached. On the other hand, over-reinforced sections exhibit larger cracking moments and show no decrease in moment resistance but rather an increasing moment resistance up to failure. It also can be seen that, because the compression zone must equilibrate larger tension forces in the beam with high percentages of reinforcement, the crack heights remain lower throughout the total range of loading. The effect of yielding can be seen by examining the curve for p = 1.42%. It is observed that

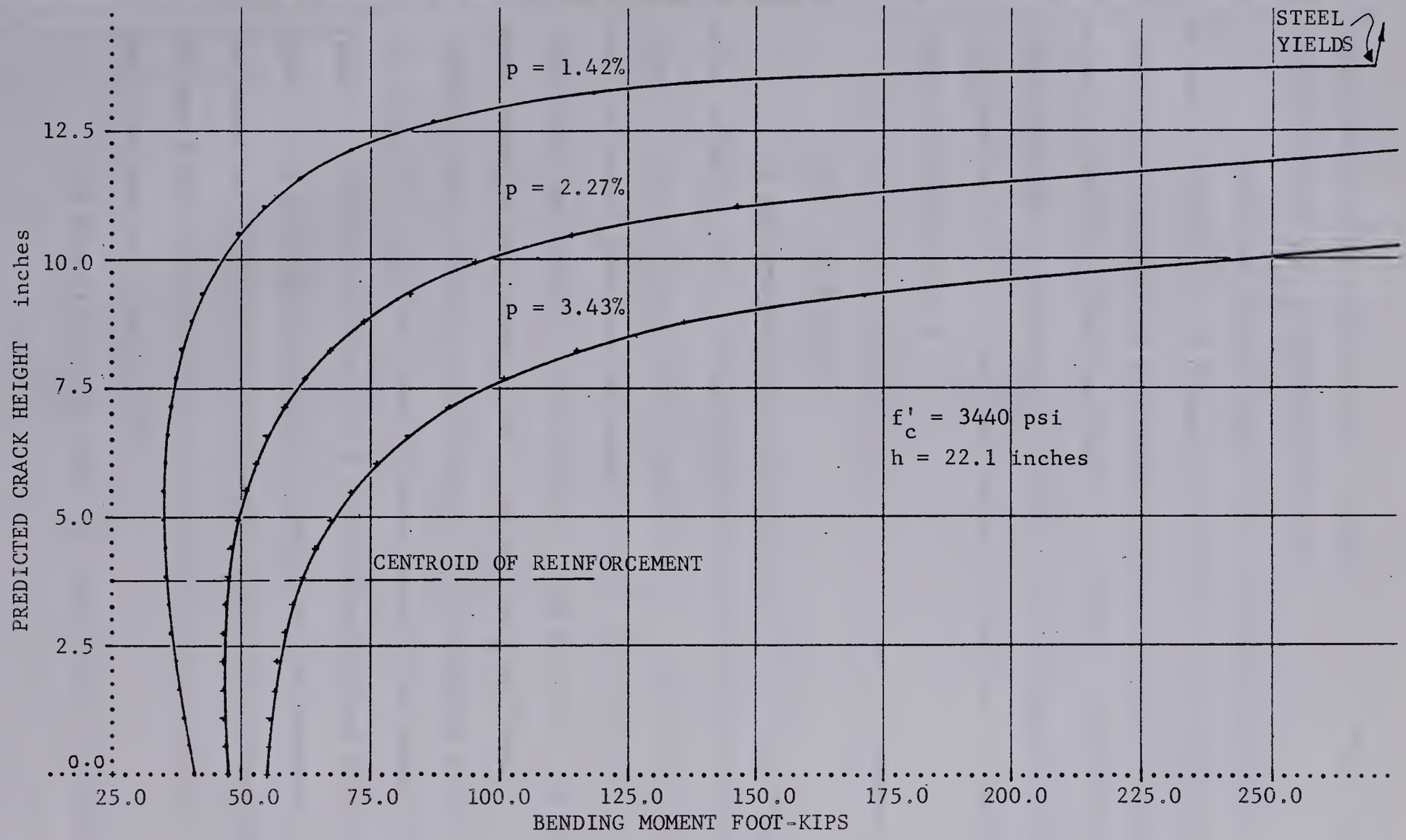

FIGURE 6.3 THE EFFECT OF A CHANGE IN STEEL PERCENTAGE ON THE PREDICTED CRACK HEIGHT

when yielding takes place, a rapid increase in crack height occurs with very little increase in moment resistance.

The effect of the steel strain compatibility factor, F , can be seen in FIGURE 6.4. A change in the steel strain factor has the same effect as a change in the percentage of reinforcement in a beam. The curves of FIGURE 6.4 thus are similar to FIGURE 6.3 and the reasons for the differences in the curve of FIGURE 6.4 are the same as those presented for FIGURE 6.3 if it is realized that an increase in, F , results in an effective increase in, p .

(b) Factors Affecting the Height of a Crack in a Region of Combined Shear and Flexure

In the introduction to this discussion of crack heights the variables affecting the crack height were divided into those directly and indirectly affecting the flexural crack height. The variables which fall into the second group are the shear force at the head of the crack, the flexibility and number of teeth and the tooth stresses. In the analysis these variables are important in altering the crack height of a purely flexural crack because of their effect on the cracking stress and strain. The larger the shear and tooth stresses become, the smaller the horizontal flexural tensile stress can be if the principal stress at the top of the crack is not to exceed the tensile strength of the concrete. The resulting reduction in the horizontal tensile stress that can be developed has the same effect on the flexural crack height as a reduction in the ultimate tensile stress and strain (FIGURE 6.1).

The direction of the crack is controlled by the relative magni-

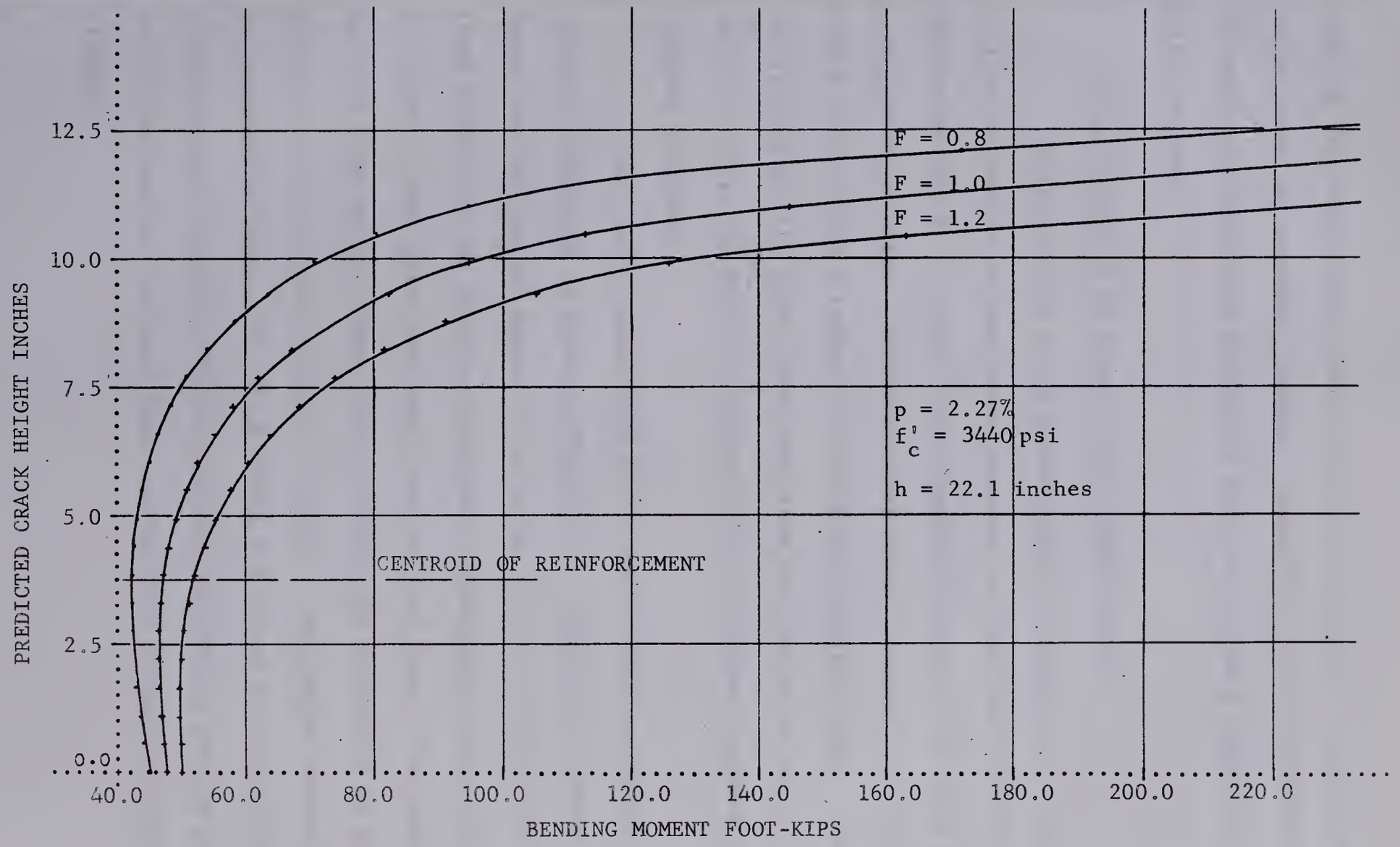

FIGURE 6.4 THE EFFECT OF CHANGING THE STEEL STRAIN COMPATIBILITY FACTOR ON THE PREDICTED CRACK HEIGHT

tudes of the shear stress, the tooth stresses and the flexural stress. The larger these two secondary stresses become relative to the flexural stress the more inclination the crack will have and the more rapidly the crack will propagate.

6.3 THE DISTRIBUTION OF SHEAR ON THE CROSS-SECTION

In this thesis it is assumed that the shear at a cracked section will be carried by the uncracked concrete, by dowel action of the longitudinal reinforcing and by the shear force transmitted across the crack by aggregate interlock or friction. The three shear force components are plotted in FIGURE 6.5 for beam C tested by Krefeld and Thurston (1962). These curves are plotted for the first crack away from the load point in this beam (crack 2). All the shear is carried by the uncracked concrete until flexural cracking.

The relative magnitudes of the shear force carried by the longitudinal reinforcing is shown in FIGURE 6.6. The values plotted for the 5 beams show the general shape of the curves and also present the upper and lower bounds for the 10 beams analyzed. In each case the curves are plotted for crack 2, the first crack away from the load point. The curves all have the same general shape indicating that the proportion of shear force carried by dowel action increases rapidly at the initial stages of cracking and eventually levels off. From FIGURE 6.6 it can also be seen that according to this analysis the longitudinal reinforcing carries between 7 and 13 per cent of the total shear on the given section at loads close to ultimate.

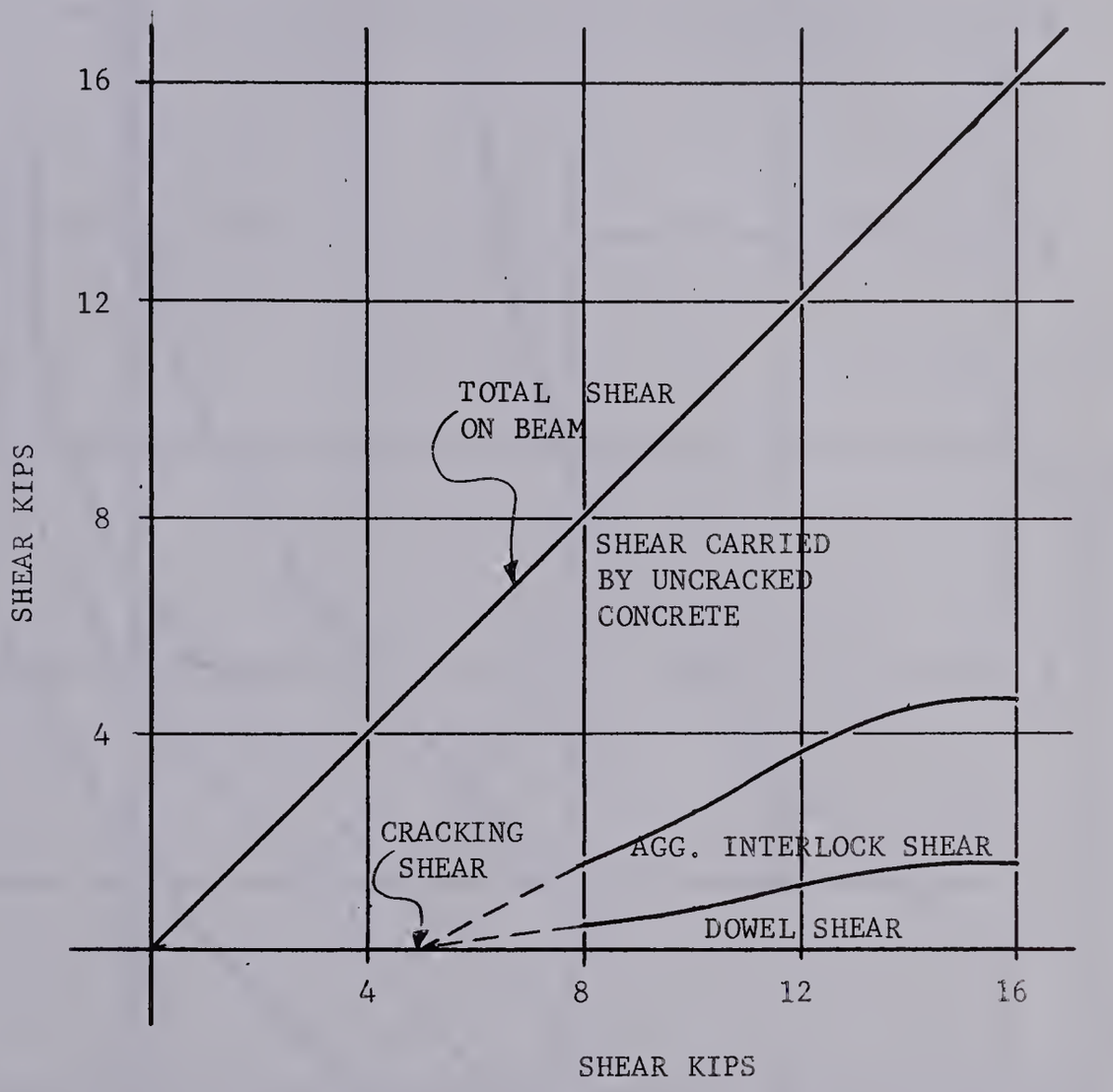

FIGURE 6.5 DISTRIBUTION OF TOTAL

SHEAR IN BEAM C

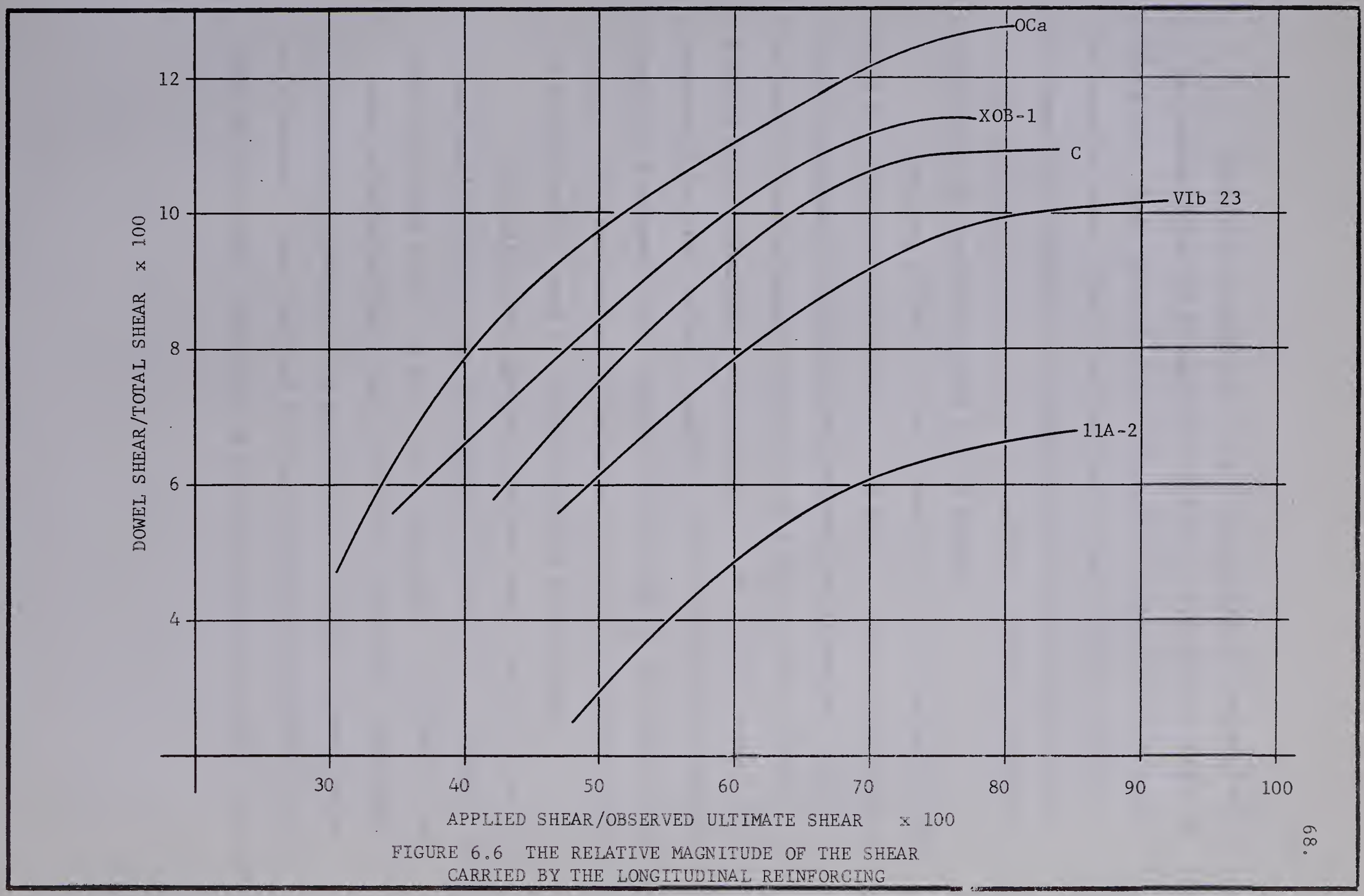

FIGURE 6.6 THE RELATIVE MAGNITUDE OF THE SHEAR CARRIED BY THE LONGITUDINAL REINFORCING

The relative magnitude of the shear transferred across crack 2 in the assumed structure by aggregate interlock or friction is shown in FIGURE 6.7. These curves have the same general shape as the curves for the doweling shear. The curves show that at loads close to ultimate, the shear force transferred by aggregate interlock and friction can be as high as 35% and as low as 20% of the total shear force on the section according to the assumptions made in this analysis.

Examining FIGURES 5.1 and 5.6 and 6.1 to 6.5 it can be seen that while the cracks propagate rapidly in the initial stages of cracking the rate of propagation decreases as the ultimate load is reached. Thus, the rate of crack propagation varies in the same way as the relative doweling shear and aggregate interlock shear. The doweling shear is a function of the crack height. Similarly, shear transferred by aggregate interlock is assumed to be a function of the height of the crack in this analysis. Thus the leveling of the curves of the shear transfer forces can be explained in terms of the rate of growth of the cracks.

The doweling and aggregate interlock shear transfer forces carry a considerable portion of the total shear at loads close to ultimate. This proportion ranges from 27 to 47 per cent. The curves in FIGURES 6.6 and 6.7 show the relative magnitudes of the forces only at the second crack in the computed structure. The magnitudes of the shear transfer forces are a maximum at this crack and thus the 47% might be considered an upper bound while the lower bound would be zero where there is no crack developed.

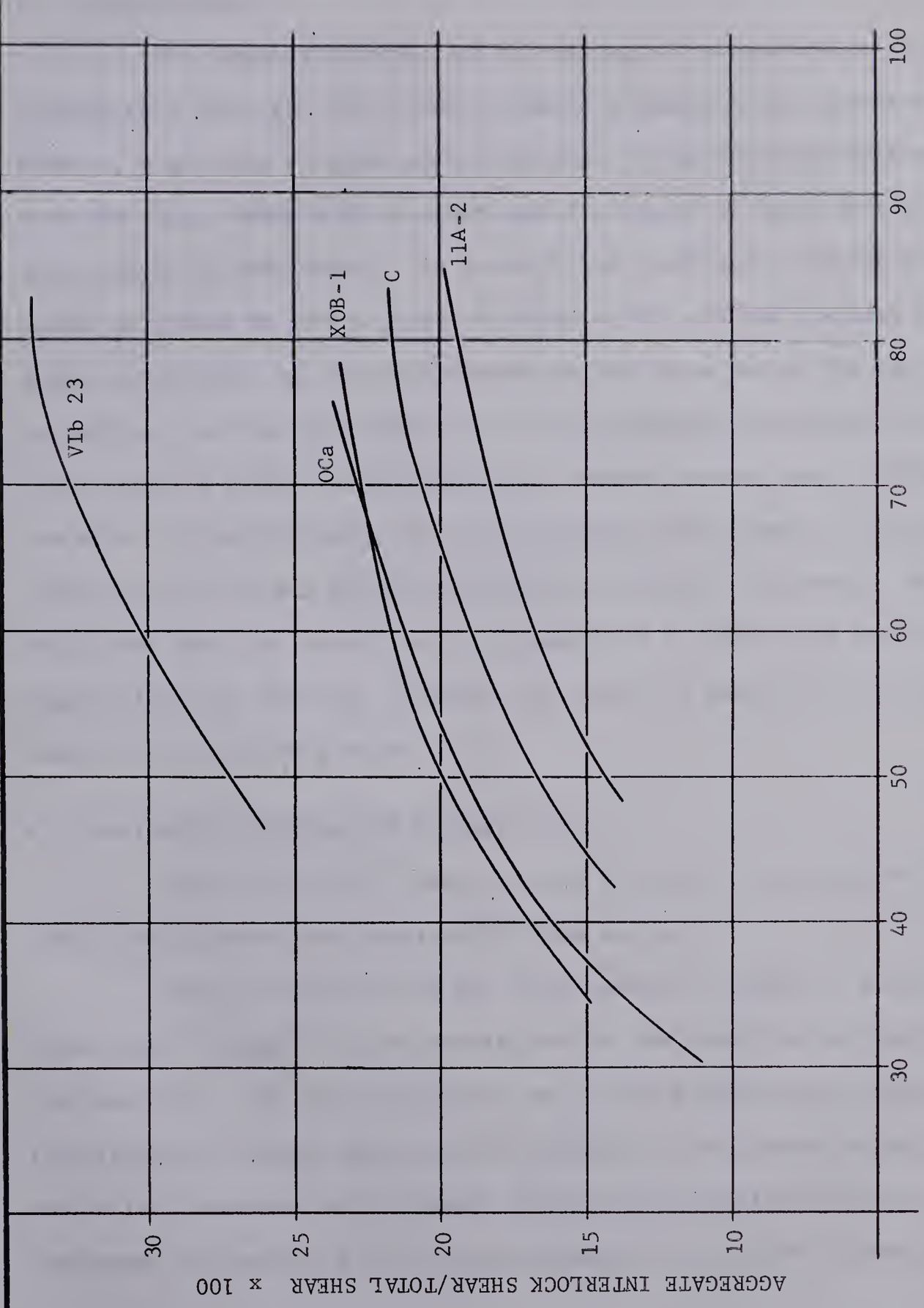

FIGURE 6.7 THE RELATIVE MAGNITUDE OF AGGREGATE INTERLOCK SHEAR

6.4 TOOTH STRESSES

The flexural stresses due to bending of the teeth were generally considerably less than the ultimate tensile strength of the concrete. However, high tooth stresses were calculated in the few teeth farthest from the load. These high stresses were the result of the relatively short cracks in this region. As a result the teeth had a greater horizontal stiffness so that a larger difference, ΔT , in the flexural tensile stress could exist in the reinforcement on the two sides of the tooth. In addition the low crack height led to low aggregate interlock and doweling shear transfer forces. Since the shear transfer forces tend to offset the effect of the ΔT force, the tooth stresses remain small in the teeth closer to the load but become quite large in the last few teeth. As a result the last few cracks tend to propagate at a faster rate than the cracks closer to the load. However, the effect is damped out if cracks form in the uncracked portion.

6.5 VARIABLES AFFECTING THE ULTIMATE LOAD

This section will concern itself with other variables which affect the ultimate load predicted by this analysis.

One such variable was the crack spacing. TABLE 6.1 shows the effect that varying the crack spacing had on the predicted failure load for beam XOB-1. It can be seen that as the crack spacing was decreased the predicted ultimate load was also decreased. This effect is partially due to the increased tooth stresses which result from the reduction in the moment of inertia of the critical section of the tooth. These larger

tooth stresses result in a more rapid propagation of the cracks. Conversely, the larger the tooth width, resulting from larger crack spacing results in lower tooth stresses and an increase in the ultimate predicted load. This increase is not linear with the increase in crack spacing, however, because the ΔT forces are increased by the increase in tooth stiffness that results from an increase in the width of the teeth.

TABLE 6.1

EFFECT OF CRACK SPACING ON THE COMPUTED

INCLINED CRACKING LOAD FOR BEAM XOB-1

Beam	Crack Spacing		P_w [2]	Predicted Failure Crack
	inches	X [1]	kips	
XOB-1 (Bresler and Scordelis, 1964)	5.65	1.5	42.0	5
	7.54	2.0	45.0	3
	11.31	3.0	45.5	2

1. The crack spacing is expressed as X ; C where C is the cover on the reinforcement.
2. The measured failure load was 57.5 kips with failure occurring at the seventh crack from the load. The average crack spacing was 7.19 inches.

It is interesting to note that as the crack spacing was reduced the predicted location of the failure approached the actual failure location.

A second factor which affects the ultimate predicted load is the size of the load increment. Ideally this load increment should be very

small but practical consideration dictated the size of the increment. If smaller increments had been used it is possible that the ultimate predicted loads shown in TABLE 5.2 would have been smaller. When the assumed structure reached equilibrium at a given load, the load was increased and if the structure was not able to achieve equilibrium under this increased load, the beam was said to have failed under the new load. This is analogous to testing a beam with dead load rather than using a reaction type of loading.

The greatest problem in predicting the ultimate load came in establishing the height of the crack as the loads approached ultimate. As was seen in FIGURE 4.10 the moment versus crack height relationship levels off at ultimate or close to ultimate loads. In the procedure outlined in SECTION 4.3 the crack height was incremented to achieve a balance between the applied moment and the resisting moment. If the increment in load were too coarse then an unstable condition resulted when the forces on the cross section were balanced. If, in future investigations, the stress-strain curve for concrete in both tension and compression could be expressed as a continuous function, algebraic expressions could be written to achieve moment and force equilibrium rather than using an iterative procedure and failure would probably be predicted at a slightly higher load than is shown in TABLE 5.2.

The accuracy of this analysis is limited by the fact that in no case was the major diagonal crack predicted by this analysis. The crack heights predicted by this analysis can never enter the compression zone of the beam since the critical element is always taken as the

element at the head of the crack. In future investigations a check of a number of sections just above the crack height predicted by this analysis may result in higher crack heights or in the formation of a new, independant crack, particularly where the shear stresses are large compared to the bending moment. Before stresses could be checked at the sections above the head of the crack it would be necessary to have some knowledge of how the tooth stresses are damped out at levels between the head of the crack and the top of the beam. In addition, the checking of additional sections in the uncracked portion of the beam may result in principal tensions which exceed f_t' an thus a diagonal crack may be predicted before flexural cracking occurs or shortly after the formation of a flexural crack.

6.6 SUMMARY

This chapter has been an attempt to explain the effects of the major variables on the ultimate predicted load. While each variable has been discussed separately, these variables are inter-dependent in this analysis and thus a very complex system results.

CHAPTER VII

CONCLUSIONS AND RECOMMENDATIONS

7.1 GENERAL REMARKS

The analysis presented in the previous chapters is an attempt to rationalize the solution to the strength of reinforced concrete beams failing in shear. This analysis was based on the observed behavior of reinforced concrete beams before the formation of the diagonal crack. The analysis was based entirely upon strength of materials and made no attempt to account for stress concentrations. For the beams analyzed, the analysis did not predict the formation of the critical diagonal crack.

7.2 CONCLUSIONS

From the results and the discussion presented in CHAPTERS 5 and 6 the following conclusions may be drawn:

(a) The predicted crack heights appeared to be low and in no case did the analysis predict the major crack which caused failure. However, the ratio of measured to predicted ultimate load ranged from 1.09 to 1.58 with an average value of 1.25.

(b) According to this analysis the magnitude of the shear transfer forces and their contribution to the shear capacity of the section is considerable, ranging from 27% to 47% of the total shear at failure.

(c) The assumed crack spacing has an effect on the failure load in that it affects the flexural stresses in the teeth and

also the ΔT forces acting on the tooth. As the crack spacing is increased the predicted failure load increases at a decreasing rate.

(d) The major factors which affect the flexural crack height are: the steel percentage, p ; the concrete strength, f_c' and f_t' and the steel strain compatibility factor F . The tooth stresses and deflections in this analysis affect the crack height by effectively reducing the tensile strength of the concrete f_t' .

7.3 RECOMMENDATIONS

The following recommendations are made to help future investigators attempting a similar analysis:

(a) The use of a continuous function to define the stress strain characteristics of concrete in tension and compression would simplify the analysis of flexural stresses and help to ensure that the true ultimate conditions were achieved.

(b) The doweling force carried by the bar could be altered to include the effect of axial tension in the bars although, the effect of this force appeared to be small. The effect of unbonding of the bar due to cracking along the reinforcement is less important since it generally occurs after the inclined crack has formed.

(c) The effective length of the bar joining the teeth in the indeterminate structure probably should be expressed as a function of the level of stress in the bar.

(d) Since the spacing of the cracks has an effect on the ultimate load, more attention should be given to this variable.

(e) Additional elements above the head of the crack should be checked to see if the cracks propagate higher or if an independent crack is formed in this region.

(f) Sections outside the cracked portion of the shear span should be checked to see if a diagonal crack will form in this region.

(g) The magnitude of the shear carried by aggregate interlock has been mentioned by several investigators but no experimental measurements of its magnitude are available. More knowledge of this variable would be helpful.

(h) Splitting of the anchorage zone due to dowel action of the reinforcement should also be checked especially with regard to its effect on reducing the carrying capacity of the dowel.

BIBLIOGRAPHY

1928

1. Gonnerman, H. and Shuman, E.C. - "Compression, Flexure and Tension Tests of Plain Concrete" Proceedings, ASTM, Volume 28, pp 571, 1928.

1951

2. Clarke, A.P. - "Diagonal Tension in Reinforced Concrete Beams", Proceedings, American Concrete Institute, Volume 48, pp 145-156, Oct. 1951.

3. Hognestad, E. - "A Study of Combined Bending and Axial Load in Reinforced Concrete Members", University of Illinois, Eng. Experimental Station Bulletin 399, 1951.

4. Price, W.H. - "Factors Influencing Concrete Strength" Proceedings, American Concrete Institute, Volume 47, pp 417-432, Feb. 1951.

1954

5. Moody, K.G., Viest, I.M., Elstner, R.C. and Hognestad, E. - "Shear Strength of Reinforced Concrete Beams - Parts 1 and 2". Proceedings, American Concrete Institute, Volume 51, Dec. 1954 and Jan. 1955.

1955

6. Hognestad, E. Hanson, N.W. and McHenry, D. - "Concrete Stress Distribution in Ultimate Strength Design", Proceedings, American Concrete Institute, Volume 27, pp 955-479, Dec. 1955.

7. Linder, C.P. and Sprague, J.C. - "Effect of Depth Upon the Modulus of Rupture of Plain Concrete", Proceedings, ASTM, Volume 55, pp 1062, 1955.

8. Wright, P.J.F. - "Comments on an Indirect Tensile Test on Concrete Cylinders", Magazine of Concrete Research, Volume 7, No. 20, pp 87, July 1955.

1956

9. A.C.I. Committee 318 - "Building Code Requirements for Reinforced Concrete (A.C.I. 318-56)", American Concrete Institute, 1956.

10. Subcommittee III, A.C.I. Committee 325 - "Structural Design Considerations for Pavement Joints", Proceedings American Concrete Institute, Volume 53, pp 1-28, July 1956.

1959

11. Sozen, M.A., Zwoyer, E.M. and Siess, C.P. - "Strength in Shear of Beams Without Web Reinforcement", University of Illinois, Eng. Experimental Station, Bulletin 452, April 1959.

1960

12. Pauw, A. - "Modulus of Elasticity of Concrete as Affected by Density", Proceedings, American Concrete Institute, Volume 32, Dec. 1960.

1962

13. A.C.I. - A.S.C.E. Committee 326 - "Shear and Diagonal Tension, Parts 1 and 2", Proceedings, American Concrete Institute, Volume 59, Jan. and Feb. 1962.

14. Krefeld, W.J. and Thurston, C.W. - "Studies of the Shear and Diagonal Tension Strength of Simply Supported Reinforced Concrete Beams", Columbia University, June 1962.

15. Moe, J. - "Discussion of A.C.I. - A.S.C.E. Committee 326 Paper on Shear and Diagonal Tension", Proceedings, American Concrete Institute, Volume 59, pp 1334 - 1339, Sept. 1962.

16. Van Den Berg, F.J. - "Shear Strength of Reinforced Concrete Beams Without Web Reinforcement, Parts 1 and 3", Proceedings, American Concrete Institute, Volume 59, Oct. and Dec. 1962.

1963

17. A.C.I. Committee 318 - "Building Code Requirements for Reinforced Concrete (A.C.I. 318-63)", American Concrete Institute, 1956.

18. Bresler, B. and Scordelis, A.C. - "Shear Strength of Reinforced Concrete Beams", Proceedings, American Concrete Institute, Volume 60, pp 51-72, Jan. 1963.

19. Kaplan, M.F. - "Strains and Stresses of Concrete at Initiation of Cracking and Near Failure", Proceedings, American Concrete Institute, Volume 60, pp 853, 1963.

20. Krahl, N.W. - "An Analytical Study of the Behavior of Reinforced Concrete Beams Without Web Reinforcement Under Combined Shear and Bending Moment", University of Illinois, Ph.D. Thesis, 1963.

21. Mathey, R.G. and Watstein, D. - "Shear Strength of Beams Without Web Reinforcement Containing Deformed Bars of Different Yield Strengths", Proceedings, American Concrete Institute, Volume 60, pp 183, 1963.

22. Narrow, I. and Ullberg, E. - "Correlation Between Tensile Splitting Strength and Flexural Strength of Concrete", Proceedings, American Concrete Institute, Volume 60, pp 27, 1963.

23. Neville, A.M. - "Properties of Concrete", Pitman and Sons, 1963.

1964

24. Bresler, B. and Scordelis, A.C. - "Shear Strength of Reinforced Concrete Beams - Series II", University of California, Dec. 1964.

25. Kani, G.N.J. - "The Riddle of Shear Failure and Its Solution", Proceedings, American Concrete Institute, Volume 61, pp 411-967, April 1964.

26. Oladapo, I.O. - "Cracking and Failure in Plain Concrete Beams", Magazine of Concrete Research, Volume 16, No. 47, June 1964.

1965

27. Broms, B.B. - "Crack Width and Crack Spacing in Reinforced Concrete Members", Proceedings, American Concrete Institute, Volume 62, pp 1237, Nov. 1965.

28. Lorentsen, M. - "Theory for the Combined Action of Bending Moment and Shear in Reinforced and Prestressed Concrete Beams", Proceedings, American Concrete Institute, Volume 62, pp 403, April 1965.

29. Morrison, E.M. - "A Critical Examination of Inclined Cracking Equations", University of Alberta, M.Sc. Thesis, Sept. 1965.

30. Reis, E.E., Mozer, J.D., Bianchini, A.C. and Kesler, C.E. - "Causes and Control of Cracking Reinforced With High-Strength Steel Bars - A Review of Research", University of Illinois, Eng. Experimental Station Bulletin 479, Aug. 1965.

1966

31. Manuel, R.F. - "Behavior of Restrained Reinforced Concrete Columns Under Sustained Load", University of Alberta, Ph.D. Thesis, Jan. 1966.

APPENDIX A

FLOW DIAGRAM FOR THE COMPUTER APPLICATION OF THE ANALYSIS

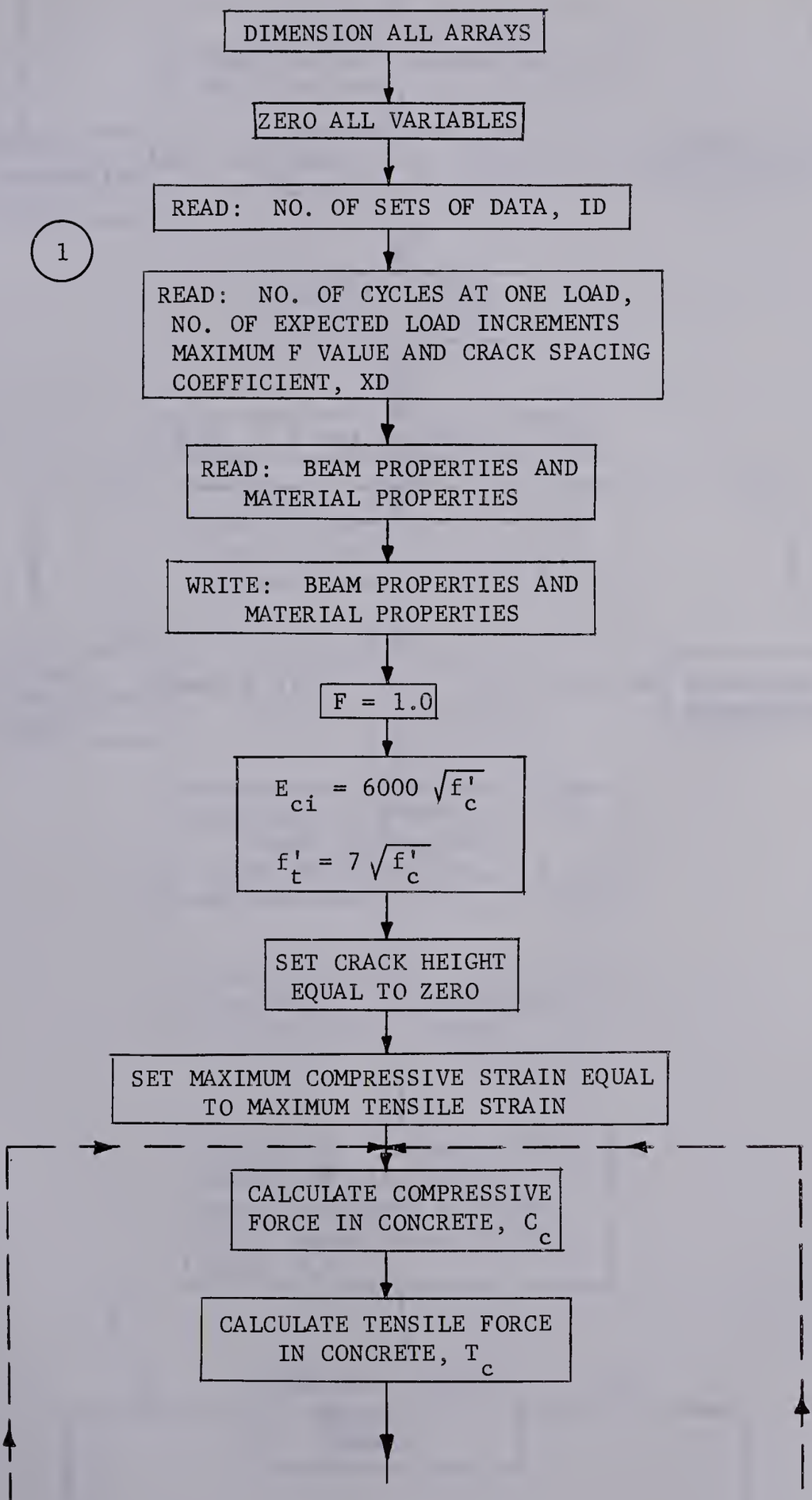
DIMENSION ALL ARRAYS
ZERO ALL VARIABLES
READ: NO. OF SETS OF DATA, ID
1
READ: NO. OF CYCLES AT ONE LOAD, NO. OF EXPECTED LOAD INCREMENTS MAXIMUM F VALUE AND CRACK SPACING COEFFICIENT, XD
READ: BEAM PROPERTIES AND MATERIAL PROPERTIES
WRITE: BEAM PROPERTIES AND MATERIAL PROPERTIES
F = 1.0
$E_{ci} = 6000 \sqrt{f'_c}$
$f'_t = 7 \sqrt{f'_c}$
SET CRACK HEIGHT EQUAL TO ZERO
SET MAXIMUM COMPRESSIVE STRAIN EQUAL TO MAXIMUM TENSILE STRAIN
CALCULATE COMPRESSIVE FORCE IN CONCRETE, C_c
CALCULATE TENSILE FORCE IN CONCRETE, T_c

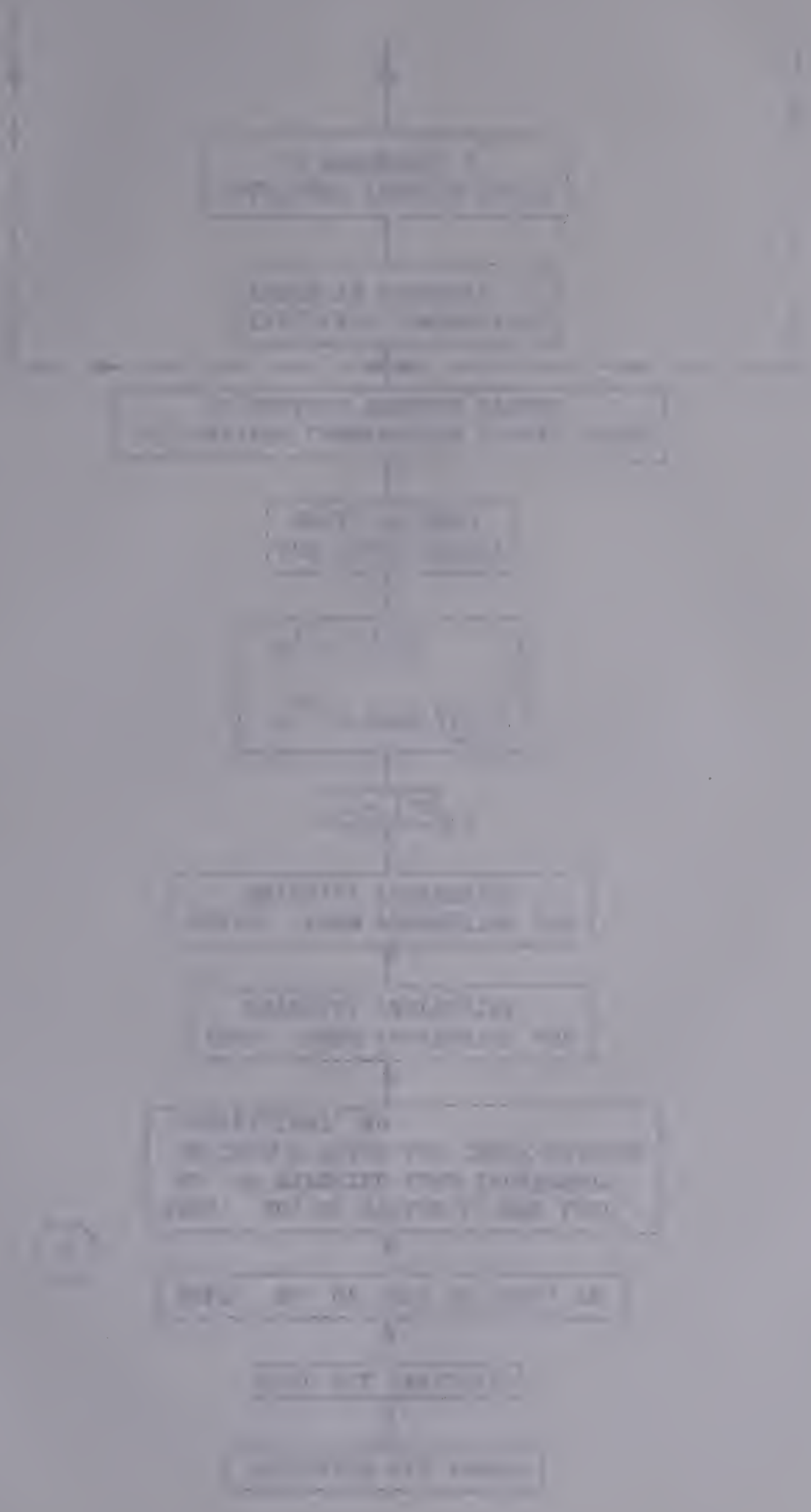

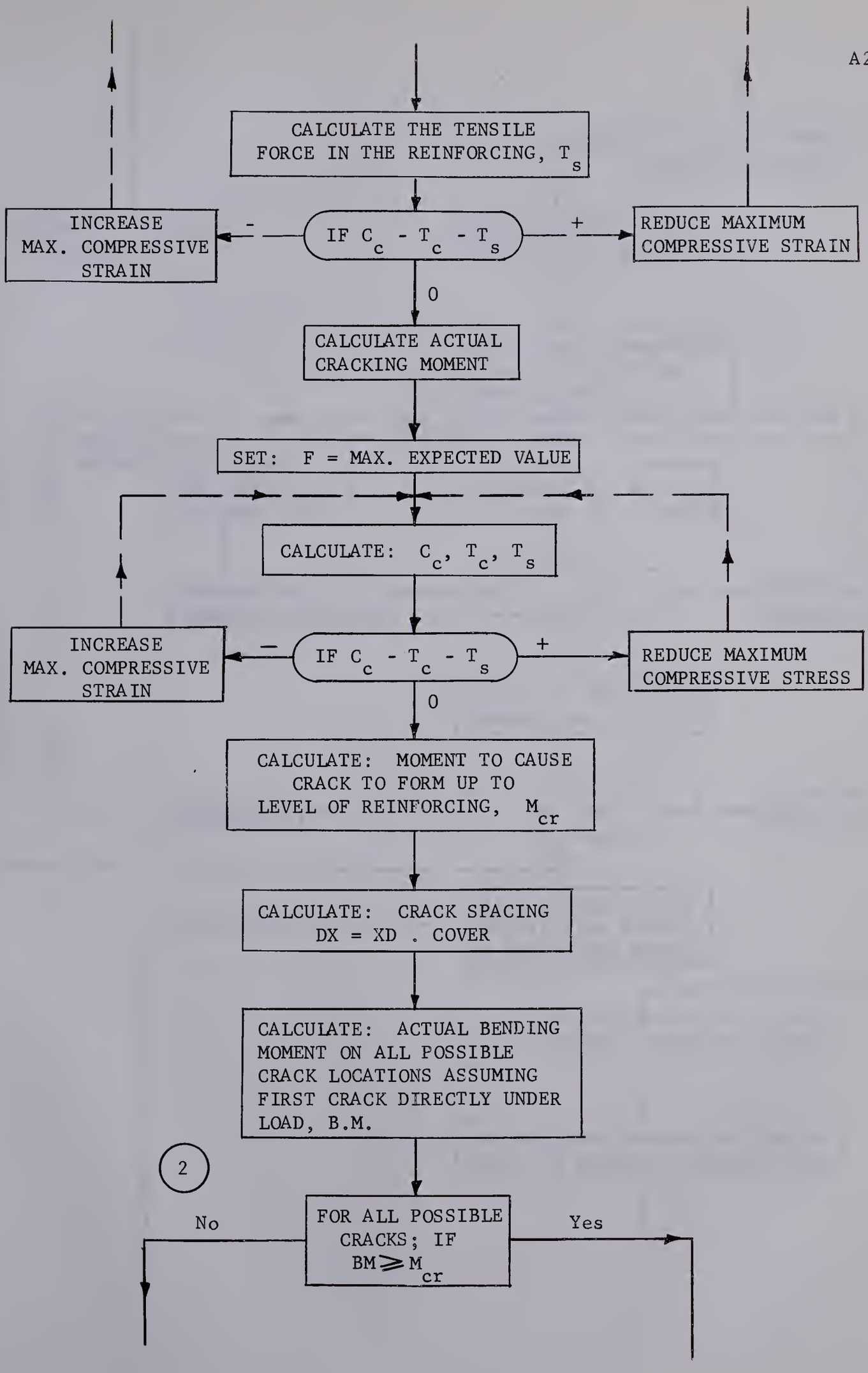
CALCULATE THE TENSILE FORCE IN THE REINFORCING, T_s
IF $C_c - T_c - T_s$
-
+
INCREASE MAX. COMPRESSIVE STRAIN
REDUCE MAXIMUM COMPRESSIVE STRAIN
0
CALCULATE ACTUAL CRACKING MOMENT
SET: F = MAX. EXPECTED VALUE
CALCULATE: C_c, T_c, T_s
IF $C_c - T_c - T_s$
-
+
INCREASE MAX. COMPRESSIVE STRAIN
REDUCE MAXIMUM COMPRESSIVE STRESS
0
CALCULATE: MOMENT TO CAUSE CRACK TO FORM UP TO LEVEL OF REINFORCING, M_{cr}
CALCULATE: CRACK SPACING DX = XD . COVER
CALCULATE: ACTUAL BENDING MOMENT ON ALL POSSIBLE CRACK LOCATIONS ASSUMING FIRST CRACK DIRECTLY UNDER LOAD, B.M.
2
FOR ALL POSSIBLE CRACKS; IF $BM \geqslant M_{cr}$
No
Yes

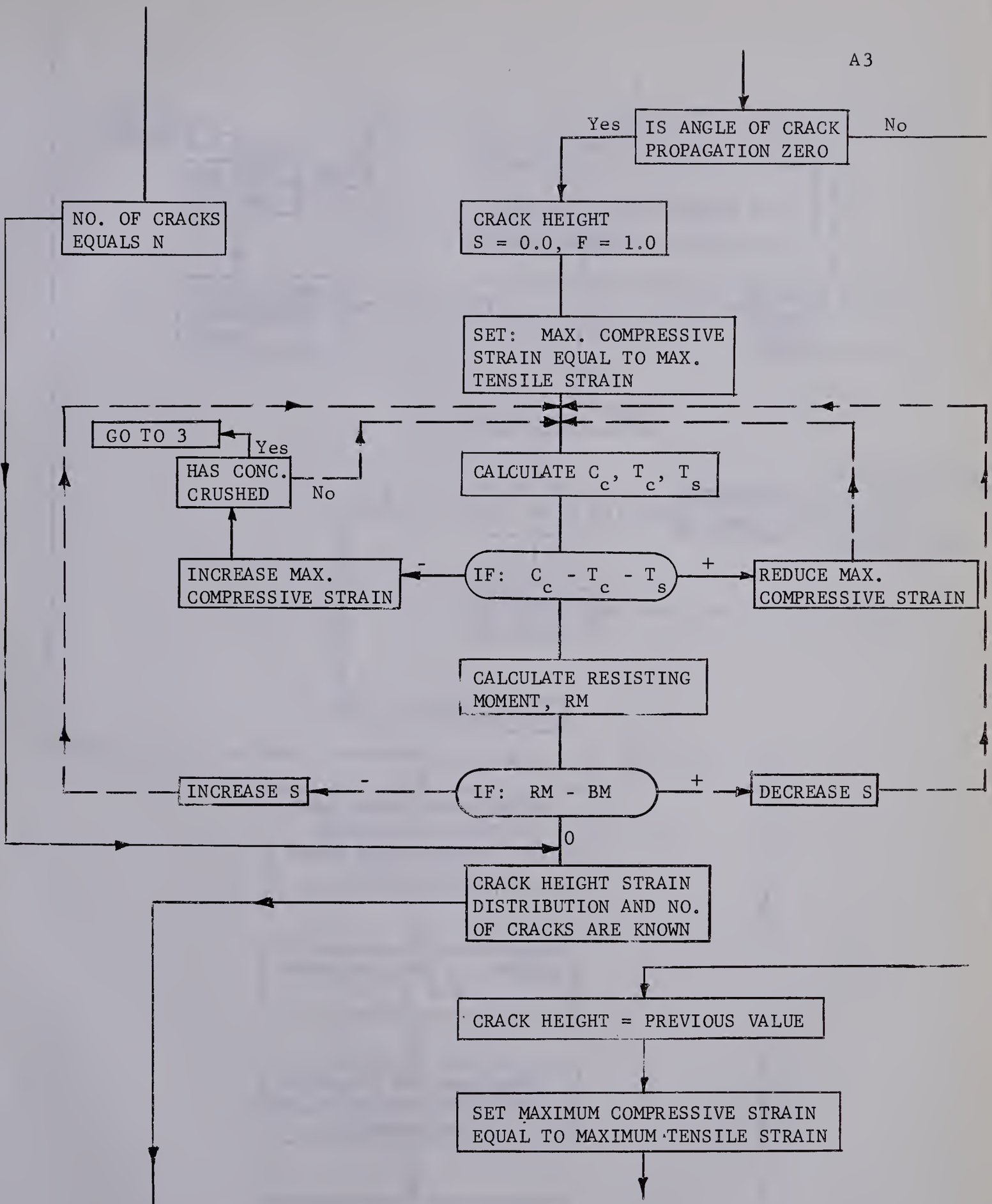
IS ANGLE OF CRACK PROPAGATION ZERO
Yes
No
NO. OF CRACKS EQUALS N
CRACK HEIGHT S = 0.0, F = 1.0
SET: MAX. COMPRESSIVE STRAIN EQUAL TO MAX. TENSILE STRAIN
GO TO 3
Yes
HAS CONC. CRUSHED
No
CALCULATE C_c, T_c, T_s
INCREASE MAX. COMPRESSIVE STRAIN
-
IF: $C_c - T_c - T_s$
+
REDUCE MAX. COMPRESSIVE STRAIN
CALCULATE RESISTING MOMENT, RM
INCREASE S
-
IF: RM - BM
+
DECREASE S
0
CRACK HEIGHT STRAIN DISTRIBUTION AND NO. OF CRACKS ARE KNOWN
CRACK HEIGHT = PREVIOUS VALUE
SET MAXIMUM COMPRESSIVE STRAIN EQUAL TO MAXIMUM TENSILE STRAIN

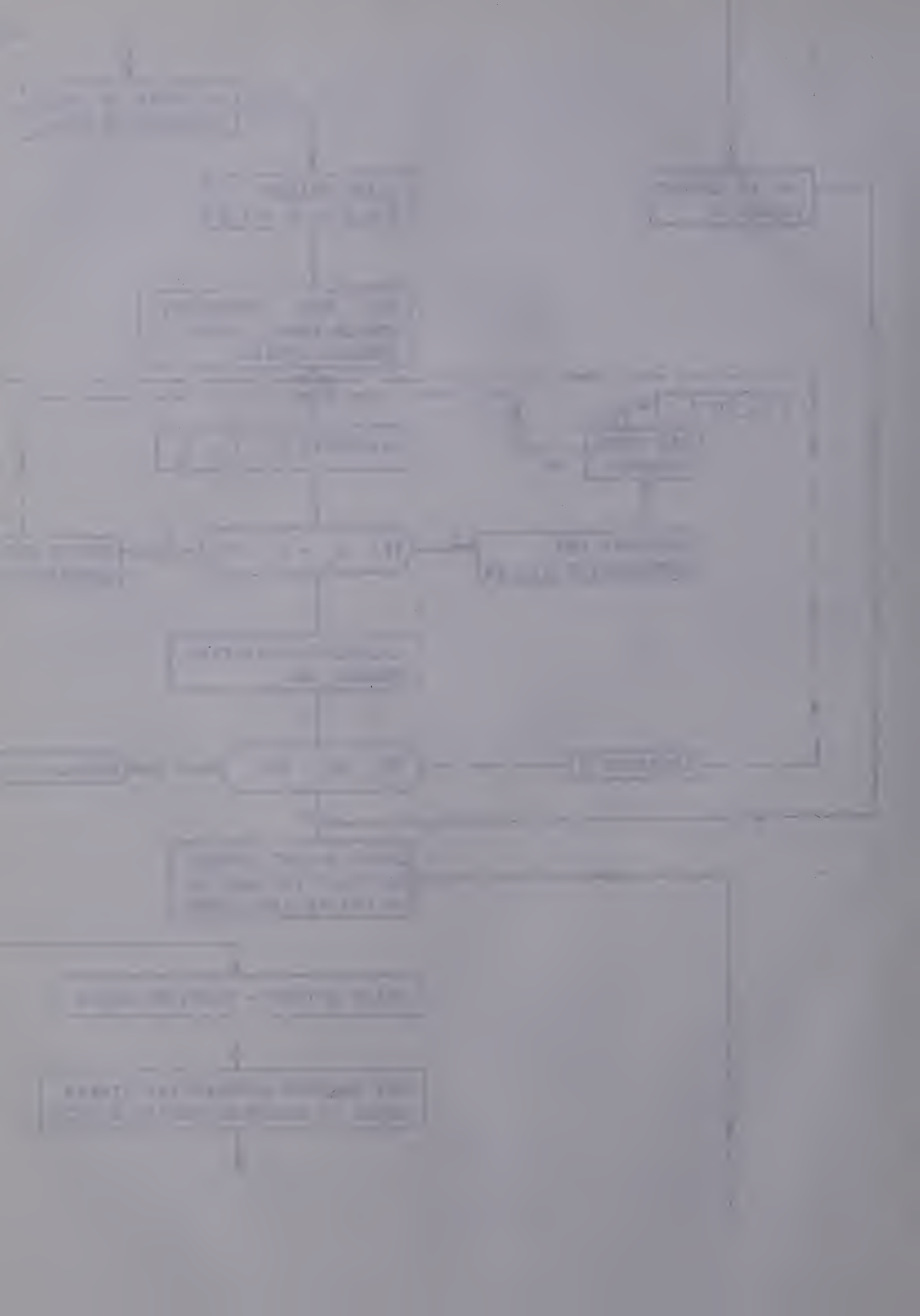

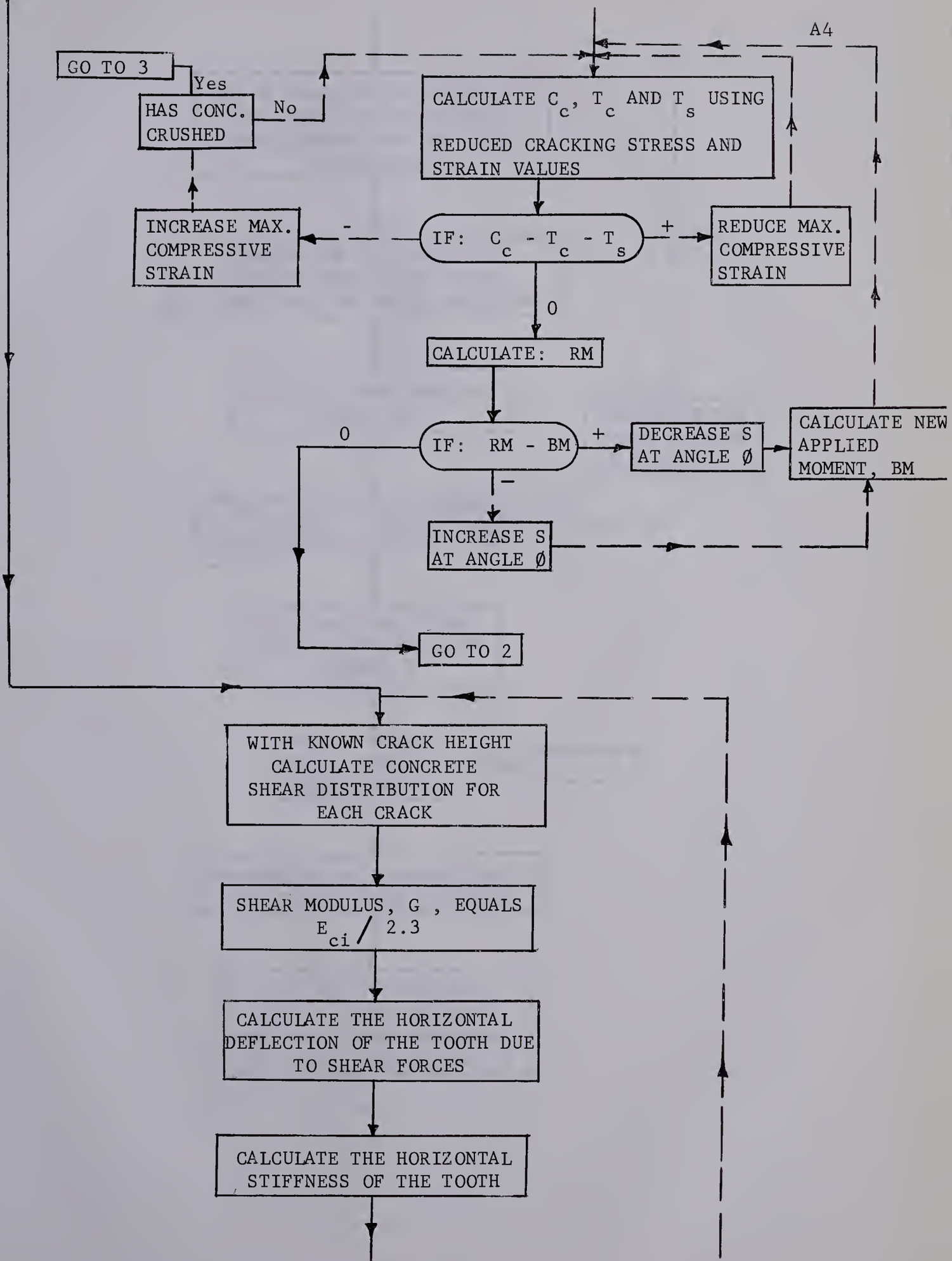
A4
GO TO 3
Yes
HAS CONC. CRUSHED
No
CALCULATE C_c, T_c AND T_s USING REDUCED CRACKING STRESS AND STRAIN VALUES
INCREASE MAX. COMPRESSIVE STRAIN
-
IF: $C_c - T_c - T_s$
+
REDUCE MAX. COMPRESSIVE STRAIN
0
CALCULATE: RM
0
IF: RM - BM
+
DECREASE S AT ANGLE Ø
CALCULATE NEW APPLIED MOMENT, BM
-
INCREASE S AT ANGLE Ø
GO TO 2
WITH KNOWN CRACK HEIGHT CALCULATE CONCRETE SHEAR DISTRIBUTION FOR EACH CRACK
SHEAR MODULUS, G , EQUALS $E_{ci} / 2.3$
CALCULATE THE HORIZONTAL DEFLECTION OF THE TOOTH DUE TO SHEAR FORCES
CALCULATE THE HORIZONTAL STIFFNESS OF THE TOOTH

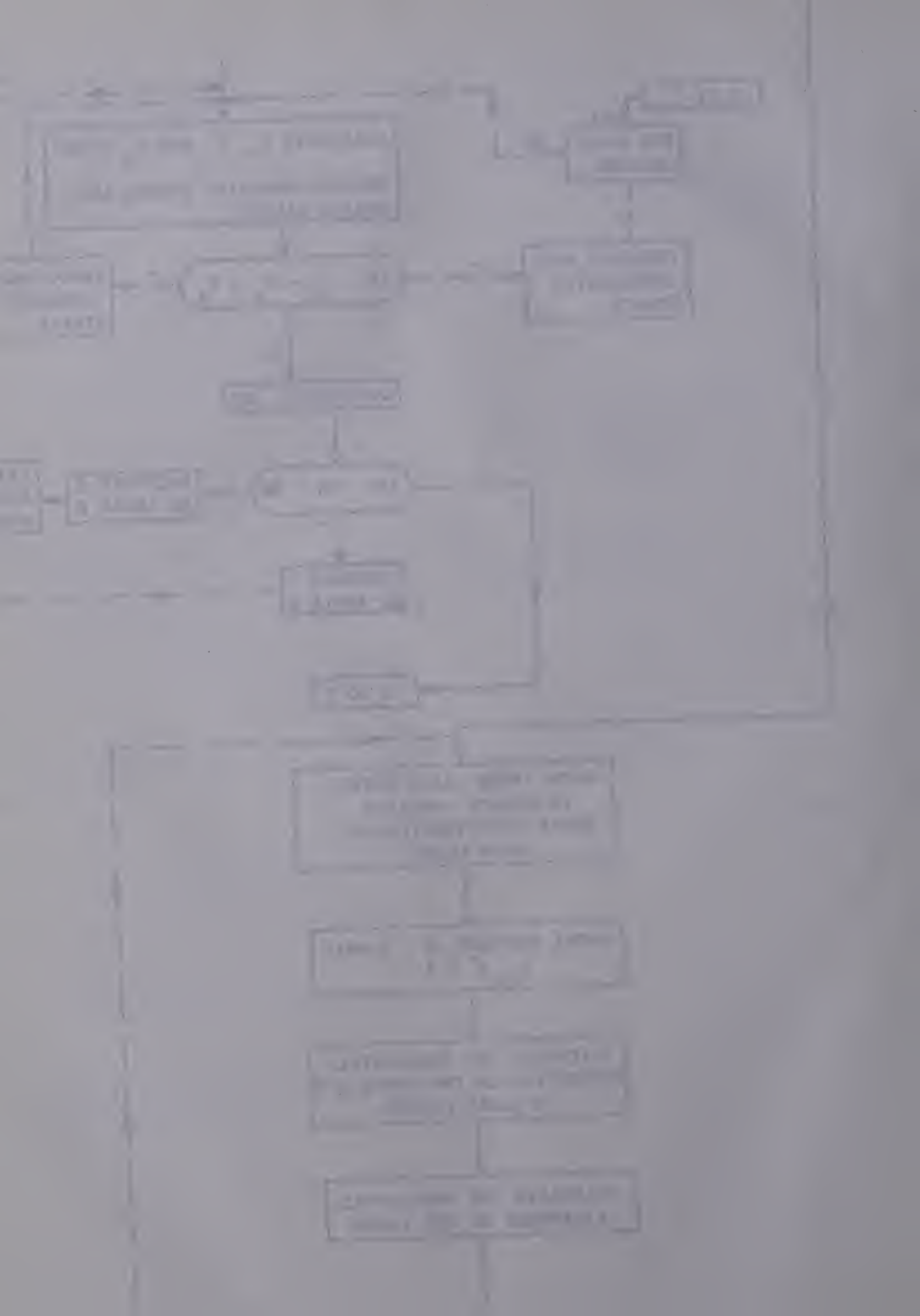

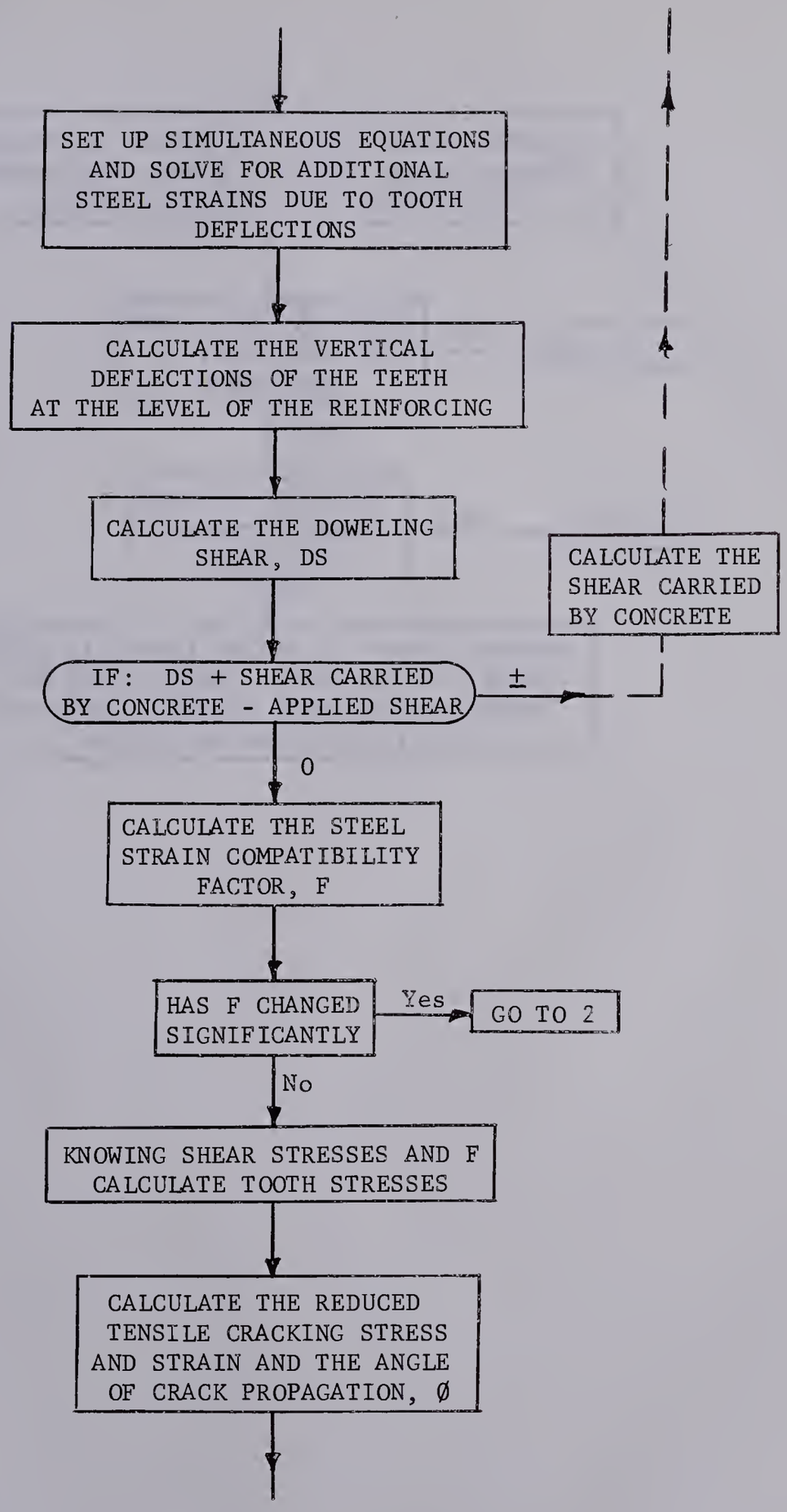
SET UP SIMULTANEOUS EQUATIONS AND SOLVE FOR ADDITIONAL STEEL STRAINS DUE TO TOOTH DEFLECTIONS
CALCULATE THE VERTICAL DEFLECTIONS OF THE TEETH AT THE LEVEL OF THE REINFORCING
CALCULATE THE DOWELING SHEAR, DS
CALCULATE THE SHEAR CARRIED BY CONCRETE
IF: DS + SHEAR CARRIED BY CONCRETE - APPLIED SHEAR
±
0
CALCULATE THE STEEL STRAIN COMPATIBILITY FACTOR, F
HAS F CHANGED SIGNIFICANTLY
Yes
GO TO 2
No
KNOWING SHEAR STRESSES AND F CALCULATE TOOTH STRESSES
CALCULATE THE REDUCED TENSILE CRACKING STRESS AND STRAIN AND THE ANGLE OF CRACK PROPAGATION, Ø

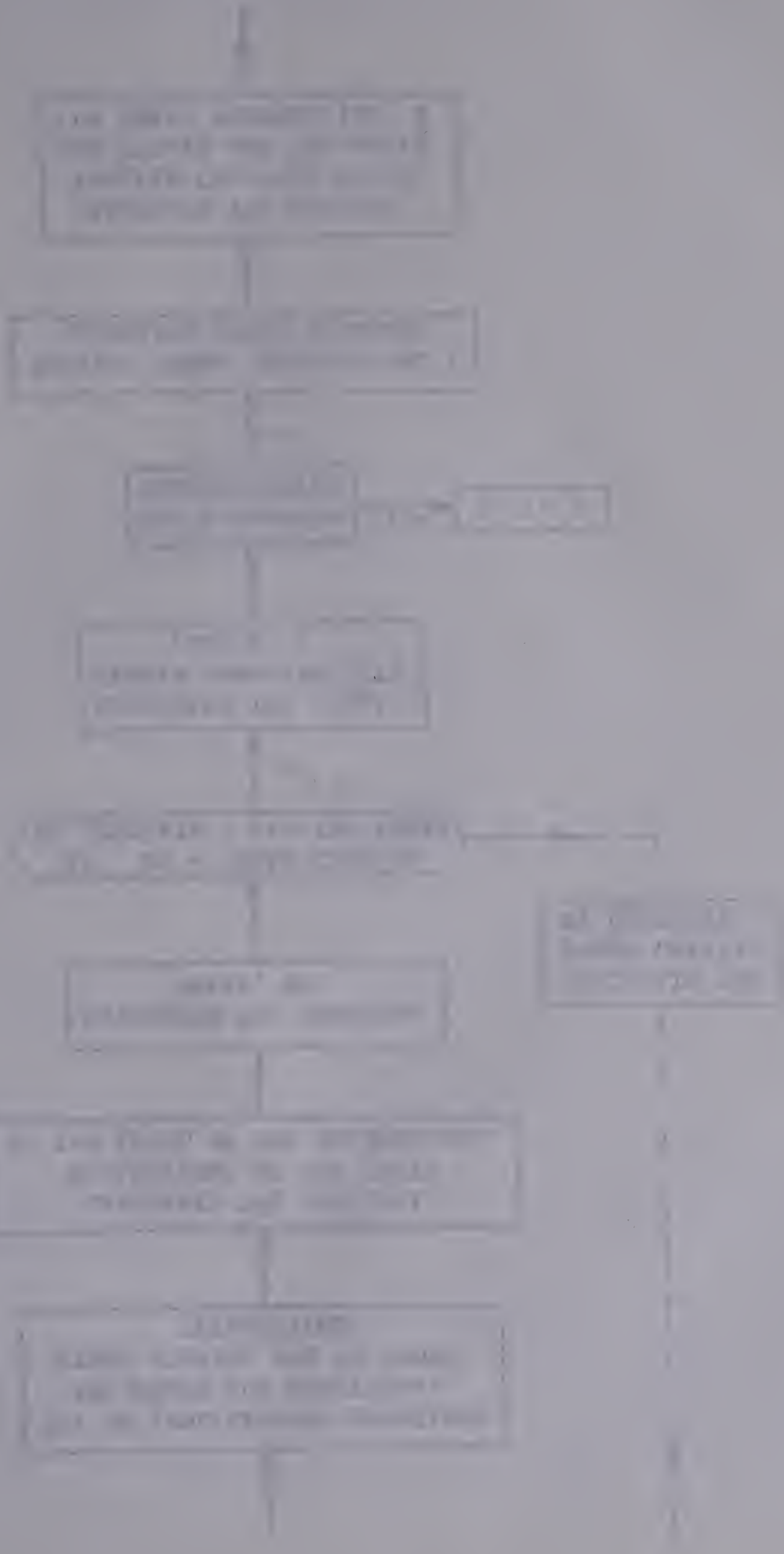

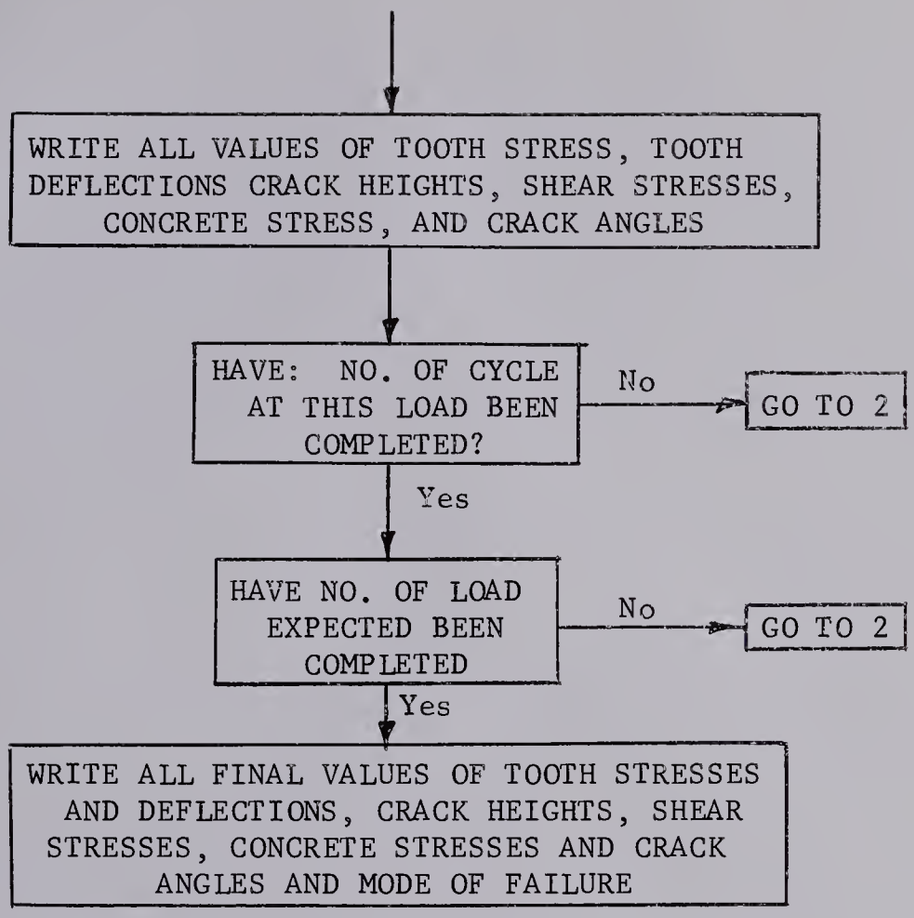
WRITE ALL VALUES OF TOOTH STRESS, TOOTH DEFLECTIONS CRACK HEIGHTS, SHEAR STRESSES, CONCRETE STRESS, AND CRACK ANGLES
HAVE: NO. OF CYCLE AT THIS LOAD BEEN COMPLETED?
No
GO TO 2
Yes
HAVE NO. OF LOAD EXPECTED BEEN COMPLETED
No
GO TO 2
Yes
WRITE ALL FINAL VALUES OF TOOTH STRESSES AND DEFLECTIONS, CRACK HEIGHTS, SHEAR STRESSES, CONCRETE STRESSES AND CRACK ANGLES AND MODE OF FAILURE

(3)